The use of positive and negative penalty functions in solving constrained optimization problems and partial differential equations

A thesis submitted in partial fulfilment

of the requirements for the degree

of

Doctor of Philosophy in

Mechanical Engineering

at

The University of Waikato

by

Luis Emilio Monterrubio Salazar

THE UNIVERSITY OF
WAIKATO
Te Whare Wānanga o Waikato

The University of Waikato

June, 2009

Abstract

The Rayleigh-Ritz Method together with the Penalty Function Method is used to investigate the use of different types of penalty parameters. The use of artificial springs as penalty parameters is a very well established procedure to model constraints in the Rayleigh-Ritz Method, the Finite Element Method and other numerical methods. Historically, large positive values were used to define the stiffness coefficient of artificial springs, until recent publications demonstrated that it is possible to use negative values to define the stiffness coefficients of the springs. Furthermore, recent publications show that constraints can be enforced using positive and negative mass or inertia in vibration problems and in a more generic sense using eigenpenalty parameters which are penalty parameters in the matrix associated with the eigenvalue. Before the commencement of this thesis, solutions using artificial inertia were published only for beams and simple spring-mass systems.

In this thesis the use of all possible types of penalty parameters are investigated in vibration problems of Euler-Bernoulli beams, thin plates and shallow shells and in elastic stability analysis of Euler-Bernoulli beams, including penalty parameters associated with the geometrical stiffness matrix. The study includes the use of penalty parameters for both enforcing support boundary conditions and continuity conditions along structural joints.

This investigation started with the selection of the set of admissible functions that would: (a) allow modelling of beams, plates and shells in completely free

boundary conditions; (b) not present any limitation in the number of functions that can be used in the solution. This gives the possibility to converge to the constraint solution and to model any type of boundary conditions.

The procedure proposed in this work combines several advantages: accuracy of the results, relative fast convergence, simplicity of the set of admissible functions and flexibility to define boundary conditions. While there are other procedures that may give better accuracy for specific cases, the proposed method is more widely applicable.

The procedure used in this work also includes a way to check for round-off errors and ill-conditioning in the results; as well as a way to bracket the “exact” solution with upper and lower-bound results.

Acknowledgements

I want to thank Dr. Ilanko for his excellent guidance and review of this thesis. I also would like to thank Dr. Harm Askes for his very valuable comments on my research and finally, I would like to thank my family and friends for their support and help during my research.

Table of Contents

List of Figures

List of Tables

Nomenclature

Roman alphabet

a	dimension along direction x of a plate or a shell
A	cross-sectional area of beams, Lamé parameter
b	dimension along direction y of a plate or a shell
B	Lamé parameter
$\mathbf{c}$	vector of arbitrary coefficients
c_i	arbitrary coefficients for beams
c_{ij}	arbitrary coefficients for plates and shells
D	flexural rigidity of a plate or a shell
E	Young's modulus
$\mathbf{E}_{ki}^{(r,s)}$	definition of a matrix in terms of its r and s partial derivatives with respect to x and the terms k and i of its admissible set of functions
$\mathbf{F}_{lj}^{(r,s)}$	definition of a matrix in terms of its r and s partial derivatives with respect to y and the terms l and j of its admissible set of functions
$\hat{g}$	non-dimensional geometric stiffness penalty parameter
$\mathbf{G}$	geometric stiffness matrix
h	thickness of a plate or a shell

$\hat{h}$ number of constrained degrees of freedom

$\hat{h}_x$ number of constrained degrees of freedom on edges parallel to axis x

$\hat{h}_y$ number of constrained degrees of freedom on edges parallel to axis y

i subscript

I second moment of area

I_x penalty parameter value due to an artificial moment of inertia at a point x for beams

$I_{(x,y)}$ penalty parameter value due to an artificial moment of inertia at a point (x,y) for plates

I_{x0} penalty parameter value per unit length due to an artificial moment of inertia along edge at $x=0$ for plates, similar coefficients are defined for springs along other edges

I_{wx0} penalty parameter value per unit length due to an artificial moment of inertia along edge at $x=0$ to enforce zero normal slope for shells, similar coefficients can be defined for springs along other edges

j subscript

k subscript

k_x penalty parameter value due to an artificial translational spring at a point x for beams

k_{rx} penalty parameter value due to an artificial rotational spring at a point x for beams

$k_{(x,y)}$ penalty parameter value due to an artificial translational spring at a point (x,y) for plates

k_{x0} penalty parameter value per unit length due to an artificial translational spring along edge at $x=0$ for plates, similar coefficients can be defined for springs along other edges

k_{ux0} penalty parameter value per unit length due to an artificial translational spring in x direction along edge at $x=0$ for shells, similar coefficients can be defined for springs constraining translation in other directions and along other edges

$k_{r(x,y)}$ penalty parameter value due to an artificial rotational spring at a point (x,y) for plates, similar coefficients can be defined for springs along other edges

k_{rx0} penalty parameter value per unit length due to an artificial rotational spring along edge at $x=0$ for plates, similar coefficients are defined for springs along other edges

k_{rwx0} penalty parameter value per unit length due to an artificial rotational spring along edge at $x=0$ to enforce zero normal slope for shells, similar coefficients can be defined for springs along other edges

$\hat{k}$ non-dimensional stiffness of artificial springs

K stiffness matrix

KUU stiffness submatrix (shells)

KUV	stiffness submatrix (shells)
KUW	stiffness submatrix (shells)
KVV	stiffness submatrix (shells)
KVW	stiffness submatrix (shells)
KWW	stiffness submatrix (shells)
l	subscript
L	beam length
m_x	penalty parameter value due to an artificial mass at a point x for beams
$m_{(x,y)}$	penalty parameter value due to an artificial mass at a point (x,y) for plates
m_{x0}	penalty parameter value per unit length due to an artificial mass along edge at $x=0$ for plates, similar coefficients can be defined for springs along other edges
m_{ux0}	penalty parameter value per unit length due to an artificial mass in x direction along edge at $x=0$ for shells, similar coefficients can be defined for springs constraining translation other directions and along other edges
M	mass matrix
MUU	mass submatrix (shells)
MVV	mass submatrix (shells)
MWW	mass submatrix (shells)
$\hat{m}$	non-dimensional artificial inertial parameters
n	number of terms included in the set of admissible functions
$\hat{n}$	number of degrees of freedom

$\hat{n}_{active}$	active number of degrees of freedom
p	superscript
P	compressive force
P_c	critical load
P_n	Legendre polynomials
$\mathbf{P}_g$	penalty matrix due to artificial geometric stiffness for beams
$\mathbf{P}_m$	penalty matrix due to artificial inertia for beams
$\mathbf{P}_{m,edge}$	penalty matrix due to artificial inertia along edges for plates
$\mathbf{P}_{m,point}$	penalty matrix due to artificial inertia at a point for plates
$\mathbf{P}_s$	penalty matrix due to artificial springs for beams
$\mathbf{P}_{s,edge}$	penalty matrix due to artificial springs along edges for plates
$\mathbf{P}_{s,point}$	penalty matrix due to artificial springs at a point for plates
$\mathbf{PI}_{s,1-2,1}$	penalty matrix to be added to the stiffness matrix of plate 1 due to its inter-connection to plate 2 using artificial springs, subscript m is used if artificial inertia is used instead
$\mathbf{PC}_{s,1-2}$	coupling penalty matrix due to artificial springs to inter-connect plates 1 and 2, subscript m is used if artificial inertia is used instead
$\mathbf{PUU}_s$	penalty submatrix due to artificial translational springs in x direction for shells, subscript m is used if artificial inertia is used instead

$\mathbf{PVV}_s$	penalty submatrix due to artificial translational springs in y direction for shells, subscript m is used if artificial inertia is used instead
$\mathbf{PWW}_s$	penalty submatrix due to artificial translational and rotational springs in/around z direction for shells, subscript m is used if artificial inertia is used instead
r	superscript, radius of beams
r_0	radius of tapered beam at $x=0$
r_L	radius of tapered beam at $x=L$
R_x	radius of curvature of a shell parallel to axis x
R_y	radius of curvature of a shell parallel to axis y
s	superscript
t	time
T_{max}	maximum kinetic energy of the structural element
T_m	maximum kinetic energy due to artificial inertia for beams
$T_{m,edge}$	maximum kinetic energy of artificial springs along edges for plates
$T_{m,point}$	maximum kinetic energy of artificial springs at a point for plates
u	displacement (or deflection) of the structure on coordinate axis x
U	displacement amplitude function of the structure on coordinate axis x
v	displacement of the structure on coordinate axis y
V	displacement amplitude function of the structure on coordinate axis y

V_a maximum potential energy due to an axial compressive force

V_g maximum potential energy of artificial geometric stiffness for beams

V_{max} maximum potential energy of the structural element

V_s maximum potential energy of artificial springs for beams

$V_{s,edge}$ maximum potential energy of artificial springs along edges for plates

$V_{s,point}$ maximum potential energy of artificial springs at a point for plates

$V_{s,transu}$ maximum potential energy of artificial springs along edges constraining translation in the x direction

$V_{s,transv}$ maximum potential energy of artificial springs along edges constraining translation in the y direction

$V_{s,transw}$ maximum potential energy of artificial springs along edges constraining translation in the z direction

$V_{s,rotw}$ maximum potential energy of artificial springs along edges to enforce zero normal slope for shells

$V_{s,1-2}$ maximum potential energy of artificial springs to inter-connect structures 1 and 2

w displacement (or deflection) of the structure on coordinate axis z

W displacement amplitude function of the structure on coordinate axis z

x coordinate axis

y coordinate axis

z	coordinate axis

Greek alphabet

α	aspect ratio
β	positive factor used to define proportionality between R_x and R_y
γ_x	penalty parameter value due to an artificial translational geometric stiffness at a point x for beams
γ_{rx}	penalty parameter value due to an artificial rotational geometric stiffness at a point x for beams
γ_{xy}	membrane shear strain component of the shell
ε_x	membrane linear strain component of the shell in x direction
ε_y	membrane linear strain component of the shell in y direction
η	non-dimensional coordinate in y direction
θ	angle between beams of a two-beam frame
κ_x	dynamic curvature of the shell in x direction
κ_y	dynamic curvature of the shell in y direction
κ_{xy}	dynamic twisting curvature of the shell
λ	non-dimensional frequency parameter, non-dimensional critical load
Λ	Lagrangian multiplier
ν	Poisson's ratio
ξ	non-dimensional coordinate in x direction
ρ	density

$\hat{\rho}$	tapering ratio of a beam
ϕ_i	set of admissible functions in x direction
χ_j	set of admissible functions in y direction
Ψ_m,	kinetic function of the artificial inertia.
Ψ_{max}	kinetic energy function of the structural element
$\Psi_{m,edge}$	kinetic energy function due to artificial inertia along edges of plates
$\Psi_{m,point}$	kinetic energy function due to artificial inertia at a point in plates
ω	circular natural frequency

Chapter 1

Introduction

1.1 Overview

This thesis presents a methodology to solve vibration and buckling problems of structural elements in completely free condition or resting on different types of supports, which restrict the motion of the structure in specific degrees of freedom. For instance, in this work the following point supports are used to model the essential boundary conditions of Euler-Bernoulli beams:

a) simple support, which constrains transverse displacement, while it allows rotation. This type of boundary condition is represented by a pin or by a roller.
b) clamped support, which constrains transverse displacement and rotation. This type of support fixes the beam at a point, and
c) guiding support, which constrains rotation, while allows translation. This type of support is represented by a sliding joint moving in vertical direction.

Supports can be defined at the ends of the beams, as well as at any internal point of the beams. Obviously, in the absence of supports the structure can move freely and the boundary condition is called free condition.

Natural frequencies and critical loads are related to the eigenvalues of the system and are characteristics of structures of specific geometry, material properties and boundary conditions. It is worth noting that supports have the effect to stiffen the structure, which means that structural elements with more supports (constraints) will have higher natural frequencies and critical loads.

The Penalty Function Method has its origin in the work by Courant (1943), where it is demonstrated that boundary conditions could be enforced in the RRM using artificial springs, which are now known widely as penalty parameters. Then as the stiffness value of the spring tends to infinity, it asymptotically approximates the effect of a rigid support. Thus, the Penalty Function Method solves the problem of having to define a set of admissible functions that individually satisfy the boundary conditions of the structure in the RRM.

The value of the coefficient of the artificial springs in the Penalty Function Method was always defined by a positive number until a publication by Ilanko and Dickinson (1999) demonstrated that it is possible to use negative values to define the stiffness of the spring in vibration problems. This technique was extended by several publications showing the advantages of the method to obtain the error of the solution due to constraint violation and its application to other type of problems (Askes and Ilanko 2006; Ilanko 2002a; Ilanko 2002b; Ilanko 2003).

Furthermore, in (Ilanko 2005b) it is proved that positive and negative penalty parameters representing inertia (mass and moments of inertia) can be used to solve vibration problems. Moreover, in a recent publication (Ilanko and Williams

2008), a general mathematical proof has been presented to show that in linear eigenvalue problems, positive and negative penalty terms can be applied to the matrix of the system associated with the eigenvalue. This type of penalty parameter was referred to as the "eigenpenalty parameter", while the penalty parameter associated to the stiffness matrix was referred as the "ordinary penalty parameter". In (Ilanko and Williams 2008) the application of the "eigenpenalty parameter" was limited to a vibration problem, using "inertial penalty parameters" introduced in (Ilanko 2005b), mentioned earlier. In the present work the use of positive and negative eigenpenalty parameters are also used in structural stability analysis, in which the eigenpenalty parameters are associated with the geometric stiffness.

The purpose of this work is to investigate how best to implement the various types of penalty functions to model constraints in practical engineering problems. This study was carried out solving vibration and buckling problems of structural continuum elements, such as Euler-Bernoulli beams, rectangular thin plates and shallow-shells of rectangular planform. Vibration problems of these three structural elements are presented in this work, while buckling problems were limited to the solution of Euler-Bernoulli beams. Results are presented in non-dimensional form, giving frequency parameters instead of natural frequencies and non-dimensional critical loads. It is worth to note here that only penalty parameters of positive stiffness type were used in plates and shells prior to the commencement of this work.

The procedure used here is very simple and in general can be divided in two steps. The first step consists of using the Rayleigh-Ritz Method (RRM) to build the system matrices of completely free structural elements (mass and elastic stiffness matrices for vibration problems or elastic stiffness and geometrical stiffness for buckling problems). In the second step, the Penalty Function Method is implemented in the RRM to define all constraints of the system and if necessary inter-connections between structural elements. The second step is not needed if there are neither constraints nor inter-connections.

Sets of admissible functions to be used in the RRM could be built by simple polynomials or transcendental functions. When a set of admissible functions built by simple polynomials is used in the RRM, ill-conditioning is found when more than a few functions are included in the solution (Li et al. 2009). For instance, implementing the RRM using simple polynomials in a MATLAB program using double precision, ill-conditioning was found when more than 13 functions were used in the set of admissible functions to model a free beam. Similarly, a maximum of seven simple polynomials could be used in each set of admissible functions in x and y directions to describe the deflection of a completely free plate (giving a total of 49 trial functions) or of a completely free shallow shell (giving a total of 147 trial functions), before reaching ill-conditioning. Sets of admissible functions composed entirely of transcendental functions are used for cases with simple boundary conditions (Li 2004). Sets of admissible functions mixing simple polynomials and trigonometric functions were also found in the literature, which converge rapidly and allow the use of artificial springs. However, in the past the mixed formulations generally did not exploit the concept of

artificial springs, as in general the proposed sets of admissible functions were always generated by solving equations to satisfy boundary conditions. This means that the procedure given in the existing literature is laborious and in many cases dependent on boundary conditions.

For this reason, it was decided to build a set of admissible functions combining trigonometric functions and simple polynomials that could represent the deflection of a free-free beam with simple functions and without solving for boundary conditions. For all beam, plate and shell problems in this work, the same set of admissible functions is used in the RRM regardless of the boundary conditions and type of problem, enforcing all essential constraints using penalty functions.

Although the set of admissible functions used here is not orthonormalized as in many publications including (Bhat 1985), no ill-conditioning was found due to the number of functions included in the solution. Whenever ill-conditioning was found in the results of this work, it was always due to the magnitude of the penalty values.

With regard to the RRM, several publications have shown its effectiveness to solve vibration and buckling problems of the structural elements covered in this work including the publications by Leissa (1969a; 1969b; 1973), Leissa and Narita (1984), Young (2000), Young and Dickinson (1995a; 1995b), Yuan and Dickinson (1992a), Baht (1985), Lim and Liew (1994), Li (2004), Zhou (1996),

Amabili *et al* (1997), Ilanko (2002a; 2002b; 2003; 2005b), Ilanko and Dickinson (1999), Askes and Ilanko (2006), Crossland and Dickinson (1997), among others.

The main contributions of this work are:

1. The development of a simple set of admissible functions that can be used in beam, plate and shell problems with any combination of boundary conditions modelled by penalty parameters. The set of admissible functions presented here does not have a limit on the number of functions that can be used due to ill-conditioning and allows fast convergence. For this reason a large number of penalty functions can be included in the solution.
2. A new type of penalty parameter to be used in buckling problems representing artificial geometric stiffness is introduced.
3. Several new findings from a study on the use of different types of penalty parameters in vibration and buckling problems of different types of structural elements.

The outline of the work carried out in this project starts with a relevant literature review presented in Section 1.2. Then, the development of the new set of functions for a free-free beam is presented in Chapter 2. This set of functions can be used in vibration and buckling problems of beams, plates and shallow shells.

Once the set of admissible functions to be used in the RRM was selected, the solutions of vibration and buckling problems presented in Chapters 3 to 7 were obtained implementing appropriate codes in the computer program MATLAB.

Results obtained with the present approach were compared with results obtained using the Finite Element Method (FEM), the RRM together with Lagrangian multipliers in which the constraints are modelled exactly, as well as with other results found in the literature. The mass, elastic stiffness and geometrical stiffness matrices of a standard beam element in the FEM used in this work as found in the literature are given in Appendix A, while a brief description of the Lagrangian Multiplier Method is given in Appendix B.

Chapter 3 shows the procedure used in this work to obtain the frequency parameters of Euler-Bernoulli beams with all types of classical boundary conditions at the ends of the beam including free, simply-supported, clamped and guiding boundary conditions. Guiding conditions constrain rotation and allow translation. This type of boundary conditions is very useful to define symmetry.

Similarly, Chapter 4 presents the procedure used to obtain the frequency parameters of rectangular thin plates with all combinations of classical boundary conditions as well as an example with internal constraints.

Chapter 5 presents the procedure to obtain the frequency parameters of shallow shells of rectangular planform with spherical, cylindrical and hyperbolic paraboloidal geometries with classical boundary conditions.

Chapter 6 presents the procedure to solve vibration problems of non-symmetrical box-type structures obtained by inter-connecting plate elements using penalty parameters.

The solution of structural stability problems for beams is presented in Chapter 7 showing the critical loads of beams with different types of boundary conditions, intermediate constrains, different tapering ratios, as well as an example of a two-beam frame.

The conclusions of the present work are given in Chapter 8.

1.2 Literature review

1.2.1 The Rayleigh-Ritz Method versus other methods

The RRM is very attractive for solving engineering problems of structures of simple geometry, especially if they can be modelled with a single structural element. The RRM presented by Ritz (1908) is an extension of the Rayleigh Method, based on the minimization of the energy functional called the Rayleigh-quotient, using a set of admissible functions to model the deflection of the structure, instead of a single function. In all cases in this work the energy functional contains only energy terms of conservative systems.

In (Williams 1987) two important characteristics of the classical RRM (without penalty parameters) are mentioned. The first characteristic is that when the RRM is used to solve vibration problems, the natural frequencies converge monotonically from above as the number of terms in the set of admissible functions is increased and the second characteristic is that the lower modes converge first. Williams (1987) also noted that these properties hold in the RRM only if all calculations are carried out in exact arithmetic. Therefore, it should be

noted that in practical computations, using the RRM even with double precision brings round-off errors.

The advantages of the RRM are that it gives upper bounds, can be used to solve problems of the three structural elements covered in this thesis, converges with a relatively low number of degrees of freedom (DOFs) and produces symmetric matrices, resulting in stable algorithms for its numerical solution (Ventsel and Krauthammer 2001).

It is important to acknowledge the existence of other methods that can be used to solve vibration and buckling problems of structural elements. First, an exact solution of a vibration or buckling problem can be derived as a boundary value problem, but in general these solutions are rare due to difficulties in satisfying the specific boundary conditions of the problem (Szilard 2004). For instance, the Navier's Method presented in (Navier 1823) can be used to solve problems of simply supported plates using double trigonometric series, whilst the Lévy's Method that uses a transcendental formulation can be used to solve plate problems having simply support conditions on two opposite edges and any type of boundary conditions on the other two edges (Lévy 1899).

Other methods have been developed to solve problems with more general sets of boundary conditions. Some of these methods such as the Rayleigh's Method, the Galerkin Method and the Collocation Method (Rao 2007) are classified as approximate analytical methods; while other methods are classified as numerical methods. Examples of the latter methods include the FEM (Zienkiewicz *et al.*

2005), the Finite Difference Method (Szilard 2004) and the Superposition Method (Gorman 1999). In (Wu and Chou 1998; Wu and Luo 1997) an analytical-and-numerical-combined-method was presented.

Although, the RRM is specially at a disadvantage when compared to the FEM to solve problems with complex geometries, it has been noted that the RRM is more efficient than the FEM in that the accuracy per degree of freedom is generally higher for the RRM than for the FEM (Kapania and Liu 2000; Smith et al. 1999). However, the FEM is used in this work to obtain results for comparison purposes with its traditional way to define boundary conditions, even though it is also very easy to implement the Penalty Function Method in the FEM. In the FEM just as the RRM the accuracy of the frequencies and modes increases as the number of DOFs increases, while their error increases in higher modes (Burnett 1987).

The procedure presented in this work has also some advantages when compared with the semi-analytical method published in (Wu and Chou 1998; Wu and Luo 1997) that also uses penalty parameters to define constraints. The disadvantages of the semi-analytical method are: (i) results are not as accurate as in the present method, (ii) no upper or lower bound is guaranteed, and (iii) it can be used only when the closed form solution to a related problem is known.

Of the other popular methods, it can be said that the Galerkin Method and RRM are equivalent for the type of problems presented in this work; the Superposition Method has not been developed for doubly curved shells; while the Collocation Method and the Finite Difference Method although simple, give non-symmetric

matrices and the latter is difficult to code (Ventsel and Krauthammer 2001). Furthermore, when using the Finite Difference Method or the Superposition Method any change in the boundary conditions would require significant alterations to the system matrices.

The Lagrangian Multiplier Method has been used in the RRM to model constraints and to join structural elements to solve problems of complex geometries as in the work by Dowell (1972) where he used this technique to model plates with beam stiffeners. Although, the Lagrangian Multiplier Method models constraints exactly, it has the following disadvantages: a) only point constraints can be modelled, b) each constraint adds a row and a column to the system matrices with zeros in the main diagonal.

The Penalty Function Method has also been used in the RRM to inter-connect elements to solve problems where the domain is defined by a complex geometry (Yuan and Dickinson 1992a; Yuan and Dickinson 1992b). Other complicated effects in the geometry of plates have been addressed in the past. This includes plates with different curved boundaries (Young and Dickinson 1994) and plates with internal constraints (Kim 1995).

1.2.2 The Rayleigh-Ritz procedure

The Rayleigh-Ritz procedure has been outlined in many publications including those by Budiansky and Pai (1946) and by Bassily and Dickinson (1975) who used the RRM to solve buckling and vibration problems of plates, respectively. The outlined procedure in these references is as follows:

1. The deflection is expressed with a set of admissible functions, which is a sum of an infinite set of functions having undetermined coefficients. In the classical RRM each term of the set of functions must satisfy the geometric boundary conditions, while in (Budiansky and Hu 1946) it is stated that this condition is not necessary when boundary conditions are defined by the Lagrangian Multiplier Method.
2. The energy of the plate is computed and minimized with respect to the undetermined coefficients.
3. The eigenvalue problem of the set of linear homogeneous equations obtained from the minimizing procedure is solved.

When the set of functions used is a complete set capable of representing the deflection, slope and curvature of any plate deformation, the solution obtained, is in principle exact.

1.2.3 Sets of admissible functions in the RRM

As stated earlier, the method presented in this thesis uses the RRM with a set of admissible functions to model the deflection of the structure with free boundary conditions to obtain the mass, stiffness and geometrical stiffness (for structural stability problems) matrices of completely free beam, plate or shell elements. Then the Penalty Function Method is used to add constraints to the system.

Some publications that use a set of admissible functions of free structures together with the Penalty Function Method to model boundary conditions were found in the literature. One of these references is the work by Yuan and Dickinson (1992a)

who used orthogonal polynomials for free boundary conditions given in (Bhat 1985) to solve vibration problems of stepped plates, plates with slits and box-type structures. Another reference that uses the same approach was published by Crossland and Dickinson (1997) to model shells with slits. Crossland and Dickinson (1997) used simple polynomials to define the sets of admissible functions of free shell elements and artificial springs were used to inter-connect the shell elements and to define boundary conditions. In (Amabili *et al.* 1997) the eigenfunctions of a free circular plate were used together with artificial springs to solve vibration problems of circular plates resting on an annular, non-uniform Winkler foundation. Similarly a method to choose admissible functions for the RRM was defined by Amabili and Garziera (1999), where it is stated that the problem should be defined as "less-constrained" than the original.

The set of admissible functions presented in this work was developed after recognizing that polynomial functions are likely to suffer ill-conditioning, while the use of only a simple trigonometric series makes it impossible to satisfy some boundary conditions. Mixing polynomials and trigonometric functions gives a set of admissible functions that allows fast convergence of most of the terms included in the set of admissible functions and avoids round-off errors and ill-conditioning as shown in (Li 2004) and (Zhou 1996). This is explained in more detail in the next paragraphs.

Set of admissible functions using polynomials

In the extensive literature on vibration of beams, plates and shells using the RRM, sets of admissible functions have often been built with simple polynomials as in

the work by Baruh and Tadikonda (1989), Crossland and Dickinson (1997), and Ilanko and Dickinson (1999). The disadvantages of using simple polynomials have been identified by many researchers including Singhvi and Kapania (1994) who used simple, orthogonal and Chebyshev polynomials in the RRM to solve free torsional vibration and buckling problems of thin-walled beams of open section resting on a Winkler-type elastic foundation subjected to an axial force. Singhvi and Kapania (1994) found that when using simple polynomials, the maximum number of terms in the set of admissible functions was limited to 6 using single precision and 10 using double precision, before the mass and stiffness matrices became singular. In (Singhvi and Kapania 1994) the penalty approach was also used to model boundary conditions when simple or Chebyshev polynomials were used as admissible functions. In comparison with simple polynomials, results using Chebyshev polynomials allow the use of more terms and converge to a more accurate solution.

Another study on the convergence of the different types of polynomials in the RRM was carried out by Smith *et al* (1999) in buckling analysis of plates. In this publication the following types of polynomials were included: simple polynomials, Chebyshev-1, Chebyshev-2, Legendre, Hermite and Laguerre. The studies of the convergence showed that the solutions of all orthogonal polynomials appeared to converge at the same rate and that as expected the results converge to more accurate results when orthogonal polynomials are used in the RRM instead of simple polynomials. However, in all cases there is a limit in the number of terms that can be used before numerical instabilities appear. Smith *et al* (1999) also reported that for fully clamped plates the solution using orthogonal

polynomials becomes unstable with less terms than with simple polynomials due to the higher degree polynomial needed to satisfy boundary conditions. Smith *et al* (1999) used double and quadruple precision in their studies of the convergence of simple polynomials. The use of quadruple precision increased the number of terms that could be used in the solution of simple polynomials to up to 16 (instead of seven to ten depending on boundary conditions), but with a price in computational effort. The study showed that the Legendre polynomials and both types of Chebyshev polynomials were the most stable, while Laguerre polynomials were the most unstable. Smith *et al* (1999) recommended the use of simple polynomials due to its simplicity and computational cost.

A set of admissible functions using orthogonal polynomials was developed by Bhat (1985), where the Gram-Schmidt process is used to construct a set of admissible functions from a polynomial that satisfies the boundary conditions and then constructing the rest of the polynomials of the set of admissible functions multiplying the original polynomial by an orthogonal weighting function. Bhat used these sets of admissible functions to solve plate problems obtaining accurate results for lower modes, particularly when plates have some free edges.

The work by Bhat (1985) has become a very popular method to define sets of admissible functions, in spite of the comments in (Brown and Stone 1997) where it is stated that the orthogonal polynomials obtained using the Gram-Schmidt process are not necessary to improve the convergence of the solution, and that the convergence depends only on the degree of the polynomial represented in the set of admissible functions. In the same publication, Brown and Stone recognized that

Bhat gives a very simple method to define sets of admissible functions for different boundary conditions and that orthogonal polynomials are more stable than simple polynomials with respect to inversion and extraction of eigenvalues of the resulting stiffness and mass matrices, especially when higher order polynomials are used.

In another publication, Bhat (1996) discussed results for cantilever beams using five different sets of admissible functions. These sets were built with the following approaches: a) using beam characteristic functions which give exact solutions, b) building orthogonal characteristic polynomials defining the first member of the series as $6x^2 - 4x^3 + x^4$, satisfying all boundary conditions, while the other five functions only satisfied the clamped constraint; c) building a series of the form $x^{i-1}\left(6x^2 - 4x^3 + x^4\right)$, this is using the first term in b) and getting the next functions by successively multiplying the first term by x; d) building orthogonal polynomials using x^2 as the first term in the series which satisfies the clamped condition and e) using the series $x^{i-1}x^2$, this is using the first term in d) and successively multiplying the first term by x. The results of the cantilever beam using six terms in all approaches were very similar for the first three modes, while the results of the upper three modes of the polynomial approaches were very different in comparison with the results using the characteristic functions. Although in the same paper Bhat included a range of results for clamped plates using beam characteristic functions, boundary characteristic orthogonal polynomials and plate characteristic functions, at least half of the upper frequencies obtained using the set of admissible functions defined by boundary characteristic orthogonal polynomials did not converge to an accurate result. For

instance, using six terms in each direction, giving a total of 36 terms, the deviation of mode 17 is higher than 17.0 % in comparison with the results for beam and plate characteristic functions.

Set of admissible functions using transcendental functions

Transcendental functions have also been used to build sets of admissible functions. For instance, Leissa (1973) presented the solution of the 21 possible cases of rectangular plates with classical boundary conditions (that is, free, simply-supported and clamped conditions). For the six cases having two opposite sides simply-supported the classical Voigt or Lévy solutions were obtained using exact characteristic functions. For all other cases, the RRM was used and the admissible functions were defined by normalized beam eigen-functions exactly satisfying simply supported and clamped boundary conditions and approximately satisfying free boundary conditions of the plates as previously presented in (Warburton 1954). Each specific set of admissible functions in (Warburton 1954) were built with transcendental functions and defined for each combination of classical boundary conditions on opposite edges, except for the cases including free modes. For the free-free case a unit function and a function built by a combination of a unit function and a linear function are included together with a series of transcendental functions, while for a simply supported-free beam only the latter function to model the rotational rigid-body mode is included. Unfortunately, simple transcendental functions do not permit all possible boundary conditions to be satisfied.

Set of admissible functions mixing transcendental functions and simple polynomials

Some researchers have also defined admissible functions combining transcendental functions and polynomials. Ilanko and Dickinson (1987) used a set of admissible functions constructed from a combination of a sine Fourier series and a linear term in the RRM to model the in-plane displacements of slightly curved rectangular plates. Zhou (1996) solved the natural frequencies of rectangular plates using a set of static beam functions, in which each function consists of the cubic polynomial and a sine function. The coefficients of each term are determined solving for boundary conditions, although for free-free and free-simply supported boundary conditions extra functions (a unit and a linear function) in the series are included to represent rigid-body modes, which are similar to the rigid-body modes defined in (Warburton 1954). The method presented in (Zhou 1996) gives accurate results for as many modes as there are number of admissible functions.

Li (2004) proposed a similar set of admissible functions to the one proposed by Zhou, but Li used the polynomial terms as separate functions. In the approach by Li, the set of admissible functions are built by a Fourier series of the cosine function and a fourth order polynomial with undetermined boundary constants, which are found by using the boundary conditions in terms of the admissible functions and their first and third derivatives for an elastically restrained rectangular plate. The polynomial terms are added to the set of admissible functions to avoid discontinuities of the displacement of the beam and its derivatives at the end points, and to improve the convergence of the solution (Li

2004). Results converge to a very good approximation with as few as four functions in each direction.

Filipich and Rosales (2000) developed the so-called ``whole element method'' that consists of the definition of a proper functional and the introduction of an extremizing sequence that defines the set of admissible functions. The set of admissible functions for plates by Filipich and Rosales (2000) is a series of a trigonometric functions and a bidimensional function combining a constant term, a linear term and a sine term that together satisfy the boundary conditions.

The set of admissible functions used in this work is built by the terms of a quadratic polynomial and a cosine series and it can be used to solve beam, plate and shell problems. Thus, the set of admissible functions presented in this work is used to build the mass, elastic stiffness and geometric stiffness matrices that define the properties of these elements in completely free condition, as well as the penalty matrices that define boundary conditions and inter-connections between elements.

In each type of structure, the mass, elastic stiffness and geometric stiffness matrices remain always the same, although they can be scaled according to the geometric and material properties of the elements included in a structure, while the penalty matrix changes according to the constraints of the problem.

Structures of complex geometry can be modelled with the set of admissible functions used in the present work inter-connecting several structural elements, as

there is no limitation on the number of terms in the set of admissible functions that can be used in the solution other than memory size. This means, that there is also no limitation on the number of penalty functions that can be used to inter-connect elements and to define boundary conditions.

1.2.4 Methods to model constraints in the RRM

The Penalty Function Method and the Lagrangian Multiplier Method are probably the most common methods to add constraints in vibration and buckling problems using the RRM. These methods can also be used in other energy methods and in the FEM. Another interesting method to define constraints in the RRM is the pb-2 method (Liew and Wang 1993; Lim and Liew 1994).

In this work results obtained using the RRM with the Penalty Function Method are compared with results using the RRM with Lagrangian multipliers, as well as results from references using RRM with the pb-2 method. For this reason these three methods are described below.

The pb-2 Rayleigh-Ritz Method

The procedure of the pb-2 RRM consists of multiplying the set of admissible functions, by a basic function formed by the product of all the boundary equations. To define the condition at the boundary, a particular boundary equation is raised to the power of 0, 1 or 2 to model free, simply supported or clamped conditions respectively. This approach has been proved to be effective solving bending, buckling and vibration problems of plate and shell elements (Liew and Lim 1994; Liew and Wang 1993; Lim and Liew 1994). These publications present

solutions of several plates and shells that will be used for comparison purposes in this work.

Other authors that have used this approach are Young and Dickinson (1993) who used simple polynomials to solve vibration problems of rectangular plates with straight or curved internal line supports. In a later publication by the same authors (Young and Dickinson 1994) an extended version of the method was presented to solve vibration problems of plates with curved edges. In this extended version of the pb-2 method, the intersections of the x and y axes and two curved edges were used to define quarters of plates. Then either symmetry or artificial springs were used to obtain the solution of the whole plate.

Lagrangian Multiplier Method in the RRM

The Lagrangian Multiplier is a well-established method to define boundary conditions in the RRM and other methods. The Lagrangian Multiplier Method consists of adding equations that force the boundary conditions to be satisfied exactly. In the RRM an extra row and column are added to the stiffness matrix for each point constraint added to the system. For a translational constraint in a flexure problem, the terms of the new row and column are obtained evaluating the corresponding function of the set of admissible functions at the point where the constraint is added. In a similar way, for a rotational constraint the terms of the new row and column are obtained evaluating the first derivative of the corresponding function of the set of admissible functions at the point where the constraint is added as shown in Appendix B.

In the work by Budiansky and Hu (1946) the Lagrangian Multiplier Method was used to add constraints to the Rayleigh-Ritz solution of a buckling plate problem. Budiansky and Hu (1946) stated that the main advantage of using the Lagrangian Multiplier Method in the RRM is that the boundary conditions do not have to be satisfied individually by the functions in the set of admissible functions, but by the expansion of the whole set of admissible functions. In contrast, the main disadvantage of the Lagrangian Multiplier Method is that it increases the size of the matrices and introduces zero diagonal terms in the stiffness matrix (Liu and Chen 2001). Another disadvantage of this method is that it is not possible to define constraints along the edges of plates or shells by integrals. Thus, for these structural elements constraints have to be defined point by point (Liu and Chen 2001).

Finally, an interesting characteristic of the method noticed by Budiansky and Hu (1946) is that the rate of convergence of the solution is faster when Lagrangian multipliers are used to constrain translation using a cosine function series than rotation using a sine function series as the set of admissible functions.

The Penalty Function Method in the RRM

As mentioned in the procedure given in 1.2.2, in the classical RRM a set of admissible functions satisfying the essential boundary conditions must be found. Finding such admissible functions can be a laborious task. In order to address this problem, Courant (1943) introduced the use of artificial springs in the RRM to model geometric constraints in structures. This has the same effect as the Lagrangian multipliers in the work by Budiansky and Pai (1946). Many

researchers have since used artificial springs to model constraints in static and dynamic analysis of structures, as well as in many other disciplines of engineering and mathematical sciences where the stiffness of the artificial springs is known as the penalty parameter (Amabili et al. 1997; Crossland and Dickinson 1997; Kapania and Kim 2006; Yuan and Dickinson 1992a; Zienkiewicz et al. 2005).

A useful characteristic of the RRM is that it produces upper-bound results for natural frequencies as stated in (Williams 1987), but when the Penalty Function Method is used to model constraints representing artificial stiffness the upper-boundness of the solutions may be compromised as the results converge from below with respect to the value of the stiffness coefficient of the spring. This has been noted by several researchers including Huang and Leissa (2009).

As mentioned earlier, recent publications (Ilanko 2003; Ilanko 2005b; Ilanko and Dickinson 1999; Ilanko and Williams 2008) demonstrated that in vibration problems it is possible to model constraints using either artificial springs or artificial inertia (representing mass or moments of inertia). Thus, in modelling constraints in an undamped vibration problem, there are four possible ways to apply a penalty parameter. These are the use of positive stiffness, positive inertia, negative stiffness and negative inertia.

The nature of convergence towards the constrained solution depends on the type and sign of penalty parameter used. Ilanko (2005b) demonstrated that when positive artificial inertial restraints are added to a system, the frequency parameters would approach those of the constrained system from above, whereas

the approach is from below if negative inertial restraints are used. Similarly, if positive artificial stiffnesses are used to model the constraints of the system the frequency parameters are approached from below and from above if negative values are used (Ilanko and Dickinson 1999).

Thus, it is worth noting here that true upper bounds of the natural frequencies of a constrained system are obtained only if penalty parameters that model constraints of the system are represented by either positive inertia (Ilanko 2005b) or by negative stiffness (Ilanko and Dickinson 1999).

In addition, the bounding theorems in (Ilanko 2002a; Ilanko and Williams 2008) show that solutions obtained from penalised models with positive and negative penalty parameters bracket the constrained solution. Thus, the maximum error is half the difference between a pair of results of positively and negatively equally restraint systems and the mean values of each pair of results would be closer to the constrained solution.

As mentioned in the work by Ilanko (2002a; 2005b) a vibration problem of a system with $\hat{n}$ DOFs and $\hat{h}$ penalty parameters approaching infinite absolute value, will give $\hat{n}-\hat{h}$ natural frequencies. Therefore when using penalty parameters in the RRM modelling rigid constraints, $\hat{h}$ DOFs are lost and their corresponding eigenvalues should be deleted from the results. Identifying the $\hat{h}$ eigenvalues and modes that do not correspond to the constrained solution is a very easy task, as they converge to either 0^+, 0^-, ∞ or $-\infty$ depending on the type of penalty parameter used in the solution. 0^+ and 0^- are obtained when positive and

negative inertial penalty parameters are used respectively, while ∞ and $-\infty$ are obtained when positive and negative stiffness penalty parameters are used respectively.

The above statements are valid in any type of linear eigenvalue problem where constraints are replaced with penalty functions, irrespective of the mathematical procedure used, providing that the system does not have rigid-body modes. The set of admissible functions presented here has rigid-body modes. This does not have a big influence on the vibration results, although in buckling problems of a single beam and in the absence of penalty parameters the stiffness matrix will have two zero rows and columns, while the geometric stiffness matrix will have one zero row and column. Thus, in the solution of the beam buckling problem presented here, one eigenvalue will become infinite when an elastic stiffness type penalty parameter is used to model constraints. Furthermore, in vibration problems the zero-frequencies of the original free structure will be included in the results when inertial penalty parameters are used to model constraints as no stiffness would be related to these DOFs. This means that it is important to identify *a priori* the number of rows and columns full of zeros of the matrices of the system.

It is important to mention that the procedure proposed in this work using the RRM and penalty functions to model constraints is an asymptotic method with respect to the absolute penalty value. This means that results approach the "exact" solution as the number of terms increases, but also as the absolute value of the

penalty functions increases. This is of course only until round-off errors or ill-conditioning is reached.

A drawback in the Penalty Function Method is that round-off errors or ill-conditioning appear when penalty parameters are defined with a very high value. For this reason, the appropriate monotonic convergence property and the "bracketing property" of the constraint solution by a pair of penalty parameters of the same type and opposite sign were used as tests to find the best set of eigenvalues free of round-off errors.

Another drawback of this procedure when using negative stiffness is the need to use a reasonably large magnitude for the penalty parameter that is greater than all critical penalty values. The critical penalty values are low negative penalty values of stiffness type that match the original stiffness value of the structure and give a zero frequency as explained in (Ilanko 2002a; Ilanko and Dickinson 1999). While critical penalty values can be computed and they are much smaller in magnitude than what would be needed to enforce constraints, it is still acknowledged as a drawback of this procedure.

However, there is a way to avoid the need to determine the critical penalty terms. This is done by using eigenpenalty functions, although it has been found in this work that a similar instability occurs when low negative eigenpenalty parameters are used if the model contains rigid-body modes. Nevertheless, in this case the maximum number of instabilities is limited to the number of rigid-body modes that have been constrained by penalty parameters and checking the convergence

of the fundamental frequency will prevent this problem as the lower eigenvalues are the last to converge. In contrast, when using ordinary penalty parameters the low frequencies converge first.

It has been found in this work that compared with ordinary type penalty functions, the magnitude of eigenpenalty parameters to effect a constraint is smaller particularly for higher modes. For this reason, eigenpenalty functions are particularly suited for vibration analysis when the number of terms used in the set of admissible functions is not too large, because as mentioned earlier in this case the fundamental frequency is the last one to converge.

Applications of the different types of penalty parameters can be found in recent publications that show with numerical results backed by mathematical theorems, that all penalty parameters mentioned above are effective in enforcing constraints in computing frequency parameters (Ilanko 2002a; 2005b), critical loads (Ilanko 2003), linear systems of equations (Askes and Ilanko 2006) and in linear stress analysis (Ilanko 2005a). However, all illustrative examples used in the above publications were simple structures. In this thesis, the implementation of the various penalty methods for more complex problems is investigated.

As mentioned earlier, the procedure used to develop the set of admissible functions used in the RRM in this thesis, built by a cosine series and a second order polynomial is presented in the next chapter.

Chapter 2

New Set of Admissible Functions for a Free-Free Beam

2.1 Introduction

The purpose of this work is to present a general procedure to solve vibration and buckling problems of structural elements such as Euler-Bernoulli beams, thin plates and shallow shells with any kind of boundary conditions using the RRM together with the Penalty Function Method. Thus, it would prove very convenient to define a set of admissible functions that adequately models completely free structural elements (beam, plate and shell), allows the use of several penalty parameters and does not have a limit in the number of terms that can be used in the series due to ill-conditioning and at the same time converges with a relatively small number of terms.

In the past some researchers gave guidelines to develop sets of admissible functions such as the ones given in (Oosterhout *et al.* 1995) as follows:

a) the set of functions must be complete in energy form (all modes of vibration must be represented and no modes must be missing),

b) the set of functions must be linearly independent,

c) the functions must satisfy boundary conditions and

d) the functions must have derivatives at least up to half of the order of the partial differential equation. In all problems solved in this work it is necessary to build the stiffness matrix of the structural elements, which in all cases presented in this work includes derivatives up to the second order with respect to the same variable.

As mentioned in Chapter 1, it is possible to build sets of admissible functions with any kind of elementary functions including simple polynomials, transcendental functions and a combination of both.

Simple polynomials have a severe limitation on the number of terms that can be included in the solution before an ill-conditioning problem arises. Other sets of admissible functions built by orthogonal polynomials using the Gram-Schmidt process presented in (Bhat 1985) have proved to give excellent results for plates involving free edges (Yuan and Dickinson 1992a). This procedure has been used to build sets of admissible functions by many researchers, even though some criticism of this work was raised in (Brown and Stone 1997), where it is stated that the convergence of a vibration problem is independent of the selection of the set of admissible functions (no need for orthogonal polynomials is suggested) and that it depends only on the degree of the polynomial represented in the set. In the same work Brown and Stone stated that for plate problems orthogonality of the functions should be targeted only on the second derivative of the functions, although they also recognized that special polynomials are only needed if higher

order polynomials are included in the set of admissible functions. This is to make the set of functions more stable with respect to inversion and the extraction of eigenvalues of the resulting stiffness and mass matrices, although in (Li 2004) it has been reported that even when orthogonal polynomials are used in the RRM, the higher order polynomials become numerically unstable due to round-off errors.

Transcendental functions also have some disadvantages. For instance, certain sets of admissible functions built by trigonometric functions have limitations converging when penalty parameters are included in the solution (Li and Daniels 2002). Further more, Fourier series can be used as set of admissible functions only for some cases with simple boundary conditions (Li 2004). Sets of functions using trigonometric and hyperbolic functions are very complex and are likely to become numerically unstable when several terms are used in the solution. This was noticed by Blevins (2000) who recommends using a high degree of precision when high modes are included, as well as by Jaworski and Dowell (2008) who used trigonometric and hyperbolic functions to solve vibration problems of beams with multiple steps using a set of functions for clamped-free beams. Jaworski and Dowell (2008) reported that numerical problems arise due to the difference between the values of the hyperbolic functions. In (Jaworski and Dowell 2008) the set of admissible functions built by trigonometric and hyperbolic functions was substituted by an approximation in higher modes with a combination of sine, cosine and exponential functions as previously used by Dowell (1984).

In contrast with all the previous options to build sets of admissible functions, several publications including (Li 2000; Li 2004; Zhou 1996), have shown that when polynomials and trigonometric functions are used to build sets of admissible functions, the solutions have a fast convergence rate and results are also accurate for higher modes. Although it is known that only the sum of the series of the functions should satisfy the boundary conditions (Budiansky and Hu 1946), many researchers have proposed to build sets of functions starting with a series containing trigonometric and polynomial functions, but enforcing boundary conditions for each term. This approach was used in (Li 2000; Li 2004; Zhou 1996).

As mentioned earlier Li (2002) built a series of admissible functions mixing polynomials and trigonometric functions. Li stated that the polynomials are introduced to take all the relevant discontinuities with the original displacement and its derivatives at the boundaries.

It is important to remember that high order polynomials are the cause of numerical instabilities and ill-conditioning. Thus to keep the solution as simple as possible and free of numerical problems the minimum number of polynomial functions with the lowest order possible are included in the set of admissible functions presented in this work.

As the main purpose of this work is to study the use of penalty parameters, a set of functions that converges rapidly and allows the use of a large number of functions without causing ill-conditioning should be used. For this reason, the set of

admissible functions to be used in this work was chosen to be a combination of polynomials and trigonometric functions.

2.2 Building a set of admissible functions

In this work, the first step to build a set of admissible functions combining trigonometric and simple polynomials is to select the trigonometric function.

Sine functions are used as a set of functions to exactly model simple supported structures as they constrain the displacement at both ends of the structure, while rotation is allowed. On the other hand, cosine functions constrain rotation and allow translation, modelling sliding structures also in an exact way. Sliding condition is very useful when symmetry is used to model symmetrical modes using half of the structure.

In (Budiansky and Hu 1946) Lagrangian multipliers were implemented in the RRM to constrain edges of a plate. Budiansky and Hu showed that the rate of convergence of the RRM together with the Lagrangian Multiplier Method is faster when a cosine series is used to build the set of admissible functions together with translational constraints to model clamped conditions than the combination of a set of admissible functions built by sine series and rotational constraints.

Similarly, in (Li 2002) a comparison of the convergence of the RRM with admissible functions built by either a sine or a cosine series plus a polynomial is also presented. In (Li 2002) convergence rates for most boundary conditions were also found to be faster using cosine series than sine series. As expected, in this

work by Li, sine series have their fastest rate of convergence for simple supported conditions, while cosine series have their fastest rate of convergence for sliding conditions. In these cases they represent exact modes if the beams are uniform and have no discontinuities.

For this reason, cosine series were selected in this work to build the set of admissible functions of a free-free beam. The cosine series used in this work is defined as

$$\cos\left(\frac{i\pi x}{L}\right), \qquad \text{for} \qquad i = 0,1,2\ldots n \tag{2.1}$$

where x is the axial coordinate of the beam, L is the beam length and n is the number of terms included in the set of admissible functions.

Now, it is only necessary to define the simple polynomials in terms of the coordinate system that should be used in the set of admissible functions together with the cosine series. This can be started knowing that the series must include the rigid-body modes of the beam and as mentioned earlier that the set of admissible functions should satisfy the boundary conditions as a whole series and not individually.

Then, the two rigid-body modes of a beam should be represented by a unit function and a linear function as in (Bassily and Dickinson 1975; Warburton 1954; Zhou 1996). The unit term releases the translational rigid-body mode and the linear term releases a rotational rigid-body mode. It is important to note that the unit function is already included in the cosine series for $i = 0$, although for simplicity the unit function will be used in the notation.

Next, by inspection it is observed that to satisfy all possible combinations of boundary conditions it is only necessary to add one more function that allows a second non-zero slope at one of the ends of the beam. Thus, a square term is added to the set of functions, because it is the lowest order polynomial that can be added to the series.

This completes the set of admissible functions $\phi_i(x)$ used in this work that it is defined as

$$\phi_i(x)=1 \qquad \text{for} \qquad i=1 \tag{2.2a}$$

$$\phi_i(x)=\left(\frac{x}{L}\right) \qquad \text{for} \qquad i=2 \tag{2.2b}$$

$$\phi_i(x)=\left(\frac{x}{L}\right)^2 \qquad \text{for} \qquad i=3 \tag{2.2c}$$

$$\phi_i(x)=\cos\frac{(i-3)\pi x}{L} \qquad \text{for} \qquad i=4,5,\ldots n \tag{2.2d}$$

The set of admissible functions given in Eqs. (2.2a)-(2.2d) are used in the RRM to model the transverse deflection of the beam as

$$w(x,t)=W(x)\sin(\omega t), \tag{2.3a}$$

where $W(x)$ is the amplitude of the deflection of the neutral axis of the beam defined as

$$W(x)=\sum_{i=1}^{n} c_i\phi_i(x), \tag{2.3b}$$

where c_i are arbitrary coefficients.

A very important property of the Fourier series is that they are nominally orthogonal functions with respect to each other. This property can be defined for cosine functions with the following relationship (Szilard 2004):

$$\int_0^L \cos\frac{i\pi x}{L}\cos\frac{j\pi x}{L}dx = \begin{cases} 0 & for \quad i \neq j \\ L/2 & for \quad i = j \end{cases} \quad \text{and} \quad (2.4)$$

A similar relationship applies for sine series. A property of orthogonal functions is that their first and second derivatives are also orthogonal (Szilard 2004). This property is very useful to obtain the terms of the elastic stiffness, geometrical stiffness and mass matrices of beams, plates and shells, as when a set of orthogonal functions are used in the RRM the mass and elastic stiffness matrices of the structural element are diagonal matrices. However, if a good set of admissible functions is chosen, off-diagonal terms will be relatively small (Mukhopadhyay 2008). In the present work, the stiffness matrix of a free-free beam element is diagonal with the first two terms equal to zero, while the mass matrix of a beam has off-diagonal terms only in the first three rows and columns, corresponding to the terms that involve the linear and square functions. This is because the linear and square functions are not orthogonal with respect to any other function of the set. However the non-zero second derivative of the series would be orthogonal as suggested by (Brown and Stone 1997). Thus, the stiffness matrix of a beam derived with the present set of admissible functions results in a diagonal matrix, although the values of the first two terms in the main diagonal are zero.

In the cases of a completely free plate and a completely free shallow-shell modelled by the set of admissible functions given in Eqs. (2.2a)-(2.2d) the stiffness and the mass matrices are sparse.

Furthermore, even though neither orthogonalization nor orthonormalization is carried out to define the set of admissible functions used in this work, no ill-conditioning was found in any case due to the number of terms used in the series.

The set of functions given in Eqs. (2.2a)-(2.2d) as was done by Li in (2000; 2004) use a cosine series and a polynomial. The main difference between the present approach and those in (Li 2000; Li 2004) is that even though the structures could be defined to be completely free in the work by Li, admissible functions were still obtained solving for boundary conditions of a structure with elastic boundary supports. This appears to have led Li to the conclusion that the set of functions must include polynomials of at least fourth order, while in this work these functions are built by the terms of a simple second order polynomial.

Next, a comparison between the present set of admissible functions with the Legendre polynomials is carried out to show that these two sets of admissible functions model a free-free beam.

The Legendre polynomials are obtained starting from a simple polynomial with the lowest degree that satisfies the boundary conditions of the problem and obtaining the rest of the polynomials using the Gram-Schmidt orthogonalization

process (Oosterhout *et al.* 1995). The Legendre polynomials have been used to solve vibration problems of completely free plates (Oosterhout *et al.* 1995).

The Legendre polynomials are defined by the following Rodrigues formula (Garcia 1994):

$$P_n(x) = \frac{1}{2^n n!}\left(\frac{d}{dx}\right)^n \left(x^2 - 1\right)^n \tag{2.5}$$

Then the first six polynomials are

$$P_0(x) = 1, \tag{2.6a}$$

$$P_1(x) = x, \tag{2.6b}$$

$$P_2(x) = \frac{1}{2}\left(3x^2 - 1\right), \tag{2.6c}$$

$$P_3(x) = \frac{1}{2}\left(5x^3 - 3x\right), \tag{2.6d}$$

$$P_4(x) = \frac{1}{8}\left(35x^4 - 30x^2 + 3\right) \quad \text{and} \tag{2.6e}$$

$$P_5(x) = \frac{1}{8}\left(63x^5 - 70x^3 + 15x\right) \tag{2.6f}$$

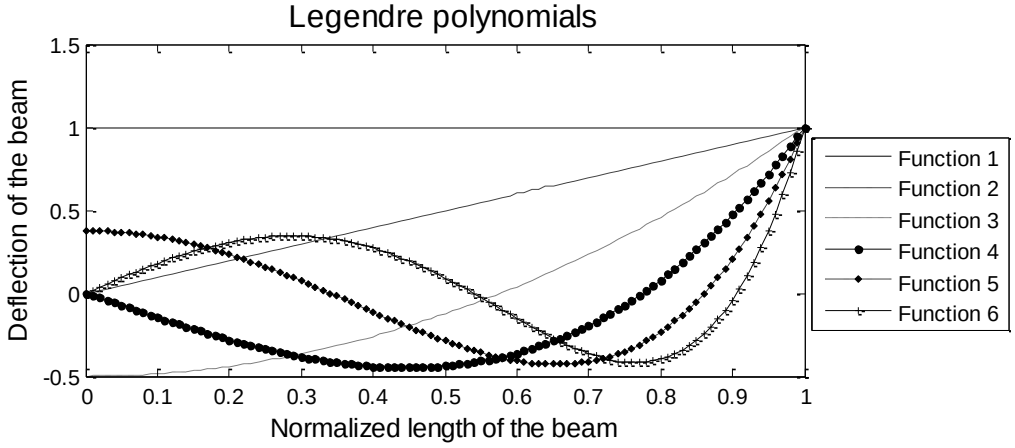

Figure 2.1. First six Legendre polynomials.

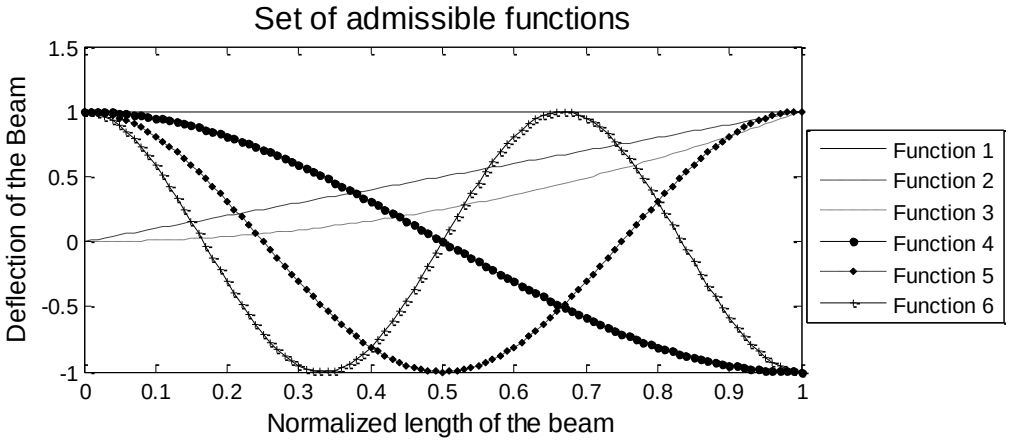

Figure 2.2. First six admissible functions of the present work.

Comparing Eqs. (2.2a) and (2.2b) with Eqs. (2.6a) and (2.6b), it is obvious that the first two functions of both the Legendre polynomials and the set of admissible functions developed in this work are identical. This can also be observed in Figs. 2.1 and 2.2.

Furthermore the third function in both sets is a square function (the function in the Legendre polynomials is a linear combination of a square term and a constant, both of which appear in the proposed set); while the following functions of both series add a nodal point to the previous function. This makes clear that not all functions satisfy the free boundary conditions at both ends, but as stated in (Budiansky and Hu 1946) and mentioned earlier in this work, the boundary conditions do not have to be satisfied individually by the functions in the set of admissible functions, but by the expansion of the whole set of admissible functions.

To further clarify the role of the functions on the boundary conditions at the ends of the beam, the manner in which the boundary conditions at both ends of the beam are satisfied by the set of admissible functions as a whole is explain below

$\phi_i(0) \neq 0$ This condition is satisfied by Eqs. (2.2a) and (2.2d),

$\phi_i(L) \neq 0$ All functions included in the set defined in Eqs. (2.2a)-(2.2d) satisfy this condition,

$\left.\frac{\partial \phi_i}{\partial x}\right|_{x=0} \neq 0$ This condition is only satisfied by the linear term defined in Eq. (2.2b) and

$\left.\frac{\partial \phi_i}{\partial x}\right|_{x=L} \neq 0$ This condition is satisfied by the liner and square terms defined in Eqs. (2.2b) and (2.2c).

The argument above shows that the proposed set of admissible functions is a complete set, which models the deflection of a free-free beam.

In the following chapter the set of admissible functions shown in Eqs. (2.2a)-(2.2d) are used in the RRM together with the Penalty Function Method to solve vibration problems of Euler-Bernoulli beams.

Chapter 3

Free Vibration of Beams

3.1 Introduction

The Euler-Bernoulli beam is the first structural element analyzed in this work. Beams are one of the most common structural members in mechanical, aerospace, civil and other engineering applications. Numerous researchers have described different approaches of the RRM and other methods to obtain the natural frequencies, modes of vibrations and critical loads of this structural element. This includes among others the work by Klein (1974) who solved problems of tapered beams inter-connecting substructures with Lagrangian multipliers in the RRM and FEM; the work by Yuan and Dickinson (1992b) who published a method to inter-connect beams using artificial springs in the RRM; the work by De Rosa and Auciello (1996) who solved the vibration problem of tapered beams with flexible ends (using translational and rotational springs) solving the equation of motion using Bessel equations; and an extensive description of existing methods and results of vibration of beams (Karnovsky and Lebed 2000; 2004).

In this chapter, as mentioned earlier, the RRM together with the Penalty Function Method are used to solve vibration problems of beams.

Throughout the years, several beam theories have been developed taking different effects into account. In this work, beams are only modelled with the Euler-Bernoulli theory, which suits slender beams subjected to bending stresses only (Karnovsky and Lebed 2004). The Euler-Bernoulli theory is based on the following assumptions (Rao 2007):

a) the beam is initially straight and unstressed,
b) the material of the beam is homogeneous and isotropic, the elastic limit is never exceeded and the Young's modulus is the same in tension and compression.
c) the length of the beam is at least ten times larger than the depth and deflections are small compared to the depth,
d) effects of rotary inertia are neglected,
e) angular distortion due to shear is considered negligible compared to bending deformation and rotation of cross-sections is neglected compared to translation,
f) plane sections that are perpendicular to the longitudinal axis of the beam before bending remain so after bending and
g) the neutral axis of the beam remains unstrained after bending.

The equation of motion of a uniform Euler-Bernoulli beams as given by (Mukhopadhyay 2008) is

$$\frac{\partial^2}{\partial x^2}\left[EI\frac{\partial^2 w}{\partial x^2}\right]+\rho A\frac{\partial^2 w}{\partial t^2}=0, \qquad 0<x<L \tag{3.1}$$

where w is the transverse deflection, E is the Young's modulus, A is the cross-sectional area of the beam, I is the second moment of area, ρ is the density of the material of the beam and t is time.

Other beam models are the Bress-Timoshenko theory that takes into account bending, shear deformation, rotary inertia and their joint contribution; the Rayleigh theory for beams under bending and shear; and the Love theory for beams that takes into account individual contributions of shear deformation, bending and rotary inertia (Karnovsky and Lebed 2004).

3.2 Theoretical derivations

The procedure using the RRM and penalty parameters to solve vibration problems of beams with all types of boundary conditions proposed in this work is described below. The matrices of a standard beam element used to obtain results with the FEM are given in Appendix A, whilst the procedure to obtain results using the RRM together with the Lagrangian Multiplier Method is briefly described in Appendix B.

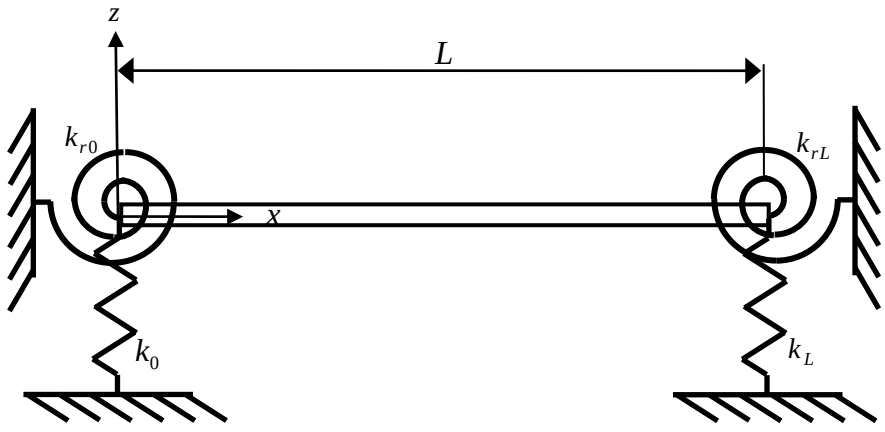

Figure 3.1. Beam of length L with artificial translational springs (k_0 and k_L) and artificial rotational springs (k_{r0} and k_{rL}).

Consider an Euler-Bernoulli beam of constant cross-section with elastic translational and rotational supports as shown in Fig. 3.1. The set of admissible functions presented in Chapter 2 are used in the RRM to solve all beam problems in this chapter. This set of functions can be rewritten as

$$\phi_i(x) = \left(\frac{x}{L}\right)^{i-1} \qquad \text{for} \quad i = 1, 2 \text{ and } 3 \tag{3.2a}$$

$$\phi_i(x) = \cos\frac{(i-3)\pi x}{L} \qquad \text{for} \quad i = 4 \text{ to } n, \tag{3.2b}$$

where x is the axial coordinate of the beam, L is the beam length and n is the number of terms in the series.

The amplitude of deflection of the neutral axis of the beam $W(x)$ can be expressed in terms of the admissible functions:

$$W(x) = \sum_{i=1}^{n} c_i \phi_i(x), \tag{3.3}$$

where c_i are arbitrary coefficients.

The maximum potential energy of an Euler-Bernoulli beam is given by

$$V_{max} = \frac{EI}{2}\int_0^L \left(\frac{\partial^2 W}{\partial x^2}\right)^2 dx \tag{3.4}$$

The maximum kinetic energy of an Euler-Bernoulli beam is given by

$$T_{max} = \frac{\omega^2}{2}\rho A\int_0^L W^2 dx \ , \tag{3.5}$$

where ω is the natural circular frequency

The maximum kinetic energy function Ψ_{max} is then given by

$$\Psi_{max} = T_{max} / \omega^2 \tag{3.6}$$

In this thesis the amplitude of deflection of all types of structures W is always defined for completely free conditions and each constraint condition not satisfied by the set of admissible functions needs to be incorporated through the use of penalty functions. In vibration problems, this may be achieved by including an energy term associated with an artificial spring of large stiffness or an inertial penalty parameter into the kinetic energy function.

Then, the strain energy of artificial translational and rotational springs of very large stiffness k_x and k_{rx} at a point x is given by

$$V_s = \frac{k_x}{2} W^2 \Big|_x + \frac{k_{rx}}{2} \left(\frac{\partial W}{\partial x} \right)^2 \Bigg|_x \tag{3.7a}$$

For instance, for a clamped-clamped beam, four penalty functions (artificial springs) are necessary to enforce the constraints (see Fig. 3.1). These include translational constraints at $x = 0$ and $x = L$ as well as rotational constraints at $x = 0$ and $x = L$ as follows:

$$V_s = \frac{k_0}{2} W^2 \Big|_{x=0} + \frac{k_L}{2} W^2 \Big|_{x=L} + \frac{k_{r0}}{2} \left(\frac{\partial W}{\partial x} \right)^2 \Bigg|_{x=0} + \frac{k_{rL}}{2} \left(\frac{\partial W}{\partial x} \right)^2 \Bigg|_{x=L}, \tag{3.8a}$$

where the stiffness coefficients k_0, k_L, k_{r0} and k_{rL} serve as penalty parameters.

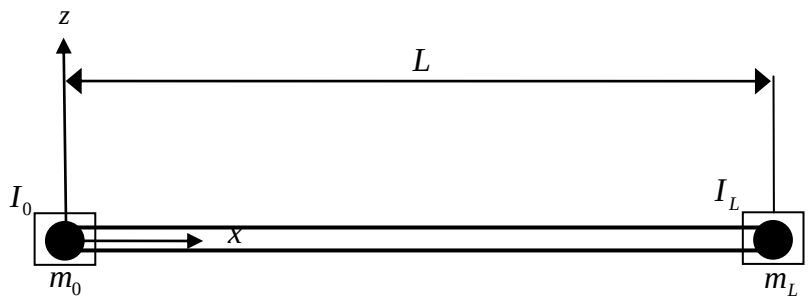

Figure 3.2. Beam of length L with artificial masses (m_0 and m_L) and artificial moments of inertia (I_0 and I_L).

Similarly, if artificial masses and moments of inertia as shown on Fig. 3.2 substitute artificial stiffness to model constraints, the kinetic energy of the artificial masses is

$$T_m = \frac{\omega^2}{2}\left(m_x W^2\Big|_x + I_x\left(\frac{\partial W}{\partial x}\right)^2\Bigg|_x \right), \tag{3.7b}$$

where m_x and I_x are the artificial mass and moments of inertia of large value at a point x.

Thus, for a clamped-clamped beam artificial masses and moments of inertia m_0, m_L, I_0 and I_L as shown in Fig, 3.2, respectively substitute the translational and rotational stiffness coefficients k_0, k_L, k_{r0} and k_{rL} in Fig. 3.1 and Eq. (3.8a). Then, for this case the kinetic energy of the artificial masses is

$$T_m = \frac{\omega^2}{2}\left(m_0 W^2\Big|_{x=0} + m_L W^2\Big|_{x=L} + I_0\left(\frac{\partial W}{\partial x}\right)^2\Bigg|_{x=0} + I_L\left(\frac{\partial W}{\partial x}\right)^2\Bigg|_{x=L} \right), \tag{3.8b}$$

where the coefficients m_0, m_L, I_0 and I_L serve as penalty parameters.

It should be noted that only the necessary penalty terms to model the chosen set of boundary conditions should be included in the solution and that Eqs. (3.7a) and (3.7b) can be used to add translational and/or rotational constraints at any point along the beam.

The stiffness matrix $\mathbf{K}$, the mass matrix $\mathbf{M}$ and the penalty matrices $\mathbf{P}_s$ (for artificial springs) or $\mathbf{P}_m$ (for artificial inertia) are obtained by applying the Rayleigh-Ritz minimization to the conservative system.

If artificial stiffness is used to model constraints, the minimization is defined as

$$\left(\frac{V_{max}}{\partial c_i}+\frac{V_s}{\partial c_i}\right)-\omega^2\frac{\Psi_{max}}{\partial c_i}=0 \qquad \text{or} \tag{3.9a}$$

if artificial inertia is used to model constraints, the minimization is defined as

$$\frac{V_{max}}{\partial c_i}-\omega^2\left(\frac{\Psi_{max}}{\partial c_i}+\frac{\Psi_m}{\partial c_i}\right)=0\,, \tag{3.9b}$$

where

$$\Psi_m=\frac{T_m}{\omega^2}\,, \tag{3.10}$$

is the kinetic function of the artificial inertia.

The minimisation is carried out by partially differentiating the total energy functional given in either Eq. (3.9a) or Eq. (3.9b) w.r.t. the unknown coefficients c_i. This would be a minimum for cases when positive penalty parameters are used. In cases where negative parameters are used the matrix may not be positive definite, but this "minimization" should still give a minimum in the restricted

domain where all available eigenvectors are orthogonal, which eliminates the unstable modes.

To present the results in non-dimensional form, the stiffness and the mass matrices are non-dimensionlized introducing a non-dimensional axial coordinate and dividing the stiffness matrix by EI / L^3 and the mass matrix by ρAL

- non-dimensional axial coordinate

$$\xi = x / L , \tag{3.11}$$

Furthermore, the penalty matrices are also non-dimensionalized introducing non-dimensional penalty parameters as follows:

- non-dimensional stiffness of the artificial springs

$$\hat{k} = \frac{k_x L^3}{EI} = \frac{k_{rx} L}{EI} , \tag{3.12a}$$

- non-dimensional artificial inertial parameters

$$\hat{m} = \frac{m_x}{\rho AL} = \frac{I_x}{\rho AL^3} . \tag{3.12b}$$

The non-dimensional eigen-problem obtained after the Rayleigh-Ritz minimization using artificial springs is

$$\left[\mathbf{K} + \mathbf{P}_s\right]\{\mathbf{c}\} - \lambda^4 \left[\mathbf{M}\right]\{\mathbf{c}\} = \{\mathbf{0}\} \tag{3.13a}$$

Similarly, the non-dimensional eigen-problem obtained after the Rayleigh-Ritz minimization using artificial inertia is

$$\left[\mathbf{K}\right]\{\mathbf{c}\} - \lambda^4 \left[\mathbf{M} + \mathbf{P}_m\right]\{\mathbf{c}\} = \{\mathbf{0}\}, \tag{3.13b}$$

where λ is the non-dimensional frequency parameter defined as (Ilanko and Dickinson 1999)

$$\lambda = \sqrt[4]{\frac{\rho A L^4 \omega^2}{EI}} \tag{3.14}$$

The non-dimensional stiffness, mass and penalty matrices of beams are presented below in a notation that will allow comparison of these matrices with their counterparts for plates and shells. Then, the mass, stiffness and penalty matrices of a beam can be defined as

$$\mathbf{K} = \mathbf{E}_{ki}^{(2,2)}, \tag{3.15}$$

$$\mathbf{M} = \mathbf{E}_{ki}^{(0,0)}, \tag{3.16}$$

where

$$\mathbf{E}_{ki}^{(r,s)} = \int_0^1 \left(\frac{d^r \phi_k}{d\xi^r} \right) \left(\frac{d^s \phi_i}{d\xi^s} \right) d\xi ,$$

$k,i = 1,2,3\ldots n$ and $r,s = 0,2$

$$\mathbf{P}_s = \hat{k} \left(\phi_k(0)\phi_i(0) + \phi_k(1)\phi_i(1) + \frac{\phi_k(0)}{\partial\xi}\frac{\phi_i(0)}{\partial\xi} + \frac{\phi_k(1)}{\partial\xi}\frac{\phi_i(1)}{\partial\xi} \right), \tag{3.17a}$$

$$\mathbf{P}_m = \hat{m} \left(\phi_k(0)\phi_i(0) + \phi_k(1)\phi_i(1) + \frac{\phi_k(0)}{\partial\xi}\frac{\phi_i(0)}{\partial\xi} + \frac{\phi_k(1)}{\partial\xi}\frac{\phi_i(1)}{\partial\xi} \right) \tag{3.17b}$$

From Eqs. (3.17a) and (3.17b) it can be observed that if $\hat{k} = \hat{m}$, then $\mathbf{P}_s = \mathbf{P}_m$.

3.3 Results and discussion

The natural frequency parameters for beams with classical boundary conditions free (F), simple supported (S) and clamped (C); as well as sliding (G) conditions are presented here. Constraints in this chapter are only defined at the ends of the beam. Intermediate constraints are treated in Chapter 7, where the methodology to solve buckling problems of tapered beams is presented.

In all beam cases presented in this chapter, the values given in (Karnovsky and Lebed 2000) are used for comparison and in some cases results using the FEM and the RRM together with Lagrangian multipliers are also included.

The last two methodologies and the method presented in this work were solved in the program MATLAB, using the command “eig” to extract the eigenvalues and eigenvectors of the eigen-problem defined by Eq. (3.13a) or Eq. (3.13b).

To identify the various support cases, two letters were used to denote the boundary conditions at the two ends of the beam. For instance, FF indicates free-free beam.

In all cases including restraints in this and all other chapters, all the penalty parameters used in translational or rotational degrees of freedom were defined with the same non-dimensional value. Similarly, in all cases presented in this and other chapters positive and negative inertial and stiffness type penalty terms were used in each case, although only the results of selected penalty parameters are presented throughout this work.

As mentioned before, in problems involving penalty parameters, the monotonic convergence property was used as a test to recognise numerical instabilities in the modes presented for all beams, plates, shells, as well as structures built by more than one structural element. A second test to avoid numerical instabilities is the use of the property described in (Ilanko and Williams 2008) that states that the eigenvalues of a constrained system can be bracketed by eigenvalues of systems

where the constraints were substituted by a pair of positive and negative penalty parameters of the same type and absolute value.

3.3.1 Frequency parameters of FF beams

Convergence with respect to discretisation (the number of terms) was investigated modelling a FF beam. The results for a FF beam using the proposed set of admissible functions give two zero frequency parameters corresponding to a rigid-body translation and a rigid body rotation. Furthermore, irrespective of the number of functions used, the last two frequency parameters were found to deviate significantly from the exact results for any number of terms in the series. The rest of the results were very close to the exact natural frequencies of the beam.

A minimum of five terms of the admissible functions must be included to obtain a good approximation to the first non-zero natural frequency of a FF beam, although a larger number of terms will in general increase the accuracy of the solution, converging from above (Williams 1987).

Table 3.1 gives the results for the first five non-zero natural frequency parameters of a FF beam obtained with the procedure proposed in this work together with the results by Karnovsky and Lebed (2000) obtained from exact frequency equations. Thus, Table 3.1 does not include the two zero frequencies of the FF beam representing the rigid-body modes and shows how the accuracy of the solution increases as the number of terms increases. For example, the first two non-zero frequency parameters obtained using 6 terms in the series match the results given

by Karnovsky and Lebed (2000) only up to the third significant number, while results using 50 terms matched the results given by Karnovsky and Lebed for the first five non-zero frequencies up to the ninth significant figure although the results presented here only show six figures.

Table 3.1. Frequency parameters of FF beams using the RRM.

Number of terms	Mode number				
	3	4	5	6	7
4	5.1800	9.0587	N/A	N/A	N/A
5	4.7307	9.0587	13.1006	N/A	N/A
6	4.7307	7.8578	13.1006	17.2090	N/A
7	4.7301	7.8578	11.0079	17.2090	21.3524
8	4.7301	7.8535	11.0079	14.1601	21.3524
9	4.7300	7.8535	10.9968	14.1601	17.3141
10	4.7300	7.8533	10.9968	14.1402	17.3141
11	4.7300	7.8533	10.9958	14.1402	17.2844
12	4.7300	7.8532	10.9958	14.1378	17.2844
15	4.7300	7.8532	10.9956	14.1373	17.2792
25	4.7300	7.8532	10.9956	14.1372	17.2788
36	4.7300	7.8532	10.9956	14.1372	17.2788
50	4.7300	7.8532	10.9956	14.1372	17.2788
100	4.7300	7.8532	10.9956	14.1372	17.2788
150	4.7300	7.8532	10.9956	14.1372	17.2788
200	4.7300	7.8532	10.9956	14.1372	17.2788
250	4.7300	7.8532	10.9956	14.1372	17.2788
300	4.7300	7.8532	10.9956	14.1372	17.2788
1000	4.7300	7.8532	10.9956	14.1372	17.2788
*	4.7300	7.8532	10.9956	14.1372	17.2788

*Results given in (Karnovsky and Lebed 2000)

Investigation of round-off errors was carried out by comparing the results using 4, 5, 6, 7, 8, 9, 10, 11, 12, 15, 25, 36, 50, 100, 150, 200, 250, 300 and 1000 terms. Although in general results converged monotonically from above, there were exceptions as the number of terms increased. These appear to be due to round-off errors which could be detected only if more than eleven decimals were recorded. The first round-off error appears on the fourteenth decimal of the second non-zero natural frequency parameter obtained using eleven terms in the series.

Results using the FEM also did not always converge monotonically from above. This is possibly due to round-off errors. Monotonic convergence of the results obtained with the FEM was interrupted as soon as three elements were used in the solution. The first mode that seems to be affected by round-off errors using three elements was the first non-zero frequency and as an element is added to the solution, the first mode in which the monotonic convergence is interrupted moves one place towards higher modes till 16 elements are used. After this, results with round-off errors move faster to higher modes.

The error always appeared in the fourth significant figure for cases using three to thirteen elements. Round-off errors in the ninth significant figure were also found in the fundamental frequency for the case using 200 terms. Some other less significant round-off errors (in higher order frequencies) were also noticed in the results obtained to build Table 3.2.

Table 3.2. Frequency parameters of FF beams using the FEM.

Number of elements	Number of DOF	Mode number				
		3	4	5	6	7
1	4	5.1800	9.5735	N/A	N/A	N/A
2	6	4.7353	8.3772	13.2469	16.7436	N/A
3	8	4.7365	7.8735	11.6608	15.6229	21.7398
4	10	4.7326	7.8776	11.0390	14.9429	18.6982
5	12	4.7312	7.8657	11.0485	14.2074	18.2256
8	16	4.7302	7.8555	11.0072	14.1748	17.3708
12	26	4.7301	7.8537	10.9981	14.1457	17.3013
16	34	4.7301	7.8534	10.9964	14.1400	17.2863
24	50	4.7300	7.8532	10.9958	14.1377	17.2803
49	100	4.7300	7.8532	10.9956	14.1372	17.2789
74	150	4.7300	7.8532	10.9956	14.1372	17.2788
99	200	4.7300	7.8532	10.9956	14.1372	17.2788
124	250	4.7300	7.8532	10.9956	14.1372	17.2788
149	300	4.7300	7.8532	10.9956	14.1372	17.2788
499	1000	4.7300	7.8532	10.9956	14.1372	17.2788
	*	4.7300	7.8532	10.9956	14.1372	17.2788

*Results given in (Karnovsky and Lebed 2000).

By comparing Tables 3.1 and 3.2 it may be seen that the RRM converges faster than the FEM. For example, with only nine terms the first non-zero frequency parameter obtained using the RRM converges to the exact results up to the fifth significant figure, while using the FEM more than 34 DOF are needed to achieve the same accuracy. However, it should be noted that the mass and stiffness matrices have a smaller band in the FEM than in the RRM.

3.3.2 Frequency parameters of CC beams using 250 terms

Convergence due to the value of the penalty parameter was investigated comparing the results for CC beams using 250 terms with different penalty values. Results for penalty parameters of stiffness type are presented in Tables 3.3 and 3.4 for positive and negative values, respectively. Similarly results for penalty parameters of inertial type are presented in Tables 3.5 and 3.6 for positive and negative values, respectively. Results given in (Karnovsky and Lebed 2000), as well as results obtained using the RRM together with Lagrangian Multiplier Method and the FEM were used for comparison, in both cases using 246 DOF.

For both stiffness and inertial penalty parameters, calculations with several values of the series $\pm 10^{p}$ were computed, where $p \in [0,1,2,3,...]$. True upper-bound solutions are obtained using negative stiffness and positive inertial penalty parameters (Ilanko 2002a; Ilanko 2005b), while the constrained solutions obtained using positive stiffness and negative inertial penalty parameters are upper bound solutions (w.r.t. discretisation) to a lower bound model (w.r.t. constraints).

Results in Tables 3.3 and 3.4 show that the first frequency is the first mode to converge when penalty parameters of stiffness type are used and that as the absolute value of the penalty parameter increases, better approximations of the frequency parameters were obtained.

Table 3.3. Frequency parameters of CC beams using 250 terms and positive stiffness penalty parameters.

$\hat{k}$	Mode Number					
	1	2	3	4	5	6
10^3	4.5257	6.9195	8.7592	10.6527	13.1151	15.9743
10^4	4.7087	7.7538	10.7148	13.5033	16.0489	18.3757
10^5	4.7279	7.8433	10.9686	14.0795	17.1719	20.2396
10^6	4.7298	7.8522	10.9929	14.1315	17.2684	20.4032
10^7	4.7300	7.8531	10.9953	14.1366	17.2777	20.4187
10^8	4.7300	7.8532	10.9956	14.1371	17.2787	20.4202
10^9	4.7300	7.8533	10.9956	14.1372	17.2788	20.4204
10^{10}	4.7300	7.8526	10.9956	14.1369	17.2788	20.4203
10^{11}	4.7300	7.8624	10.9956	14.1384	17.2788	20.4200
10^{12}	4.7299	7.8351	10.9957	14.1463	17.2789	20.4163
10^{13}	4.7295	5.1446	10.9954	14.2495	17.2778	20.4551
*	4.7300	7.8532	10.9956	14.1372	17.2788	20.4204

*Results given in (Karnovsky and Lebed 2000), FEM and RRM together with Lagrangian Multiplier Method

Table 3.4. Frequency parameters of CC beams using 250 terms and negative stiffness penalty parameters.

$\hat{k}$	Mode Number					
	1	2	3	4	5	6
-10^3	4.9488	8.6122	12.1548	15.4912	18.7299	21.9248
-10^4	4.7515	7.9506	11.2456	14.6065	17.9869	21.3396
-10^5	4.7322	7.8631	11.0223	14.1930	17.3788	20.5808
-10^6	4.7303	7.8542	10.9983	14.1428	17.2891	20.4373
-10^7	4.7301	7.8533	10.9959	14.1377	17.2798	20.4221
-10^8	4.7300	7.8532	10.9956	14.1372	17.2789	20.4205
-10^9	4.7300	7.8532	10.9956	14.1372	17.2788	20.4204
-10^{10}	4.7300	7.8539	10.9956	14.1370	17.2788	20.4203
-10^{11}	4.7300	7.8637	10.9956	14.1378	17.2788	20.4207
-10^{12}	4.7301	7.8554	10.9955	14.1407	17.2788	20.4232
-10^{13}	4.7303	8.3046	10.9959	14.4403	17.2792	20.4234
*	4.7300	7.8532	10.9956	14.1372	17.2788	20.4204

*Results given in (Karnovsky and Lebed 2000), FEM and RRM together with Lagrangian Multiplier Method

Checking for solutions free of ill-conditioning through monotonic convergence test, it was observed that the best approximation of the upper and lower bound frequency parameters were found using stiffness values equal to $\pm 10^9$. Beyond these values, the calculated frequency parameters do not follow the expected monotonic convergence as the absolute value of the stiffness penalty parameter increases. This can only be explained by round-off errors associated with large penalty terms. Results with even higher stiffnesses show that results do not change drastically as would be expected in ill-conditioning, until a very high absolute value of the penalty parameter is used ($\pm 10^{13}$ or higher). With these values, results for the second frequency began to deviate significantly from the values given by Karnovsky and Lebed (2000). This shows that there is a limitation in the maximum penalty parameter value that can be used due to numerical problems. This applies to all problems analyzed in this work including beam, plate and shell elements.

Furthermore making a second test, comparing the frequency parameters given in Tables 3.3 and 3.4 obtained with stiffness penalty parameters of magnitudes of $\pm 10^9$ show that the lower bound of second frequency parameter is higher than the upper bound. This contradicts the bracketing property described in (Ilanko and Williams 2008). This can also only be explained as a round-off error as the upper bound should always be higher than the lower bound and both results should bracket the solution obtained with the Lagrangian Multiplier Method that models the constraints exactly. Computing the values of the frequencies using penalty values $8x10^8$ and $9x10^8$ gave 7.85322 and 7.85318. This shows that the results of the second frequency parameter using a penalty value of $9x10^8$ has a round-off

error (as results should monotonically increase), whilst results using penalty values of $8x10^8$ obey the monotonic convergence giving results identical to the results in (Karnovsky and Lebed 2000) up to the fifth significant figure.

Tables 3.5 and 3.6 show that when using small inertial penalty parameters in beams all the frequencies give a good approximation of the exact results. For the CC beam case all frequencies were obtained within 1% of the exact value using an inertial penalty parameter equal to 10, (i.e. a mass equal ten times that of the beam).

Although the best approximation free of ill-conditioning was obtained with an inertial penalty parameter value of 10^7, the results remained unchanged up to the fourth decimal included in Table 3.5 for the next penalty parameters (up to 10^{10}). Then the results started to change when the inertial penalty parameter reached the value 10^{11}, giving different values only on the fourth decimal place. The solution started to deviate significantly from the values given in (Karnovsky and Lebed 2000) when the penalty parameter was assigned a value of 10^{14}. In all beam cases using inertial penalty parameters, the results included two extra rigid-body frequencies (zero frequencies), because there is no restraint attached to the rigid-bodies. These extra zero frequencies are not included in the tables presented in this work.

Similar observations to the ones in the above paragraph can be made regarding Table 3.6. It is also worth to note that when negative inertial penalty parameter of

value -10^{13} is used, results already reached ill-conditioning giving infinite values for almost all modes.

Table 3.5. Frequency parameters of CC beams using 250 terms and positive inertial penalty parameters.

$\hat{m}$	Mode number					
	1	2	3	4	5	6
1	5.0631	8.0767	11.1611	14.2687	17.3878	20.5135
10	4.7715	7.8787	11.0138	14.1513	17.2903	20.4301
10^2	4.7343	7.8558	10.9974	14.1386	17.2799	20.4213
10^3	4.7305	7.8535	10.9958	14.1373	17.2789	20.4205
10^4	4.7301	7.8532	10.9956	14.1372	17.2788	20.4204
10^5	4.7300	7.8532	10.9956	14.1372	17.2788	20.4204
10^6	4.7300	7.8532	10.9956	14.1372	17.2788	20.4204
10^7	4.7300	7.8532	10.9956	14.1372	17.2788	20.4204
10^8	4.7300	7.8532	10.9956	14.1372	17.2788	20.4204
10^9	4.7300	7.8532	10.9956	14.1372	17.2788	20.4204
10^{10}	4.7300	7.8532	10.9956	14.1372	17.2788	20.4204
10^{11}	4.7300	7.8533	10.9956	14.1370	17.2787	20.4202
10^{12}	4.7300	7.8522	10.9959	14.1386	17.2791	20.4210
10^{13}	4.7364	7.8614	11.0001	14.1565	17.2844	20.4149
10^{14}	4.7300	7.9935	10.9552	14.3009	17.1401	20.4839
*	4.7300	7.8532	10.9956	14.1372	17.2788	20.4204

*Results given in (Karnovsky and Lebed 2000), FEM and RRM together with Lagrangian Multiplier Method

Table 3.6. Frequency parameters of CC beams using 250 terms and negative inertial penalty parameters.

$\hat{m}$	Mode number					
	1	2	3	4	5	6
-1	4.1160	7.5448	10.7905	13.9827	17.1547	20.3167
-10	4.6861	7.8269	10.9771	14.1228	17.2671	20.4105
-10^2	4.7258	7.8506	10.9938	14.1357	17.2776	20.4194
-10^3	4.7296	7.8529	10.9954	14.1370	17.2786	20.4203
-10^4	4.7300	7.8532	10.9956	14.1372	17.2788	20.4204
-10^5	4.7300	7.8532	10.9956	14.1372	17.2788	20.4204
-10^6	4.7300	7.8532	10.9956	14.1372	17.2788	20.4204
-10^7	4.7300	7.8532	10.9956	14.1372	17.2788	20.4204
-10^8	4.7300	7.8532	10.9956	14.1372	17.2788	20.4204
-10^9	4.7300	7.8532	10.9957	14.1372	17.2787	20.4204
-10^{10}	4.7302	7.8531	10.9957	14.1373	17.2788	20.4204
-10^{11}	4.7336	7.8545	10.9917	14.1355	17.2825	20.4203
-10^{12}	4.7446	7.8606	11.0482	14.1372	17.2628	20.3983
-10^{13}	0.0000	4.9700	INF	INF	INF	INF
*	4.7300	7.8532	10.9956	14.1372	17.2788	20.4204

*Results given in (Karnovsky and Lebed 2000), FEM and RRM together with Lagrangian Multiplier Method

Comparison of results using artificial stiffness and artificial inertia with the same type of monotonic convergence, leads to comparison of Table 3.3 (positive stiffness) against Table 3.6 (negative inertia) and of Table 3.4 (negative stiffness) against Table 3.5 (positive inertia). This shows that accuracy of the fundamental frequency is similar when the penalty value of the artificial stiffness is 1000 times larger than the value of the artificial inertia. As mentioned earlier, the fundamental frequency is the first one to converge when artificial springs are used and the last one when artificial inertia is used. Furthermore, negative artificial stiffness has critical values that give extra zero frequencies as explained earlier. For these reasons, positive inertial penalty parameters will be used in the rest of this chapter.

3.3.3 Frequency parameters of beams with classical boundary conditions using inertial penalty parameters

Table 3.7 contains the best approximations to the non-dimensional frequency parameters of beams with all combinations of classical boundary conditions using 10, 50, 250 and 1000 terms and positive inertial penalty parameters with values 10^p where $p \in [0,1,2,3,...]$. Table 3.8 presents results for cases that contain sliding conditions (denoted by G), which may be useful when symmetry is applied to a structure; sliding conditions allow lateral displacement while rotation is fixed. All results are compared only to the results given by Karnovsky and Lebed (2000).

Results using at least 250 terms in Tables 3.7 and 3.8 are the same as those published by Karnovsky and Lebed (2000) with one exception: the second frequency of the CG case using the present method is slightly lower. The

published figure by Karnovsky and Lebed (2000) is 5.4988. However, by symmetry one can deduce the CG case results from that of the CC case, where each frequency parameter for the CG case has a frequency parameter of twice the magnitude corresponding to the symmetrical modes of CC beam. Using the second symmetrical frequency parameter for the CC beam (third mode), it can be seen that the second frequency parameter for the CG beam should be 5.4978 which is the result obtained using the present method. Therefore, the correct figure is given in Table 3.7. It is believed that the figure in (Karnovsky and Lebed 2000) contains a transcription error. With this correction, there is complete agreement between the results by Karnovsky and Lebed (2000) and the present results.

For most beam cases, penalty parameters that gave the best approximations to the frequency parameters do not change as the number of terms included in the solution increased. In most cases solutions converge up to the fourth decimal place, well before the monotonic convergence is interrupted. For instance, for GG beams using positive inertial penalty parameters, a value of 10^3 is enough to get all sets of results presented in Table 3.8.

Furthermore, as mentioned for the CC beam, in beam problems, it was found that all frequencies gave good approximations to the exact result using very small inertial penalty parameter values. For instance with an inertial penalty parameter of 10 (ten times that of the beam itself) for all beam cases included in Tables 3.7 and 3.8 and for any number of terms used in this work, the first frequency has a deviation lower than 3% in comparison with the values given in (Karnovsky and

Lebed 2000). It should be emphasised here that this deviation corresponds to the first frequency, which is the last one to converge, and is therefore the worst case scenario. The results for all other frequencies present a lower deviation.

Table 3.7. Frequency parameters of beams with classical boundary conditions.

Case	$\hat{m}$	Mode number					
		1	2	3	4	5	6
SF							
10	10^6	0	3.9271	7.0716	10.2222	13.3774	16.5883
50	10^6	0	3.9266	7.0686	10.2102	13.3518	16.4935
250	10^6	0	3.9266	7.0686	10.2102	13.3518	16.4934
1000	10^6	0	3.9266	7.0686	10.2102	13.3518	16.4934
*		0	3.9266	7.0686	10.2102	13.3518	16.4934
CF							
10	10^6	1.8752	4.6958	7.8623	11.0192	14.1795	17.4005
50	10^6	1.8751	4.6941	7.8548	10.9956	14.1373	17.2791
250	10^6	1.8751	4.6941	7.8548	10.9955	14.1372	17.2788
1000	10^6	1.8751	4.6941	7.8548	10.9955	14.1372	17.2788
*		1.8751	4.6941	7.8548	10.9955	14.1372	17.2788
SS							
10	10^5	3.1422	6.2866	9.4447	12.6010	15.8510	19.0328
50	10^5	3.1416	6.2832	9.4248	12.5665	15.7082	18.8500
250	10^5	3.1416	6.2832	9.4248	12.5664	15.7080	18.8496
1000	10^5	3.1416	6.2832	9.4248	12.5664	15.7080	18.8496
*		3.1416	6.2832	9.4248	12.5664	15.7080	18.8496
SC							
10	10^6	3.9283	7.0757	10.2438	13.4047	16.6759	19.8580
50	10^6	3.9266	7.0686	10.2103	13.3520	16.4938	19.6357
250	10^6	3.9266	7.0686	10.2102	13.3518	16.4934	19.6350
1000	10^6	3.9266	7.0686	10.2102	13.3518	16.4934	19.6350
*		3.9266	7.0686	10.2102	13.3518	16.4934	19.6350
CC							
10	10^7	4.7340	7.8658	11.0472	14.2118	17.4959	20.6671
50	10^7	4.7301	7.8533	10.9958	14.1375	17.2794	20.4214
250	10^7	4.7300	7.8532	10.9956	14.1372	17.2788	20.4204
1000	10^7	4.7300	7.8532	10.9956	14.1372	17.2788	20.4204
*		4.7300	7.8532	10.9956	14.1372	17.2788	20.4204

*Results given in (Karnovsky and Lebed 2000).

Table 3.8. Frequency parameters of beams with classical and sliding boundary conditions.

Case	$\hat{m}$	Mode number					
		1	2	3	4	5	6
FG							
10	10^4	0	2.3650	5.4978	8.6395	11.7817	14.9265
50	10^4	0	2.3650	5.4978	8.6394	11.7810	14.9226
250	10^4	0	2.3650	5.4978	8.6394	11.7810	14.9226
1000	10^4	0	2.3650	5.4978	8.6394	11.7810	14.9226
*		0	2.3650	5.4978	8.6394	11.7810	14.9226
GG							
10	10^{16}	0	3.1416	6.2832	9.4248	12.5664	15.7080
50	10^9	0	3.1416	6.2832	9.4248	12.5664	15.7080
250	10^7	0	3.1416	6.2832	9.4248	12.5664	15.7080
1000	10^8	0	3.1416	6.2832	9.4248	12.5664	15.7080
*		0	3.1416	6.2832	9.4248	12.5664	15.7080
SG							
10	10^6	1.5708	4.7133	7.8584	11.0095	14.1728	17.3639
50	10^6	1.5708	4.7124	7.8540	10.9956	14.1373	17.2789
250	10^6	1.5708	4.7124	7.8540	10.9956	14.1372	17.2788
1000	10^6	1.5708	4.7124	7.8540	10.9956	14.1372	17.2788
*		1.5708	4.7124	7.8540	10.9956	14.1372	17.2788
CG							
10	10^7	2.3652	5.5005	8.6498	11.8074	14.9774	18.1666
50	10^7	2.3650	5.4978	8.6394	11.7811	14.9228	18.0645
250	10^7	2.3650	5.4978	8.6394	11.7810	14.9226	18.0642
1000	10^7	2.3650	5.4978	8.6394	11.7810	14.9226	18.0642
*		2.3650	5.4987	8.6394	11.7810	14.9226	18.0642

*Results given in (Karnovsky and Lebed 2000).

3.3.4 Concluding remarks

In this work the new set of admissible functions derived for a FF beam in Chapter 2 was implemented in the RRM to solve beam problems including classical boundary conditions as well as sliding boundary conditions. This is similar to the approach used by Amabili *et al* (1997) where the authors used an admissible function of a less constrained problem including rigid body modes and replaced the excluded constraints by elastic restraints.

In the present approach the set of admissible functions is a combination of polynomial and trigonometric functions as in (Li 2000; Zhou 1996), but the procedure used here does not require the enforcement of essential boundary conditions for each function which have instead been imposed approximately on the final solution using the Penalty Function Method. The accuracy of the solution depends on the absolute value of the penalty parameter and the number of terms used. Although there is a limit in the maximum value of the penalty parameter of any kind, for the problems presented here, the range of penalty values that give a good approximation to the exact solution is relatively large.

In this work, it was noticed that when inertial penalty parameters were used, the higher modes converged first. This is because the force of the constraint is proportional to the square of the frequency, which means that penalty against violation of higher modes, was greater for the same absolute value of the inertial penalty parameter. Therefore, inertial penalty parameters are recommended for natural frequency calculations of beams if higher modes are of interest. This may be important in acoustics. In contrast when using stiffness type penalty parameters, it has been noted (Ilanko 2002a) that the value of the artificial stiffness penalty parameter required to effect a constraint increased with the number of modes. This means that to obtain accurate frequency parameters for high frequencies a stiffness penalty parameter with higher magnitude must be defined.

In the next chapter the same procedure is used to solve vibration problems of thin rectangular plates. Results are presented only for square plates with F, S and C

conditions, although plates with a different aspect ratios or with G conditions can also be solved using the same procedure. An example of a plate with internal constraints is also presented.

Chapter 4

Free Vibration of Plates

4.1 Introduction

This chapter investigates the use of the proposed set of admissible functions in the RRM in conjunction with penalty parameters of different types to solve vibration problems of thin rectangular plates.

Several researchers have used the RRM to solve vibration problems of plates. Some relevant to this work are (Amabili et al. 1997; Bhat 1985; Leissa 1969a; Leissa 1973; Li 2004; Liew and Wang 1993; Young and Dickinson 1993; Young and Dickinson 1994; Yuan and Dickinson 1992a; Zhou 1996). These references include solutions using artificial springs to model boundary conditions and to inter-connect plate elements, plates with different geometries and discussions about different sets of admissible functions.

Plates, just as beams, are commonly used in many engineering fields and have been the subject of study by numerous researchers, probably the first to produce a mathematical model of a plate element being Euler in 1776 (Ventsel and Krauthammer 2001).

In this thesis plates are always modelled following the classical Kirchhoff's plate theory, which is based on the following assumptions:

a) the material of the plate is homogeneous and isotropic, the elastic limit is never exceeded and the Young's modulus is the same in tension and compression,
b) thin plates typically have side a to thickness h ratios in the range $8 \leq a/h \leq 100$ (plates with lower ratios classify as thick plates, while plates with higher ratios classify as membranes) and the deflection of the middle plane is also small in comparison to the thickness of the plate,
c) rotary inertia is neglected,
d) the plate is initially flat,
e) the stress normal to the middle plane is neglected,
f) plane sections perpendicular to the middle plane of the plate remain plane before and after bending and
g) the middle surface remains unstrained after bending.

These assumptions are analogous to the those listed in Chapter 3 for Euler-Bernoulli beams and reduces the plate problem from a three-dimensional problem to a two-dimensional one (Ventsel and Krauthammer 2001). The last four assumptions above are known as Kirchhoff's hypotheses (Ventsel and Krauthammer 2001)

Another relevant plate theory developed to deal with thicker and composite plates is the Reissner-Mindlin theory (also called first-order shear deformation theory) that takes into account the transverse shear deformation on the deflection of the

plate (Amabili 2008). Thus, in the Reissner-Mindlin theory straight lines perpendicular to the middle plane do not remain perpendicular after bending and instead it takes two rotational DOFs, but this theory does not satisfy the transverse shear boundary conditions at the top and bottom surfaces, due to the assumption of a constant shear angle through the thickness.

Other theories that include geometric nonlinearities based on the Kirchhoff's plate theory and the Reissner-Mindlin plate theory were developed by Von Karman (von Kármán 1910) and by Reddy (Reddy 1990), respectively as mentioned in (Amabili 2008).

4.2 Theoretical derivations

The set of admissible functions for beams presented in Chapter 2 will be used to model the deflection of a rectangular plate as shown in Fig. 4.1, with dimensions a and b along directions x and y, thickness h and flexural rigidity D defined as

$$D = \frac{Eh^3}{12\left(1-\nu^2\right)}, \tag{4.1}$$

where ν is Poisson's ratio and E is Young's modulus.

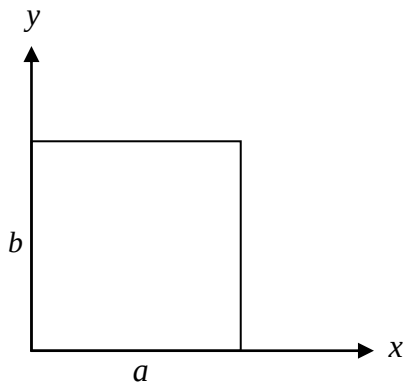

Figure 4.1. Completely free rectangular plate.

The amplitude of the deflection of the plate defined in terms of the set of admissible functions is

$$W(x,y)=\sum_{j}^{n}\sum_{i}^{n}c_{ij}\phi_i(x)\chi_j(y), \tag{4.3}$$

where c_{ij} are arbitrary coefficients.

The maximum potential energy of the plate V_{max} due to the strain energy of bending and twisting of the plate is (Oosterhout et al. 1995)

$$V_{max}=\frac{D}{2}\int_0^a\int_0^b\left[\left(\frac{\partial^2 W}{\partial x^2}\right)^2+\left(\frac{\partial^2 W}{\partial y^2}\right)^2+2\nu\frac{\partial^2 W}{\partial x^2}\frac{\partial^2 W}{\partial y^2}+2(1-\nu)\left(\frac{\partial^2 W}{\partial x\partial y}\right)^2\right]dxdy \tag{4.4}$$

The maximum kinetic energy T_{max} of the plate is (Oosterhout et al. 1995)

$$T_{max}=\frac{\rho h\omega^2}{2}\int_0^a\int_0^b W^2 dxdy, \tag{4.5}$$

The maximum kinetic energy function Ψ_{max} is given by (Oosterhout et al. 1995)

$$\Psi_{max}=T_{max}/\omega^2 \tag{4.6}$$

As explained in Chapter 2, the selected set of admissible functions are used to model the deflection of completely free structures. For this reason, in this chapter all constraint conditions are incorporated through the use of either stiffness or inertial type penalty parameters.

Then, the strain energy of translational and rotational springs along all four edges of the plate ($x=0$, $x=a$, $y=0$ and $y=b$) is defined as

$$V_{s,edge} = \frac{1}{2}\int_0^b \left(k_{x0}W^2\Big|_{x=0} + k_{xa}W^2\Big|_{x=a}\right)dy + \frac{1}{2}\int_0^a \left(k_{y0}W^2\Big|_{y=0} + k_{yb}W^2\Big|_{y=b}\right)dx$$

$$+ \frac{1}{2}\int_0^b \left(k_{rx0}\left(\frac{\partial W}{\partial x}\right)^2\Big|_{x=0} + k_{rxa}\left(\frac{\partial W}{\partial x}\right)^2\Big|_{x=a}\right)dy$$

$$+ \frac{1}{2}\int_0^a \left(k_{ry0}\left(\frac{\partial W}{\partial y}\right)^2\Big|_{y=0} + k_{ryb}\left(\frac{\partial W}{\partial y}\right)^2\Big|_{y=b}\right)dx, \qquad (4.7a)$$

where k_{x0}, k_{xa}, k_{y0} and k_{yb} are the stiffness per unit length of the translational spring supports, while k_{rx0}, k_{rxa}, k_{ry0} and k_{ryb} are the stiffness per unit length of the rotational spring supports located along the edges at $x=0$, $x=a$, $y=0$ and $y=b$, respectively. To model each of the 20 cases of plates with classical boundary conditions along the edges only the appropriate stiffness coefficients should have a non-zero value.

Springs can be used to model a constraint at a point (x, y), but in this case, no integration is necessary and both values x and y defining the location of the constraint should be substituted in the amplitude of the deflection of the plate W in the terms defining a translational constraint or a rotational constraint. For instance, the additional strain energy terms of a translational spring and rotational springs around axes x and y are

$$V_{s,point} = \frac{1}{2}k_{(x,y)}W^2\Big|_{x,y} + \frac{1}{2}k_{r(x,y)}\left(\frac{\partial^2 W}{\partial x^2}\right)\Bigg|_{x,y} + \frac{1}{2}k_{r(x,y)}\left(\frac{\partial^2 W}{\partial y^2}\right)\Bigg|_{x,y}, \qquad (4.8a)$$

where $k_{(x,y)}$ and $k_{r(x,y)}$ are the stiffness coefficients of the point translational and rotational artificial springs (assuming that both rotational springs have the same stiffness).

Similarly, if masses are used to model constraints, the maximum kinetic energy equation must include terms, similar to those in Eqs. (4.7a) and (4.8a). But in this case the energy terms contain masses per unit length m_{x0}, m_{xa}, m_{y0} and m_{yb}, and rotational inertias per unit length I_{x0}, I_{xa}, I_{y0} and I_{yb}. The maximum kinetic energy $T_{m,edge}$ of the artificial inertia to constrain the four edges of the plate in the same order as defined in Eq. (4.7a) is

$$T_{m,edge} = \frac{\omega^2}{2}\int_0^b \left(m_{x0}W^2\Big|_{x=0} + m_{xa}W^2\Big|_{x=a}\right)dy + \frac{\omega^2}{2}\int_0^a \left(m_{y0}W^2\Big|_{y=0} + m_{yb}W^2\Big|_{y=b}\right)dx$$
$$+ \frac{\omega^2}{2}\int_0^b \left(I_{x0}\left(\frac{\partial W}{\partial x}\right)^2\Big|_{x=0} + I_{xa}\left(\frac{\partial W}{\partial x}\right)^2\Big|_{x=a}\right)dy$$
$$+ \frac{\omega^2}{2}\int_0^a \left(I_{y0}\left(\frac{\partial W}{\partial y}\right)^2\Big|_{y=0} + I_{yb}\left(\frac{\partial W}{\partial y}\right)^2\Big|_{y=b}\right)dx, \qquad (4.7b)$$

The kinetic energy due to artificial point inertial parameters is

$$T_{m,point} = \frac{\omega^2}{2}\left(m_{(x,y)}W^2\Big|_{x,y} + I_{(x,y)}\left(\frac{\partial^2 W}{\partial x^2}\right)\Big|_{x,y} + I_{(x,y)}\left(\frac{\partial^2 W}{\partial y^2}\right)\Big|_{x,y}\right), \qquad (4.8b)$$

where $m_{(x,y)}$ and $I_{(x,y)}$ are the coefficients of the point artificial masses and moments of inertia (the same notation was used for both moments of inertia as they are assumed to have the same value).

Then the set of linear homogeneous equations of the system are found by minimizing the potential and kinetic energy of the plate including the energy of the artificial springs or the energy of the artificial inertia.

If artificial springs are used to model constraints the minimization is defined as

$$\left(\frac{V_{max}}{\partial c_{ij}} + \frac{V_{s,edge}}{\partial c_{ij}} + \frac{V_{s,point}}{\partial c_{ij}} \right) - \omega^2 \frac{\Psi_{max}}{\partial c_{ij}} = 0 \qquad \text{or} \qquad (4.9a)$$

if artificial inertia is used to model constraints, the minimization is defined as

$$\frac{V_{max}}{\partial c_{ij}} - \omega^2 \left(\frac{\Psi_{max}}{\partial c_{ij}} + \frac{\Psi_{m,edge}}{\partial c_{ij}} + \frac{\Psi_{m,point}}{\partial c_{ij}} \right) = 0 , \qquad (4.9b)$$

where

$$\Psi_{m,edge} = \frac{T_{m,edge}}{\omega^2} \qquad \text{and} \qquad (4.10a)$$

$$\Psi_{m,point} = \frac{T_{m,point}}{\omega^2} \qquad (4.10b)$$

To obtain results in non-dimensional form non-dimensional coordinates of the plate are introduced and the stiffness and mass matrices are non-dimensionalized by dividing them by D/ab and ρhab, respectively. Furthermore, the penalty matrices are also non-dimensionalized introducing non-dimensional penalty parameters. Examples for distributed penalty parameters along the edge at $x = 0$ and for point parameters at $x = y = 0$ are presented, while all other non-dimensional penalty parameters can be obtained in a similar way

- non-dimensional coordinates of the plate

  $\xi = x/a$ and $\eta = y/b$ (4.11a, 4.11b)

- non-dimensional distributed translational and rotational stiffness parameter

$$\hat{k} = \frac{k_{x0} a^3}{D} = \frac{k_{rx0} a}{D} \qquad (4.12a)$$

- non-dimensional distributed mass and inertia parameter

$$\hat{m} = \frac{m_{x0}}{\rho h a} = \frac{I_{rx0}}{\rho h a^3} \qquad (4.12b)$$

- non-dimensional translational and rotational point stiffness parameter

$$\hat{k} = \frac{k_{xy} a^2}{D} = \frac{k_{rxy}}{D} \tag{4.13a}$$

- non-dimensional point mass and inertia parameter

$$\hat{m} = \frac{m_{(x,y)}}{\rho h a b} = \frac{I_{(x,y)}}{\rho h a^2 b^2} \tag{4.13b}$$

The non-dimensional eigen-problem obtained after the Rayleigh-Ritz minimization using artificial springs is

$$\left[\mathbf{K} + \mathbf{P}_{s,edge} + \mathbf{P}_{s,point}\right]\{\mathbf{c}\} - \lambda^2 [\mathbf{M}]\{\mathbf{c}\} = \{\mathbf{0}\} \tag{4.14a}$$

Similarly, the non-dimensional eigen-problem obtained after the Rayleigh-Ritz minimization using artificial inertia is

$$[\mathbf{K}]\{\mathbf{c}\} - \lambda^2 \left[\mathbf{M} + \mathbf{P}_{m,edge} + \mathbf{P}_{m,point}\right]\{\mathbf{c}\} = \{\mathbf{0}\}, \tag{4.14b}$$

where λ is the non-dimensional frequency parameter defined as (Young and Dickinson 1993)

$$\lambda = \sqrt{\frac{\rho h a^2 b^2 \omega^2}{D}} \tag{4.15}$$

Using a notation that is consistent for beams, plates and shells, the non-dimensional version of the matrices in Eqs. (4.14a) and (4.14b) are written below.

First the non-dimensional mass and stiffness matrices of a plate are

$$\mathbf{M} = \mathbf{E}_{ki}^{(0,0)} \mathbf{F}_{lj}^{(0,0)}, \tag{4.16}$$

$$\mathbf{K} = a^2 b^2 \left[\frac{1}{a^4} \mathbf{E}_{ki}^{(2,2)} \mathbf{F}_{lj}^{(0,0)} + \frac{1}{b^4} \mathbf{E}_{ki}^{(0,0)} \mathbf{F}_{lj}^{(2,2)} \right.$$

$$+\frac{v_p}{a^2b^2}\left[\mathbf{E}_{ki}^{(0,2)}\mathbf{F}_{lj}^{(2,0)}+\mathbf{E}_{ki}^{(2,0)}\mathbf{F}_{lj}^{(0,2)}\right]+\frac{2(1-v)}{a^2b^2}\mathbf{E}_{ki}^{(1,1)}\mathbf{F}_{lj}^{(1,1)}\Bigg], \tag{4.17}$$

where $\mathbf{E}_{ki}^{(r,s)}=\int_0^1\left(\frac{d^r\phi_k}{d\xi^r}\right)\left(\frac{d^s\phi_i}{d\xi^s}\right)d\xi$, $\mathbf{F}_{lj}^{(r,s)}=\int_0^1\left(\frac{d^r\chi_l}{d\eta^r}\right)\left(\frac{d^s\chi_j}{d\eta^s}\right)d\eta$,

$k,i,l,j=1,2,3\ldots n$ and $r,s=0,1,2$

Then the non-dimensional penalty matrices due to the artificial stiffness as defined in Eqs. (4.7a,4.8a) are

$$\begin{aligned}\mathbf{P}_{s,edge}=\hat{k}\Big[&\phi_k(0)\phi_i(0)\mathbf{F}_{lj}^{(0,0)}+\phi_k(1)\phi_i(1)\mathbf{F}_{lj}^{(0,0)}\\&+\mathbf{E}_{ki}^{(0,0)}\chi_l(0)\chi_j(0)+\mathbf{E}_{ki}^{(0,0)}\chi_l(1)\chi_j(1)\\&+\frac{\partial\phi_k(0)}{\partial\xi}\frac{\partial\phi_i(0)}{\partial\xi}\mathbf{F}_{lj}^{(0,0)}+\frac{\partial\phi_k(1)}{\partial\xi}\frac{\partial\phi_i(1)}{\partial\xi}\mathbf{F}_{lj}^{(0,0)}\\&+\mathbf{E}_{ki}^{(0,0)}\frac{\partial\chi_l(0)}{\partial\eta}\frac{\partial\chi_j(0)}{\partial\eta}+\mathbf{E}_{ki}^{(0,0)}\frac{\partial\chi_l(1)}{\partial\eta}\frac{\partial\chi_j(1)}{\partial\eta}\Big]\end{aligned}\quad\text{and} \tag{4.18}$$

$$\begin{aligned}\mathbf{P}_{s,point}=\hat{k}\Big[&\phi_k(\xi)\phi_i(\xi)\chi_l(\eta)\chi_j(\eta)+\frac{\partial\phi_k(\xi)}{\partial\xi}\frac{\partial\phi_i(\xi)}{\partial\xi}\chi_l(\eta)\chi_j(\eta)\\&+\phi_k(\xi)\phi_i(\xi)\frac{\partial\chi_l(\eta)}{\partial\eta}\frac{\partial\chi_j(\eta)}{\partial\eta}\Big],\end{aligned} \tag{4.19}$$

Penalty matrices due to artificial inertia can be obtained substituting $\hat{k}$ by $\hat{m}$ in Eqs. (4.18) and (4.19).

It is observed that all terms in Eqs. (4.16)-(4.19) are in function of four subscripts. Then the two-dimensional matrices are obtained carrying out the double summation of W defined in Eq. (4.3). Thus, the two-dimensional matrices are

obtained combining every term in the double summation (with subscripts i and j with a term with subscripts k and l using the following relationships:

$$o = i + (k-1)n \qquad \text{and} \qquad p = j + (l-1)n, \qquad (4.20a,4.20b)$$

With this reduction all matrices defining properties of a plate in Eqs. (4.16)-(4.19) are square matrices of size $\hat{n} \times \hat{n}$,

$$\hat{n} = n^2 , \qquad (4.21)$$

where $\hat{n}$ is the original number of DOFs of the system.

Moreover, $\alpha = a/b$ is the aspect ratio of the plate. In this chapter only results for square plates are presented. This means that in all cases $\alpha = 1$. Also, for all solutions presented in this chapter the Poisson's ratio has a fixed value $\nu = 0.3$.

It should be clear as explained in Chapter 3, that $\hat{h}$ DOFs are lost when $\hat{h}$ penalty parameters are applied to the solution. The total number of active DOFs of the plate can be calculated by subtracting the number of edge constraints parallel to axis y from the number of terms used on the x direction, then subtracting the number of edge constraints parallel to axis x from the number of terms used on the y direction and multiplying the results. This can be written as

$$\hat{n}_{active} = \left(n - \hat{h}_x\right)\left(n - \hat{h}_y\right) \qquad (4.22)$$

For instance the number of DOFs of a SCSC plate setting $n = 10$ is

$$\hat{n}_{active} = (10-2)(10-4) = 48$$

Then for a SCSC plate with $n=10$ size of the matrices remain 100x100, although there are only 48 $\hat{n}_{active}$. Thus there are 52 eigenvalues that should be erased from the solution. Identifying these 52 eigenvalues is a very easy task as they tend to 0^+ and 0^- when positive and negative artificial inertia is used or to $-\infty$ or to $+\infty$ when positive and negative artificial stiffness is used, respectively. This applies to vibration problems of all types of structural elements analyzed in this thesis.

4.3 Results and discussion

This section presents frequency parameters for plates with F, S or C boundary conditions. To identify the boundary conditions of the different plate cases, four letters representing the edges at the non-dimensional coordinates are necessary and they are given in the following order $\xi=0$, $\eta=0$, $\xi=1$ and $\eta=1$. For all cases the same number of terms is used in both directions.

4.3.1 Frequency parameters of a FFFF plate

To demonstrate the robustness of the solution using the proposed set of admissible functions, first solutions of a FFFF plate are presented in Table 4.1. This case shows that ill-conditioning is not due to the number of terms used as it is the only case without penalty parameters.

Furthermore, for comparison the solution of a FFFF plate using the RRM with a set of admissible functions built by simple polynomials is also included in Table 4.1. The maximum number of terms in the solution using simple polynomials free of ill-conditioning was found to be seven, which gives very accurate results, but

for lower modes only. On the other hand, the solution with five terms does not converge for all the first eight modes given on Table 4.1 and the solution with eight terms already gives inaccurate results due to ill-conditioning, as results include negative and complex eigenvalues. From the comparison between both solutions using seven terms in each direction, it is clear that the set of admissible functions built by simple polynomials gives lower frequency parameters for the first five lower frequencies and the eighth frequency. For all other modes lower frequencies were obtained using the set of admissible functions given in Chapter 2, although these results are not shown here.

Table 4.1. Convergence of FFFF plates with respect to the number of terms n.

			Present work			
n	1	2	3	4,5	6,7	8
6	13.4967	19.6065	24.2903	34.9087	61.2251	64.3716
7	13.4967	19.5978	24.2744	34.8825	61.1877	63.9576
10	13.4725	19.5967	24.2718	34.8206	61.1040	63.8078
15	13.4695	19.5962	24.2705	34.8059	61.0952	63.7088
20	13.4686	19.5962	24.2703	34.8027	61.0941	63.6967
25	13.4684	19.5962	24.2703	34.8018	61.0936	63.6905
30	13.4683	19.5961	24.2702	34.8014	61.0935	63.6889
35	13.4683	19.5961	24.2702	34.8012	61.0934	63.6876
40	13.4682	19.5961	24.2702	34.8011	61.0933	63.6872
45	13.4682	19.5961	24.2702	34.8010	61.0933	63.6868
50	13.4682	19.5961	24.2702	34.8010	61.0933	63.6867
55	13.4682	19.5961	24.2702	34.8010	61.0933	63.6865
60	13.4682	19.5961	24.2702	34.8009	61.0933	63.6864
			Simple polynomial			
	1	2	3	4,5	6,7	8
6	13.4687	19.7257	24.5412	35.2880	63.0195	66.1691
7	13.4687	19.5963	24.2707	34.8083	62.9471	63.6896

4.3.2 Frequency parameters of plates with classical boundary conditions

Table 4.2 shows the frequency parameters of the 21 cases of plates with classical boundary conditions obtained using the proposed set of admissible functions in the RRM. Results for 10 and 20 terms in each direction of the plate are presented. Results obtained with the proposed set of admissible functions are compared with the results given by Leissa (1973).

As mentioned earlier, a pair of results using positive and negative penalty parameters brackets the constrained solution of the vibration problem. For this reason, the sets of results presented in Table 4.2 were obtained using positive and negative inertial penalty parameters with absolute values from the series 2^{i-1}, for $i = 1,2,3...$ and checking for monotonic convergence towards the constrained solution in the first six non-zero frequencies. For all cases except one, results presented in Table 4.2 were found when results using positive and negative inertial penalty parameters of the same absolute value converged to the same results up to the second decimal place. The exception was found in the second frequency parameter of a SFSF plate using 20 terms in each direction, where a difference of 0.01 persisted. Results presented for this case is the average of the last pair of results with monotonic convergence with positive and negative penalty parameters.

Table 4.2. Results of 21 plate cases with classical boundary conditions.

Case		$\hat{m}$	Mode number					
			1	2	3	4	5	6
1 SSSS	10x10	8192	19.74	49.38	49.38	79.00	99.04	99.04
	20x20	4096	19.74	49.35	49.35	78.96	98.72	98.72
	Leissa		19.74	49.35	49.35	78.96	98.70	98.70
2 SCSC	10x10	16384	29.01	54.89	69.58	94.99	102.74	130.38
	20x20	131072	28.96	54.75	69.35	94.62	102.25	129.19
	Leissa		28.95	54.74	69.33	94.59	102.22	129.10
3 SCSS	10x10	32768	23.67	51.75	58.77	86.34	100.67	113.96
	20x20	8192	23.65	51.68	58.66	86.15	100.30	113.28
	Leissa		23.65	51.67	58.65	86.13	100.27	113.23
4 SCSF	10x10	16384	12.69	33.10	41.76	63.13	72.57	91.03
	20x20	131072	12.69	33.07	41.71	63.03	72.41	90.64
	Leissa		12.69	33.07	41.70	63.01	72.40	90.61
5 SSSF	10x10	8192	11.69	27.76	41.25	59.12	61.91	90.70
	20x20	262144	11.68	27.76	41.20	59.07	61.86	90.32
	Leissa		11.68	27.76	41.20	59.07	61.86	90.29
6 SFSF	10x10	131072	9.64	16.14	36.74	39.00	46.79	70.83
	20x20	131072	9.63	16.14	36.73	38.95	46.74	70.75
	Leissa		9.63	16.13	36.73	38.95	46.74	70.74
7 CCCC	10x10	16384	36.11	73.76	73.76	108.99	133.09	133.63
	20x20	8192	35.99	73.43	73.43	108.29	131.69	132.31
	Leissa		35.99	73.41	73.41	108.27	131.64	132.64
8 CCCS	10x10	8192	31.91	63.57	71.36	101.36	117.27	131.70
	20x20	16384	31.83	63.35	71.10	100.85	116.42	130.45
	Leissa		31.83	63.35	71.08	100.83	116.40	130.37
9 CCCF	10x10	8192	24.00	40.15	63.49	77.07	81.00	117.55
	20x20	32768	23.93	40.01	63.26	76.74	80.62	116.75
	Leissa		24.02	40.04	63.49	76.76	80.71	116.80
10 CCSS	10x10	16384	27.09	60.70	60.94	93.20	115.36	115.49
	20x20	4096	27.06	60.55	60.80	92.87	114.61	114.76
	Leissa		27.06	60.54	60.79	92.87	114.57	114.72
11 CCSF	10x10	8192	17.57	36.09	51.96	71.32	74.56	106.56
	20x20	16384	17.54	36.03	51.83	71.10	74.35	105.85
	Leissa		17.62	36.05	52.07	71.19	74.35	106.28

Table 4.2 (continued).

Case		$\hat{m}$	Mode number					
			1	2	3	4	5	6
12 CCFF	10x10	8192	6.93	23.95	26.62	47.79	62.88	65.72
	20x20	65536	6.92	23.91	26.59	47.67	62.72	65.56
	Leissa		6.94	24.03	26.68	47.79	63.04	65.83
13 CSCF	10x10	8192	23.44	35.69	63.13	67.00	77.73	109.48
	20x20	32768	23.38	35.58	62.91	66.78	77.42	108.93
	Leissa		23.46	35.61	63.13	66.81	77.50	108.99
14 CSSF	10x10	8192	16.82	31.16	51.53	64.13	67.72	101.45
	20x20	65536	16.80	31.12	51.41	64.03	67.56	101.15
	Leissa		16.87	31.14	51.63	64.04	67.65	101.21
15 CSFF	10x10	131072	5.36	19.09	24.70	43.16	52.78	63.92
	20x20	65536	5.35	19.08	24.67	43.10	52.71	63.78
	Leissa		5.36	19.17	24.77	43.19	53.00	64.05
16 CFCF	10x10	16384	22.23	26.51	43.78	61.42	67.50	80.09
	20x20	32768	22.18	26.42	43.62	61.21	67.22	79.84
	Leissa		22.27	26.53	43.66	61.47	67.55	79.90
17 CFSF	10x10	32768	15.22	20.62	39.80	49.58	56.45	77.42
	20x20	131072	15.20	20.59	39.74	49.46	56.30	77.34
	Leissa		15.29	20.67	39.78	49.73	56.62	77.37
18 CFFF	10x10	131072	3.47	8.52	21.31	27.22	31.01	54.33
	20x20	131072	3.47	8.51	21.29	27.20	30.97	54.21
	Leissa		3.49	8.52	21.43	27.33	31.11	54.44
19 SSFF	10x10	16384	3.37	17.32	19.30	38.23	51.09	53.54
	20x20	65536	3.37	17.32	19.29	38.21	51.04	53.49
	Leissa		3.37	17.41	19.37	38.29	51.32	53.74
20 SFFF	10x10	65536	6.64	14.91	25.39	26.00	48.50	50.63
	20x20	65536	6.64	14.90	25.38	26.00	48.45	50.58
	Leissa		6.65	15.02	25.49	26.13	48.71	50.85
21 FFFF	10x10	N/A	13.47	19.60	24.27	34.82	34.82	61.10
	20x20	N/A	13.47	19.60	24.27	34.80	34.80	61.09
	Leissa		13.49	19.79	24.43	35.02	35.02	61.53

As observed in Chapter 3, once again the frequency parameters for the higher modes converge first and with lower magnitudes of artificial masses than those required for the lower modes. For instance, using 10 terms in both directions of the plate in all 20 cases including constraints in the boundary conditions and assigning a value of 8 to the inertial parameter index, at least half of the upper

frequency parameters converged within 1% of the best approximation (using the penalty value on Table 4.2 for 10 terms).

Results presented in Tables 4.1 and 4.2 for FFFF plate do not include three zero frequencies (rigid body frequencies) corresponding to one translation and two rotations.

Fig. 4.2 shows the expected monotonic convergence according to the type and sign of penalty parameter used in the solution. Fig. 4.2 also shows that there is a linear relationship between the inverse of the penalty values and the frequency parameters in a range close to the optimum penalty value, which is the highest penalty value that gives results free of round-off errors. This is similar to what was observed in the case of a linear stress problem in (Askes and Ilanko 2006).

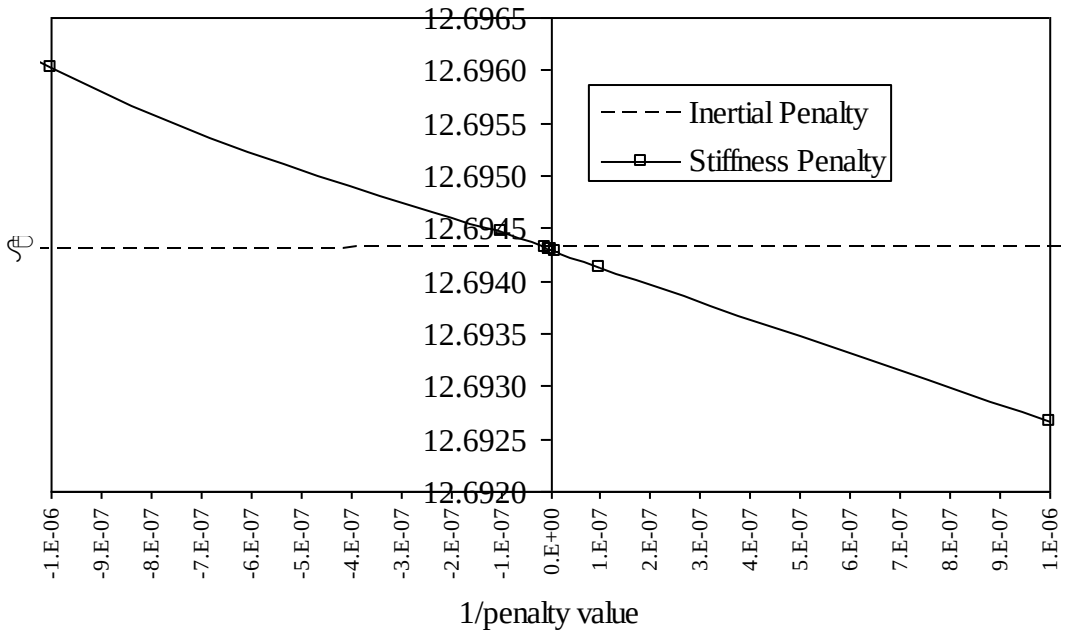

Figure 4.2. Convergence of the fundamental frequency parameter versus the inverse of the penalty values of a SCSF plate with n=10.

4.3.3 Frequency parameters of FFFF plates simply supported along a diagonal

Penalty parameters can be applied at any interior point of plate elements to model more sophisticated constraints. As an example, a series of ten non-dimensional masses were defined along a diagonal from the origin to the opposite corner of the plate to model a simply supported diagonal.

Results of this case are compared with those presented by Kim (1995), who reported results for plates with any combination of classical boundary conditions along its edges and supported along a diagonal using a simple polynomial as admissible function in a similar way to that presented in (Young and Dickinson 1993). In both cases the pb-2 Method was used to define boundary conditions and constraints along a diagonal.

Results are presented in Table 4.3, which show a very good agreement with the solution published by Kim (1995). Both solutions used 10 terms in each direction of the plate.

Table 4.3. Frequency parameters of FFFF plates with a diagonal support.

Present	Mode number					
$\hat{m}$	1	2	3	4	5	6
2048	12.648	19.597	34.821	35.980	53.054	61.104
[Kim]	[12.650]	[19.596]	[34.801]	[35.991]	[52.013]	[61.093]

In this case, results were obtained again using positive and negative masses, checking for monotonic convergence and convergence of the results up to the fifth significant figure which was achieved with positive and negative inertial parameters of magnitude 2048. For this case, some frequencies using inertial

penalty values of 2048 included very small round-off errors, typically of order 10^{-9}.

4.3.4 Concluding remarks

Solving plate problems, the number of terms in the set of admissible functions was found to be limited only by machine memory provided the penalty parameter is chosen carefully to avoid round-off errors associated with large penalty parameters. For instance, a maximum of about 60 terms in each direction of a rectangular plate could be used on a machine with 1 Gb of RAM memory. This gives an eigenvalue problem of a square mass and stiffness matrices of size of 3600. In (Oosterhout et al. 1995) it is mentioned that when using the Legendre polynomials in the RRM to model a completely free plate at least 15 terms in each direction can be used, but no specific limit in the number of terms was mentioned. It was also mentioned that for this case the lowest 25% natural frequencies can be considered to be accurate. In the present work, when 15 terms are used in each direction (leading to 225 terms in total) 221 natural frequencies can be considered to be accurate (within 1% error), including three zero frequencies. This shows that while the procedure is simple, it is also robust.

In the next chapter, the same procedure is used to study the use of the different types of penalty parameters in vibration problems of shallow shells of rectangular planform with several types of geometries (plates, cylindrical, spherical and hyperbolic paraboloidal) with F, S and C conditions.

Chapter 5

Free Vibration of Shells

5.1 Introduction

This chapter deals with applications of the set of admissible functions developed in Chapter 2 to obtain frequency parameters of thin shallow shells of rectangular planform with constant thickness h subjected to any combination of boundary conditions.

Several researchers have used the RRM in the past to solve problems of shallow shells. Some of the most relevant publications for the present work are (Crossland and Dickinson 1997; Leissa 1969b; Leissa and Narita 1984; Liew and Lim 1994; Lim and Liew 1994; Young and Dickinson 1995a; Young and Dickinson 1995b). These publications deal with completely free shallow shells, shallow shells with slits, shallow shells with different boundary conditions defined using the pb-2 Method, shallow shells of planforms with outer and inner-curves and inter-connected by artificial springs.

Shell elements can be described as curved plates the thickness of which is small in comparison with the other dimensions of the element. Another characteristic of

shell elements that makes them different from plates is that their bending can not be separated from their stretching (Ventsel and Krauthammer 2001).

Shells are classified as shallow if the rise does not exceed 1/5 of the smallest dimension of the shell in its plane, which are defined as length a and width b as shown in Fig. 5.1a (Ventsel and Krauthammer 2001).

Shell elements can adopt very different shapes depending on the curvatures to define the structure, and their efficiency in carrying loads make them very appealing for many engineering applications. It can be understood that shell elements are more efficient than plate elements to carry loads, just as an arch can be more efficient than a straight beam under lateral load. This is because of their increased stiffness arising from the curvature.

As with beams and plates, shells have been analyzed using different mathematical models that have been improved over time and that take into account different effects. In this chapter the theory of shallow shells is used to solve all vibration problems of shells. The shallow shell theory is a special case of the linear theory of thin elastic shells or first order approximation shell theory (Ventsel and Krauthammer 2001), which is derived from Love's assumptions presented below (Leissa 1969b)

a) the thickness of the shell is small compared with the other dimensions of the shell including the radius of curvature of the middle surface of the shell,

b) strains and displacements are sufficiently small. Thus, strain-displacement relations of second and higher-order magnitude may be neglected,
c) the transverse normal stress is small compared with other normal stress components and may be neglected and
d) normals to the undeformed middle surface remain straight and normal to the deformed middle surface and undergo no extension.

The fourth assumption is known as the Kirchhoff's hypothesis. It has been reported that the theory defined by Love has the following inconsistencies (Rao 2007):

a) the transverse normal stress can not be zero, especially when the outer surface of the shell is loaded and
b) shear forces are assumed to be present, which causes non-zero shear strains.

Other shell theories have been developed to try to improve the first order approximation shell theory given above. For instance, the Donell-Mushtari-Vlasov theory for thin shells that adds two more assumptions to the Love's assumptions. These are the static assumption (effect of transverse shear forces in the in-plane equilibrium equations is neglected) and the geometric assumption (influence of transverse displacement predominates over in-plane displacements in bending) as explained in (Ventsel and Krauthammer 2001).

The theory of shallow shells was developed using both sets of assumptions mentioned above, fixing the Lamé parameters $A = B = 1$ and defining the

curvatures of the shell as given in Eqs. (5.5a)-(5.5c) (Ventsel and Krauthammer 2001).

Another linear theory presented by Novozhilov is the second-order approximation theory, in which the strain-displacement relationships are obtained from three-dimensional elasticity based on Love's assumptions (Leissa 1969b). In (Amabili 2008) several theories and examples of non-linear shallow shells are presented.

5.2 Theoretical derivations

As the theoretical derivation of shallow shells is more complex than the derivations of the previous two structural elements (beams and plates), these are given in three sub-sections. In 5.2.1 the geometric properties of shallow shells are presented, then the theoretical derivations to obtain the stiffness and mass matrices are given in 5.2.2, while the description of the penalty parameters to enforce constraints on the edges of the shells are given in 5.2.3.

5.2.1 Geometry and properties of shallow shells

The material of the shell is assumed to be isotropic with Young's modulus E, Poisson ratio ν and density ρ. The geometric properties of the shallow shells are defined placing the midpoint of the middle surface of the shell at $z=0$, one corner of the middle surface of the shell at $x=0$ and $y=0$ and aligning the edges of the shells with the x and y axes as shown in Fig. 5.1a. The projections of the edges on their respective axis are defined as length a and width b as shown in Fig. 5.1b.

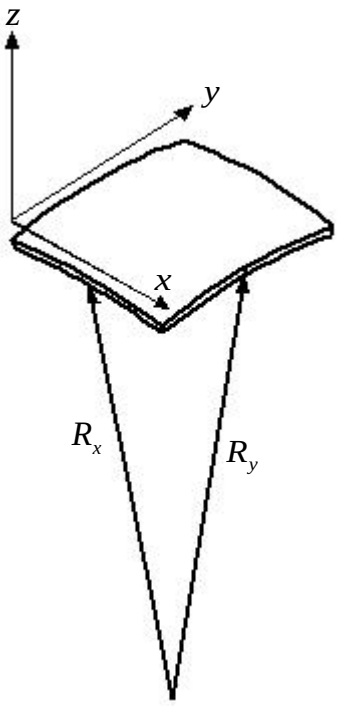

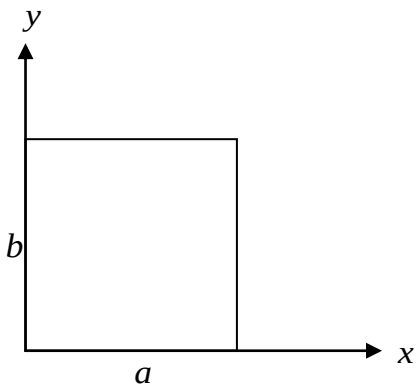

Fig. 5.1a Fig. 5.1b

Figure 5.1. Coordinate axes and main dimensions of a free shallow shell of rectangular planform.

The middle surface of the shell is defined by two constant curvatures of radii R_x and R_y, which are parallel to the x and y axes. The radii R_x and R_y have their origins located on points along the line at the midpoint of the shells defined by $x = a/2$ and $y = b/2$. Thus, the middle surface of the shell is described by

$$z = -\frac{\left(x - \frac{a}{2}\right)^2}{2R_x} - \frac{\left(y - \frac{b}{2}\right)^2}{2R_y} \tag{5.1}$$

The special cases of geometries of the shallow shells used in this chapter can be classified according to their radii of curvature as

- plate $R_x = R_y = \infty$,
- cylindrical $R_x = \infty$ and $R_y \neq \infty$

- spherical $R_x = R_y \neq \infty$
- hyperbolic paraboloidal $R_x = -\beta R_y$, where β is a positive factor

5.2.2 Frequency parameters of fully free shallow shells

As the RRM is an energy method, it is necessary to first define the maximum potential and kinetic energies of the free shell.

Then, the kinetic energy of the shell (Leissa and Narita 1984) is

$$T = \frac{\rho h}{2}\int_0^b \int_0^a \left[\left(\frac{\partial u}{\partial t}\right)^2 + \left(\frac{\partial v}{\partial t}\right)^2 + \left(\frac{\partial w}{\partial t}\right)^2\right] dxdy, \tag{5.2}$$

where u, v and w are the displacements of the middle surface of the shell in the x, y and z directions.

The potential energy of a shallow shell as defined by Leissa and Narita (1984) is

$$V = \frac{Eh}{2(1-\nu^2)}\int_0^b \int_0^a \left[(\varepsilon_x + \varepsilon_y)^2 - 2(1-\nu)(\varepsilon_x\varepsilon_y - \gamma_{xy}^2/4)\right] dxdy$$

$$+ \frac{Eh^3}{24(1-\nu^2)}\int_0^b \int_0^a \left[(\kappa_x + \kappa_y)^2 - 2(1-\nu)(\kappa_x\kappa_y - \kappa_{xy}^2)\right] dxdy, \tag{5.3}$$

where the first term on the right hand side of Eq. (5.3) is the potential energy due to stretching of the middle surface of the shell and the second term is the potential energy due to bending of the shell. In Eq. (5.3) ε_x and ε_y are the membrane direct strain components and γ_{xy} is the shear strain component (Ventsel and Krauthammer 2001). These are related to the displacements by (Leissa and Narita 1984)

$$\varepsilon_x = \partial u/\partial x + w/R_x, \tag{5.4a}$$

$$\varepsilon_y = \partial v/\partial y + w/R_y \quad \text{and} \tag{5.4b}$$

$$\gamma_{xy} = \partial v/\partial x + \partial u/\partial y \tag{5.4c}$$

Similarly, in Eq. (5.3) κ_x and κ_y are the dynamic curvatures and κ_{xy} is the twist of the shell. These curvatures are defined as (Leissa and Narita 1984)

$$\kappa_x = \partial^2 w/\partial x^2, \tag{5.5a}$$

$$\kappa_y = \partial^2 w/\partial y^2 \ , \tag{5.5b}$$

$$\kappa_{xy} = \partial^2 w/\partial x \partial y, \tag{5.5c}$$

and assuming the free vibration of the shell to be small, the displacements of the middle surface of the shell u, v and w are defined as

$$u(x,y,t) = U(x,y)\sin\omega t, \tag{5.6a}$$

$$v(x,y,t) = V(x,y)\sin\omega t \quad \text{and} \tag{5.6b}$$

$$w(x,y,t) = W(x,y)\sin\omega t \tag{5.6c}$$

Substituting Eqs. (5.6a)-(5.6c) in Eq. (5.2) gives the following equation for the kinetic energy (Kurpa et al. 2005):

$$T_{max} = \frac{\rho h \omega^2}{2}\int_0^b\int_0^a \left[U^2 + V^2 + W^2\right]dxdy, \tag{5.7}$$

where ω is the circular frequency of the shell.

Substituting Eqs. (5.4a)-(5.6c) in Eq. (5.3) gives the following equation for the potential energy of the shell (Kurpa et al. 2005):

$$V_{max} = \frac{12D}{h^2}\int_0^b\int_0^a \left\{\left(\frac{\partial U}{\partial x} + \frac{\partial V}{\partial y} + \frac{W}{R_x} + \frac{W}{R_y}\right)^2\right.$$

$$-2(1-\nu)\left[\left(\frac{\partial U}{\partial x}+\frac{W}{R_x}\right)\left(\frac{\partial V}{\partial y}+\frac{W}{R_y}\right)-\frac{1}{4}\left(\frac{\partial U}{\partial y}+\frac{\partial V}{\partial x}\right)^2\right]\Bigg\}dxdy$$

$$+\frac{D}{2}\int_0^b\int_0^a\left\{\left(\frac{\partial^2 W}{\partial x^2}+\frac{\partial^2 W}{\partial y^2}\right)^2-2(1-\nu)\left[\left(\frac{\partial^2 W}{\partial x^2}\frac{\partial^2 W}{\partial y^2}\right)-\left(\frac{\partial W}{\partial x\partial y}\right)^2\right]\right\}, \quad (5.8)$$

where $D=Eh^3/12(1-\nu^2)$ is the flexural rigidity of the shell.

Then, the maximum kinetic energy function of the free shell is

$$\Psi_{max}=\frac{T_{max}}{\omega^2} \quad (5.9)$$

The displacement amplitude functions $U(x,y)$, $V(x,y)$ and $W(x,y)$ are defined by two orthogonal sets of admissible functions $\phi_i(x)$ and $\chi_j(y)$ as

$$U(x,y)=\sum_i^n\sum_j^n c_{ij}\phi_i(x)\chi_j(y), \quad (5.10a)$$

$$V(x,y)=\sum_{i+n}^{2n}\sum_{j+n}^{2n} c_{ij}\phi_i(x)\chi_j(y), \quad (5.10b)$$

$$W(x,y)=\sum_{i+2n}^{3n}\sum_{j+2n}^{3n} c_{ij}\phi_i(x)\chi_j(y), \quad (5.10c)$$

where n is he maximum number of terms included in each set of admissible functions and c_{ij} are arbitrary coefficients.

In the present work no separation of symmetric and anti-symmetric modes was implemented and the same number of terms and modes were used for all subscripts i and j.

The two orthogonal complete sets of admissible functions for a fully free shallow shell, used in this work are the same functions defined in Chapter 2 given here for two different coordinates as $\phi_i(x)$ and $\chi_j(y)$:

$$\phi_i(x)=\left(\frac{x}{a}\right)^{i-1} \qquad \text{for} \qquad i=1,2 \text{ and } 3, \tag{5.11a}$$

$$\phi_i(x)=\cos\frac{(i-3)\pi x}{a} \qquad \text{for} \qquad i=4,5,\ldots n, \tag{5.11b}$$

$$\chi_j(y)=\left(\frac{y}{b}\right)^{j-1} \qquad \text{for} \qquad j=1,2 \text{ and } 3 \tag{5.11c}$$

$$\chi_j(y)=\cos\frac{(j-3)\pi y}{b} \qquad \text{for} \qquad j=4,5,\ldots \text{n} \tag{5.11d}$$

The Rayleigh-Ritz minimization to obtain the stiffness and mass matrices of the completely free shallow shell is

$$\frac{\partial V_{max}}{\partial c_{ij}}-\omega^2\frac{\Psi_{max}}{\partial c_{ij}}=0\ , \tag{5.12}$$

To obtain results in non-dimensional form the stiffness and mass matrices are non-dimensionalized by dividing them by D/ab and by ρhab and by using non-dimensional coordinates of the shell defined as

$$\xi=\frac{x}{a} \qquad \text{and} \qquad \eta=\frac{y}{b} \tag{5.13a,5.13b}$$

Then the non-dimensional eigen-problem obtained after the Rayleigh-Ritz minimization is

$$[\mathbf{K}]\{\mathbf{c}\}-\lambda^2[\mathbf{M}]\{\mathbf{c}\}=\{\mathbf{0}\}, \tag{5.14}$$

where λ is the non-dimensional frequency parameter defined as (Lim and Liew 1994)

$$\lambda = \omega a b \sqrt{\rho h / D}\,, \tag{5.15}$$

Then, the stiffness and mass matrices are defined as

$$\mathbf{K} = \begin{vmatrix} \mathbf{KUU} & \mathbf{KUV} & \mathbf{KUW} \\ \mathbf{KUV}^{\mathrm{T}} & \mathbf{KVV} & \mathbf{KVW} \\ \mathbf{KUW}^{\mathrm{T}} & \mathbf{KVW}^{\mathrm{T}} & \mathbf{KWW} \end{vmatrix}, \tag{5.16a}$$

$$\mathbf{M} = \begin{vmatrix} \mathbf{MUU} & 0 & 0 \\ 0 & \mathbf{MVV} & 0 \\ 0 & 0 & \mathbf{MWW} \end{vmatrix}, \tag{5.17a}$$

where

$$\mathbf{KUU} = \left(\frac{b}{h}\right)^2 \mathbf{E}_{ki}^{(1,1)} \mathbf{F}_{lj}^{(0,0)} + \frac{(1-\nu)}{2}\left(\frac{a}{h}\right)^2 \mathbf{E}_{ki}^{(0,0)} \mathbf{F}_{lj}^{(1,1)}, \tag{5.16b}$$

$$\mathbf{KUV} = \nu\left(\frac{a}{h}\right)\left(\frac{b}{h}\right) \mathbf{E}_{ki}^{(1,0)} \mathbf{F}_{lj}^{(0,1)} + \frac{(1-\nu)}{2}\left(\frac{a}{h}\right)\left(\frac{b}{h}\right) \mathbf{E}_{ki}^{(0,1)} \mathbf{F}_{lj}^{(1,0)} \tag{5.16c}$$

$$\mathbf{KUW} = \left(\frac{b}{R_x} + \frac{\nu b}{R_y}\right)\left(\frac{a}{h}\right)\left(\frac{b}{h}\right) \mathbf{E}_{ki}^{(1,0)} \mathbf{F}_{lj}^{(0,0)}, \tag{5.16d}$$

$$\mathbf{KVV} = \left(\frac{a}{h}\right)^2 \mathbf{E}_{ki}^{(0,0)} \mathbf{F}_{lj}^{(1,1)} + \frac{(1-\nu)}{2}\left(\frac{b}{h}\right)^2 \mathbf{E}_{ki}^{(1,1)} \mathbf{F}_{lj}^{(0,0)}, \tag{5.16e}$$

$$\mathbf{KVW} = \left(\frac{\nu a}{R_x} + \frac{a}{R_y}\right)\left(\frac{a}{h}\right)\left(\frac{b}{h}\right) \mathbf{E}_{ki}^{(0,0)} \mathbf{F}_{lj}^{(1,0)}, \tag{5.16f}$$

$$\mathbf{KWW} = \left[\left(\frac{b}{R_x}\right)^2 + 2\nu\left(\frac{b}{R_x}\right)\left(\frac{b}{R_y}\right) + \left(\frac{b}{R_y}\right)^2\right]\left(\frac{a}{h}\right)^2 \mathbf{E}_{ki}^{(0,0)} \mathbf{F}_{lj}^{(0,0)}$$

$$+ \frac{1}{12}\left(\frac{b}{a}\right)^2 \mathbf{E}_{ki}^{(2,2)} \mathbf{F}_{lj}^{(0,0)} + \frac{1}{12}\left(\frac{a}{b}\right)^2 \mathbf{E}_{ki}^{(0,0)} \mathbf{F}_{lj}^{(2,2)}$$

$$+\frac{\nu}{12}\mathbf{E}_{ki}^{(0,2)}\mathbf{F}_{lj}^{(2,0)}+\frac{\nu}{12}\mathbf{E}_{ki}^{(2,0)}\mathbf{F}_{lj}^{(0,2)}+\frac{2(1-\nu)}{12}\mathbf{E}_{ki}^{(1,1)}\mathbf{F}_{lj}^{(1,1)}, \tag{5.16g}$$

$$\mathbf{MUU}=\mathbf{MVV}=\mathbf{MWW}=\mathbf{E}_{ki}^{(0,0)}\mathbf{F}_{lj}^{(0,0)}, \tag{5.17b}$$

$$\mathbf{E}_{ki}^{(r,s)}=\int_0^1\left(\frac{d^r\phi_k}{d\xi^r}\right)\left(\frac{d^s\phi_i}{d\xi^s}\right)d\xi, \quad \mathbf{F}_{lj}^{(r,s)}=\int_0^1\left(\frac{d^r\chi_l}{d\eta^r}\right)\left(\frac{d^s\chi_j}{d\eta^s}\right)d\eta,$$

$k,i,l,j=1,2,3\ldots n$ and $r,s=0,1,2$

The reduction of these four dimensional arrays to two-dimensional matrices should be carried out using the procedure described in Chapter 4. Thus the mass and stiffness matrices have a size of $3n^2 \text{ x } 3n^2$.

5.2.3 Penalty parameters of shallow shells

In this work, any combination of boundary conditions containing constraints is modelled through the use of penalty parameters of stiffness type or inertial type. In both cases, it is possible to use positive and negative values. Although, constraints can be defined at the edges of the shell as well as at locations in the interior of the shell, in this work, only results for constraints along the edges are presented.

As in the previous chapters penalty parameters of stiffness type represent artificial translational and rotational springs, while penalty parameters of inertial type represent artificial masses and moments of inertia. To implement the penalty parameters in the Rayleigh-Ritz approach it is necessary to add the energy terms of the artificial stiffness to the stiffness matrix or alternatively the energy of the artificial inertia to the mass matrix.

Then using penalty parameters four different constraints can be defined at each edge (Young and Dickinson 1995b). For instance, constraints along edge $x=0$ using artificial springs can be modelled as follows:

- translational constraints in the in-plane displacements U and V

$$V_{s,transu}=\frac{1}{2}k_{ux0}\int_0^b\left(\left(U\right)_{x=0}\right)^2 dy, \tag{5.18a}$$

$$V_{s,transv}=\frac{1}{2}k_{vx0}\int_0^b\left(\left(V\right)_{x=0}\right)^2 dy, \tag{5.18b}$$

- translational constraints in the out-of-plane displacement W

$$V_{s,transw}=\frac{1}{2}k_{wx0}\int_0^b\left(\left(W\right)_{x=0}\right)^2 dy, \tag{5.18c}$$

- rotational constraints to enforce zero normal slope $\partial W/\partial x$

$$V_{s,rotw}=\frac{1}{2}k_{rwx0}\int_0^b\left(\left(\partial W/\partial x\right)_{x=0}\right)^2 dy, \tag{5.18d}$$

where k_{ux0}, k_{vx0} and k_{wx0} represent the artificial stiffness per unit length of the translational springs of the displacements u, v and w; while k_{rwx0} represents the stiffness per unit length of the artificial rotational spring. The last two subscripts of the penalty parameters in Eqs. (5.18a)-(5.18d) indicate the location of the constraint $\left(x=0\right)$.

Artificial inertia can also be used to define constraints. In this case, the kinetic energy can be obtained substituting the coefficient of the stiffness of the artificial springs by the values of the artificial masses per unit length m_{ux0}, m_{vx0}, m_{wx0} and artificial moment of inertia per unit length I_{wx0}.

For comparison with the results in (Lim and Liew 1994) the boundary conditions modelled in this chapter will be called free (F) when there are no constraints, simply supported (S) when both in-plane and out-of-plane translational DOFs are constrained and clamped (C) when the appropriate rotational spring is added to the S condition to enforce zero slope on w. Other boundary conditions along an edge as a guiding conditions or hinge edge with free support, that allows translation in the out-plane direction are not presented in this chapter, although it is possible to define these type of boundary conditions using the present method.

To present results in non-dimensional form all penalty parameters are non-dimensionalized. For instance, the penalty parameters to constrain the edge at $x=0$ are

- non-dimensional distributed translational and rotational stiffness

$$\hat{k} = \frac{k_{ux0}a^3}{D} = \frac{k_{rwx0}a}{D}, \tag{5.19a}$$

- non-dimensional distributed mass and inertia parameter for shells

$$\hat{m} = \frac{m_{ux0}}{\rho h a} = \frac{I_{wx0}}{\rho h a^3}, \tag{5.19b}$$

Then, the penalty matrices are obtained minimizing Eqs. (5.18a)-(5.18d) as

$$\frac{\partial V_{s,transu}}{\partial c_{ij}} = \mathbf{PUU}_s, \tag{5.20a}$$

$$\frac{\partial V_{s,transv}}{\partial c_{ij}} = \mathbf{PVV}_s \text{ and} \tag{5.20b}$$

$$\frac{\partial V_{s,transw}}{\partial c_{ij}} + \frac{\partial V_{s,rotw}}{\partial c_{ij}} = \mathbf{PWW}_s \tag{5.20c}$$

The terms of these matrices are identical to their counterparts to model constraints in plates. Thus, matrices $\mathbf{PUU}_s$ and $\mathbf{PVV}_s$ are defined by the first four terms of Eq. (4.18) related with translational constraints, while matrix $\mathbf{PWW}_s$ is defined by all terms of Eq. (4.18) as in general contains translational as well as rotational constraints.

If artificial inertia is used the penalty matrices $\mathbf{PUU}_m$, $\mathbf{PVV}_m$ and $\mathbf{PWW}_m$ can be obtained substituting $\hat{m}$ for $\hat{k}$ in the penalty matrices defined in Eq. (4.18).

Finally, the penalty matrices due to artificial springs should be included in the stiffness matrix of the shell before solving the eigen-problem as follows:

$$\mathbf{K} = \begin{vmatrix} \mathbf{KUU} + \mathbf{PUU}_s & \mathbf{KUV} & \mathbf{KUW} \\ \mathbf{KUV}^{\mathrm{T}} & \mathbf{KVV} + \mathbf{PVV}_s & \mathbf{KVW} \\ \mathbf{KUW}^{\mathrm{T}} & \mathbf{KVW}^{\mathrm{T}} & \mathbf{KWW} + \mathbf{PWW}_s \end{vmatrix} \tag{5.21}$$

Alternatively, the penalty matrices due to artificial inertia could be added to the appropriate mass submatrices of the shell as follows:

$$\mathbf{M} = \begin{vmatrix} \mathbf{MUU} + \mathbf{PUU}_m & 0 & 0 \\ 0 & \mathbf{MVV} + \mathbf{PVV}_m & 0 \\ 0 & 0 & \mathbf{MWW} + \mathbf{PWW}_m \end{vmatrix} \tag{5.22}$$

5.3 Results and discussions

As in the previous chapter for plates, four letters are necessary to fully identify the boundary conditions of the shells and they are given in the following order with respect to the location of the edges were the constraints are modelled: $\xi = 0$,

$\eta = 0$, $\xi = 1$ and $\eta = 1$. With the present approach, any thin shallow-shell of rectangular planform can be solved using a single Matlab code, changing the geometric and materials properties, as well as activating the appropriate penalty parameters that define the desired boundary conditions.

In the Matlab code used in this work, the values for R_x and R_y to model plates and the value for R_x to model cylindrical shells were defined with an infinite value.

Results presented in this section are compared with the results obtained by Leissa and Narita (1984), Lim and Liew (1994) and Liew and Lim (1994). Leissa and Narita (1984) used the RRM to solve FFFF shallow shells, separating the problem in four parts depending on the particular symmetry class. The four cases of symmetry are: SS, SA, AS, AA, where S and A identify symmetric modes an antisymmetric modes, respectively. This allows using only either the odd or the even terms of the sets of admissible functions in a specific displacement function to formulate the eigenproblem. Although this reduces the size of the matrices, eigenproblems of the four different cases have to be developed to obtain the whole solution. Results by Leissa and Narita were obtained using four terms in each set of admissible functions.

5.3.1 Frequency parameters of FFFF shallow shells

In (Liew and Lim 1994) results for FFFF plates using the RRM and the pb-2 method fixing the number of terms n to 20 in the displacement functions for U and V and to 18 terms for W were published. Results for FFFF shells in the

present work were obtained by setting up the aspect ratio $a/b=1$ and $n=20$, except for results in Table 5.1, which presents convergence of the results of two FFFF shallow shells of square planform in function of n. The geometry of these cases corresponds to a plate and to a cylindrical shell. In both cases a good approximation to the published results can be obtained by fixing $n=7$.

Table 5.2 presents results of three more cases of FFFF shallow shells: a flat plate with $\nu=0.333$ (for all other cases $\nu=0.3$), a spherical shell and hyperbolic paraboloidal shell.

Solutions for any number of terms were free of ill-conditioning and the limit of the maximum number of terms to be used in the solution was due to memory of the machine. Thus a PC with 1 Gb of RAM memory allows solution of vibration problems of completely free shells up to $n=40$. This corresponds to stiffness and mass matrices of 4800 DOFs.

5.3.2 Frequency parameters of cylindrical CFFF shallow shells

Results using the present approach are compared with results presented by Lim and Liew (1994), who used the RRM together with the pb-2 method to solve vibration problems of shells setting the number of terms in each displacement function n to 15. Results using the procedure described in this work are also obtained fixing n to 15.

Tables 5.3 and 5.4 present a study of the convergence of a CFFF shell with respect to stiffness penalty parameters and inertial penalty parameters,

respectively. Each table contains results for positive and negative values. All four cases converged monotonically to the same results up to the third decimal place.

Some interesting characteristics in the solutions of vibration problems of shallow shells were found in the study of the use of the four types of penalty parameters described above. These characteristics are described below.

When artificial stiffness is used to model constraints the eigenvalues of the solution have the following characteristics:

a) $\hat{h}$ eigenvalues tend to ∞ or to $-\infty$ (depending on the sign of the penalty parameters),

b) the fundamental frequency is the first one to converge,

c) after round-off errors appear, negative eigenvalues are obtained, although the remaining positive eigenvalues may resemble the solution free of round-off errors and

d) no complex eigenvalues were found in any case.

When artificial inertia is used to model constrains the eigenvalues of the solution have the following characteristics:

a) $\hat{h}$ eigenvalues tend to 0^+ or 0^- (depending on the sign of the penalty parameters),

b) the fundamental frequency is the last one to converge,

d) after round-off errors appear, negative eigenvalues also start to appear and

c) complex eigenvalues can be found, when round-off errors or ill-conditioning are present in the solution and this may happen before the lower eigenvalues

converge to similar results to those obtained using artificial stiffness. This depends also on the series that define the penalty parameter values, if the step is relatively big the optimum penalty parameter could be missed.

Due to the characteristics of the eigenvalues mentioned above, it was decided to present the remaining sets of results using only negative artificial stiffness as the solution using artificial stiffness is more robust than using artificial inertia and because when negative artificial stiffness is used, real upper-bound solutions are obtained.

5.3.3 Frequency parameters of CFFF, SSSS and CCCC shallow shells

Tables 5.5 to 5.7 present the first eight frequency parameters of shallow shells of cylindrical-type with different curvatures R_y with three different boundary conditions: CFFF, SSSS and CCCC.

In general, results using the method proposed in this work are very close to the results given in the literature. For FFFF cases, it seems to give slightly lower results and in the cases including constraints slightly higher results as constraints reduce the active number of DOFs in a similar way as described in Chapter 4. For instance, the number of DOFs for FFFF, CFFF, SSSS and CCCC shells using the methodology presented in this work fixing $n=15$ are 675, 615, 507 and 459, respectively. Even reducing the number of degrees of freedom when constraints are added, the results obtained in this work differed from the results in the literature only in the fourth significant figure.

5.3.4 Concluding remarks

The use of the admissible functions developed in Chapter 2 for vibration analysis of thin shells proved successful. The advantages of this method are: a) it gives a single general solution for any kind of boundary conditions b) the mass and stiffness matrices are defined by simpler terms than in other approaches and c) it gives more flexibility than the pb-2 method to define boundary conditions. For instance, guiding boundary conditions can be easily defined.

In the following chapter the same procedure is used again to study the use of different penalty parameters to define boundary conditions and to inter-connect plate elements in box-type structures. The model of the box is built with six plate elements to allow modelling of non-symmetric structures and more importantly as a test of the convergence of vibration problems that use a large number of penalty parameters.

Table 5.1. Convergence study of frequency parameters of FFFF shells with respect to n ($a/h=100$).

						Frequency parameters							
a/b	ν	R_x/R_y	b/R_y	n	Reference	SS-1	SS-2	SA-1	SA-2	AS-1	AS-2	AA-1	AA-2
SQUARE PLATE													
1	0.3	-	0	≈20	Liew and Lim	19.523	24.381	34.947	61.255	34.947	61.255	13.523	69.268
		Uses Symmetry		4	Leissa and Narita	19.596	24.271	34.801	61.111	34.801	61.111	13.468	69.279
				7	Present work	19.598	24.274	34.882	61.188	34.882	61.188	13.497	69.405
				10	Present work	19.597	24.272	34.821	61.104	34.821	61.104	13.473	69.298
				15	Present work	19.596	24.270	34.806	61.095	34.806	61.095	13.470	69.277
				20	Present work	19.596	24.270	34.803	61.094	34.803	61.094	13.469	69.269
				30 & 40	Present work	19.596	24.270	34.801	61.093	34.801	61.093	13.468	69.266
SQUARE CYLINDRICAL SHELL													
1	0.3	0	0.2	≈20	Liew and Lim	21.942	38.640	35.003	75.552	37.807	61.283	13.539	70.965
		Uses Symmetry		4	Leissa and Narita	21.904	38.473	34.852	75.298	37.643	61.154	13.483	70.952
				7	Present work	21.907	38.539	34.939	75.504	37.759	61.216	13.514	71.126
				10	Present work	21.904	38.491	34.871	75.322	37.665	61.128	13.488	70.958
				15	Present work	21.903	38.473	34.856	75.275	37.648	61.119	13.485	70.933
				20	Present work	21.903	38.471	34.853	75.269	37.644	61.118	13.484	70.925
				25	Present work	21.903	38.470	34.852	75.267	37.643	61.117	13.484	70.923
				30 & 40	Present work	21.903	38.469	34.851	75.266	37.643	61.117	13.483	70.922

Table 5.2. Frequency parameters of FFFF shallow shells ($a/h=100$)

						Frequency parameters							
a/b	ν	R_x/R_y	b/R_y	n	Reference	SS-1	SS-2	SA-1	SA-2	AS-1	AS-2	AA-1	AA-2
SQUARE SPHERERICAL SHELL													
1	0.3	1	0.2	≈ 20	Liew and Lim	19.755	42.675	36.013	74.172	36.013	74.172	13.580	69.573
		Uses Symmetry		4	Leissa and Narita	19.757	42.353	35.880	73.890	35.880	73.890	13.524	69.598
				20	Present work	19.754	42.335	35.881	73.816	35.881	73.816	13.524	69.574
SQUARE HYPERBOLIC PARABOLOIDAL SHELL													
1	0.3	-1	0.2	≈ 20	Liew and Lim	24.851	52.563	37.145	77.217	37.145	77.217	13.517	78.325
		Uses Symmetry		4	Leissa and Narita	24.741	52.574	36.957	77.063	36.957	77.063	13.462	77.647
				20	Present work	24.738	52.563	36.957	77.029	36.957	77.029	13.462	77.607
SQUARE PLATE													
1	0.333			≈ 20	Liew and Lim	19.224	24.535	34.376	61.099	34.376	61.099	13.223	68.132
		Uses Symmetry		4	Leissa and Narita	19.224	24.423	34.233	60.951	34.233	60.951	13.169	68.142
				20	Present work	19.224	24.423	34.234	60.933	34.234	60.933	13.169	68.133

Table 5.3. Convergence study of the frequency parameters of CFFF cylindrical shallow shells with respect to stiffness penalty values, ($n=15$, $a/b=1$, $a/h=100$, $\nu=0.3$, $R_y=5$ and $R_x=\infty$).

	Frequency Parameters							
	1	2	3	4	5	6	7	8
Lim and Liew	8.3633	8.9029	26.824	33.237	35.105	58.714	64.603	73.829
$\hat{k}$								
10^3	4.2382	8.3351	13.285	25.741	30.298	30.454	31.575	50.470
10^4	4.5028	8.5484	26.397	32.595	32.976	41.330	56.965	64.304
10^5	5.6988	8.6319	26.560	32.862	33.585	57.936	64.478	72.891
10^6	7.5890	8.7992	26.745	33.078	34.520	58.493	64.559	73.533
10^7	8.2619	8.8889	26.817	33.223	35.022	58.714	64.603	73.813
10^8	8.3534	8.9035	26.827	33.249	35.104	58.745	64.611	73.862
10^9	8.3630	8.9051	26.828	33.252	35.113	58.748	64.612	73.868
10^{10}	8.3640	8.9052	26.828	33.253	35.114	58.748	64.612	73.868
$\hat{k}$								
-10^3	413.05	415.94	424.37	449.67	455.38	458.19	462.21	468.90
-10^4	382.64	401.78	418.48	437.43	443.56	446.56	450.59	456.26
-10^5	323.69	328.52	345.88	346.89	351.62	374.07	388.42	417.45
-10^6	200.73	204.84	205.58	212.67	225.65	228.00	244.01	251.86
-10^7	8.4868	8.9270	26.840	33.297	35.244	58.789	64.623	73.951
-10^8	8.3750	8.9070	26.829	33.256	35.125	58.752	64.613	73.874
-10^9	8.3652	8.9054	26.828	33.253	35.115	58.749	64.612	73.869
-10^{10}	8.3642	8.9053	26.828	33.253	35.114	58.748	64.612	73.868

Table 5.4. Convergence study of the frequency parameters of CFFF cylindrical shallow shells with respect to inertial penalty values ($n=15$, $a/b=1$, $a/h=100$, ν =0. 3, $R_y=5$ and $R_x=\infty$).

	Frequency Parameters							
	1	2	3	4	5	6	7	8
Lim and Liew	8.3633	8.9029	26.824	33.237	35.105	58.714	64.603	73.829
$\hat{m}$								
10^0	318.33	325.34	331.03	341.22	345.58	351.19	373.94	387.49
10^1	228.20	241.44	248.77	252.83	265.68	274.27	276.17	281.94
10^2	125.81	130.55	131.53	133.91	139.72	142.12	142.85	150.57
10^3	53.797	58.858	61.853	63.524	64.648	73.972	75.026	85.003
10^4	26.837	26.859	27.718	33.290	35.210	58.759	64.614	73.880
10^5	8.7431	8.9521	26.830	33.256	35.123	58.750	64.612	73.869
10^6	8.3796	8.9075	26.828	33.253	35.115	58.749	64.612	73.868
10^7	8.3657	8.9055	26.828	33.253	35.114	58.748	64.612	73.868
10^8	8.3643	8.9053	26.828	33.253	35.114	58.748	64.612	73.868
$\hat{m}$								
-10^0	0.0000	0.0000	0.0000	0.0224	25.380	29.971	30.235	55.108
-10^1	4.0153	8.2303	26.358	32.610	33.004	57.613	64.439	72.672
-10^2	4.2816	8.5371	26.533	32.868	33.626	58.253	64.528	73.388
-10^3	4.7611	8.6164	26.723	33.087	34.586	58.655	64.593	73.775
-10^4	7.1187	8.7807	26.813	33.225	35.038	58.738	64.610	73.857
-10^5	8.2158	8.8849	26.826	33.250	35.106	58.747	64.612	73.867
-10^6	8.3488	8.9030	26.828	33.252	35.114	58.748	64.612	73.868
-10^7	8.3626	8.9050	26.828	33.253	35.114	58.748	64.612	73.868
-10^8	8.3640	8.9052	26.828	33.253	35.114	58.748	64.612	73.868

Table 5.5. Frequency parameters of CFFF shallow shells of rectangular planform ($n=15$, $a/b=1$, $a/h=100$, $\nu=0.3$ and $R_x=\infty$).

Lim and Liew		Frequency Parameters							
	b/Ry	1	2	3	4	5	6	7	8
Plate	0	3.4714	8.5083	21.288	27.199	30.962	54.195	61.260	64.143
Cylindrical	0.1	5.2146	8.6107	24.769	28.226	31.555	55.144	64.298	65.033
Cylindrical	0.2	8.3633	8.9029	26.824	33.237	35.105	58.714	64.603	73.829
Cylindrical	0.3	9.3516	11.600	27.711	35.767	41.712	64.896	66.649	79.363
Cylindrical	0.4	9.9229	14.546	28.910	38.852	45.418	65.165	78.495	84.560
Cylindrical	0.5	10.589	16.981	30.641	42.211	47.688	65.439	89.727	89.947
Present Work		Frequency Parameters							
$\hat{k}$	b/Ry	1	2	3	4	5	6	7	8
-10^8	0	3.4722	8.5107	21.295	27.203	30.977	54.231	61.292	64.154
-10^{10}	0.1	5.2154	8.6130	24.775	28.231	31.570	55.180	64.308	65.066
-10^{10}	0.2	8.3642	8.9053	26.828	33.253	35.114	58.748	64.612	73.868
-10^{10}	0.3	9.3540	11.601	27.715	35.785	41.728	64.904	66.680	79.425
-10^{10}	0.4	9.9253	14.547	28.915	38.871	45.441	65.173	78.527	84.633
-10^{10}	0.5	10.592	16.982	30.647	42.233	47.695	65.448	89.812	90.021

Table 5.6. Frequency parameters of SSSS shallow shells of rectangular planform ($n=15$, $a/b=1$, $a/h=100$, $\nu=0.3$ and $R_x=\infty$).

Lim and Liew		Frequency Parameters							
	b/Ry	1	2	3	4	5	6	7	8
Plate	0	19.739	49.348	49.348	78.957	98.696	98.696	128.30	128.30
Cylindrical	0.1	36.841	51.576	58.383	82.302	99.527	103.66	129.41	131.11
Cylindrical	0.2	57.708	63.834	79.217	91.542	102.84	117.23	132.85	139.15
Cylindrical	0.3	66.574	85.624	103.77	104.95	113.70	136.68	139.33	151.49
Cylindrical	0.4	77.080	95.127	120.83	125.76	137.71	151.89	159.40	167.01
Cylindrical	0.5	88.431	99.889	137.82	140.07	166.64	171.88	174.16	182.95
Present Work		Frequency Parameters							
$\hat{k}$	b/Ry	1	2	3	4	5	6	7	8
-10^{10}	0	19.740	49.358	49.358	78.970	98.743	98.743	128.345	128.35
-10^{12}	0.1	36.840	51.579	58.389	82.301	99.561	103.69	129.44	131.13
-10^{12}	0.2	57.708	63.839	79.222	91.543	102.86	117.26	132.86	139.16
-10^{11}	0.3	66.576	85.653	103.78	104.96	113.71	136.71	139.36	151.52
-10^{12}	0.4	77.076	95.165	120.84	125.78	137.71	151.88	159.43	167.03
-10^{12}	0.5	88.430	99.927	137.84	140.09	166.65	172.05	174.15	182.98

Table 5.7. Frequency parameters of CCCC shallow shells of rectangular planform ($n=15$, $a/b=1$, $a/h=100$, $\nu=0.3$ and $R_x=\infty$).

Lim and Liew		Frequency Parameters							
	b/Ry	1	2	3	4	5	6	7	8
Plate	0	35.985	73.394	73.394	108.22	131.58	132.20	165.00	165.00
Cylindrical	0.1	46.281	74.657	79.290	110.35	132.54	135.55	165.82	166.97
Cylindrical	0.2	67.681	78.294	94.610	116.46	135.00	145.76	168.32	172.71
Cylindrical	0.3	83.923	90.397	115.05	125.87	140.53	161.25	172.80	181.83
Cylindrical	0.4	91.066	108.46	136.89	137.70	152.43	180.12	180.41	193.74
Cylindrical	0.5	99.263	119.00	151.13	156.35	172.52	192.43	201.67	207.80
Present Work		Frequency Parameters							
$\hat{k}$	b/Ry	1	2	3	4	5	6	7	8
-10^{9}	0	36.005	73.490	73.490	108.46	131.83	132.44	165.47	165.47
-10^{10}	0.1	46.292	74.748	79.376	110.58	132.78	135.78	166.28	167.42
-10^{10}	0.2	67.693	78.373	94.678	116.66	135.21	145.97	168.76	173.14
-10^{10}	0.3	83.986	90.446	115.11	126.04	140.69	161.44	173.21	182.21
-10^{11}	0.4	91.114	108.60	136.99	137.85	152.50	180.45	180.57	194.07
-10^{11}	0.5	99.303	119.21	151.27	156.55	172.54	192.64	201.85	208.10

Chapter 6

Free Vibration of Box-Type Structures

6.1 Introduction

This chapter aims to address one of the main drawbacks of the RRM, which is the difficulty in solving engineering problems involving complex structures. This problem arises because of the difficulty in building sets of admissible functions for complex structures, although in the past many researchers have used the Lagrangian Multiplier Method (Ilanko and Dickinson 1999; Klein 1974) or more recently artificial springs (Penalty Function Method) in the RRM to join structural elements (Amabili 1997; Yuan and Dickinson 1992a; Yuan and Dickinson 1992b). The advantages of the Penalty Function Method over the Lagrangian Multiplier Method are that the size of the matrices does not change when constraints are added, no zeros are introduced in the main diagonal and constraints can be modelled along a line, instead of at points. In spite of the development of these techniques, the RRM is not usually employed to solve problems with very complex geometries as these can be easily solved using commercial FEM software.

This chapter also aims to show the advantages of using the same set of admissible functions to model beams, plates and shells. In contrast Yuan and Dickinson (1992a) suggested that different sets of admissible functions composed of trigonometric and/or hyperbolic functions could be used to generate the matrices of each element. It is also worth noting that Yuan and Dickinson (1992b) suggested that the procedure could be used in structures comprising of different structural elements such as beams, plates and shells, providing that each component is in "free" condition, which is the case in the present work.

Furthermore, this chapter shows that the advantage of using a set of admissible functions that does not have a limitation in the number of terms due to ill-conditioning, also holds for complicated structures built by several elements. But in this case the benefit is more significant as a large number of terms and penalty parameters may be needed.

Yuan and Dickinson (1992a) presented solutions of box-type structures with all edges simply-supported using the RRM with the orthogonal polynomials given in (Bhat 1985). The model of the box-type structure presented by Yuan and Dickinson (1992a) was reduced to an eighth of the box using symmetry with respect to three planes. Yuan and Dickinson (1992a) also obtained results using a sine series solution, which was developed earlier by Dill and Pister (1958) and previously used by Dickinson and Warburton (1967) to obtain the natural frequencies of a steel box with side length ratio $a:b:c=1:1.25:1.5$, as well as by Dickinson (1968) to study the effect of the flexibility of the joints.

In this work the results in (Yuan and Dickinson 1992a) are used for comparison. Although for some cases similar sets of results can be found in (Dickinson 1968; Dickinson and Warburton 1967), these previous publications presented results as natural frequencies in Hertz with three significant numbers making comparison of the accuracy of the solution more difficult. For this reason, the non-dimensional results in Yuan and Dickinson (1992a) with five significant figures are used.

In this work two cubic box-type structures are analysed. One box is symmetric in the three directions and simply-supported on all edges to allow comparison with results presented by Yuan and Dickinson (1992a). The second box although still cubic, has different thickness on each plate element and two clamped edges to enforce non-symmetry.

6.2 Theoretical derivations

In this chapter results of box-type structures are presented using the RRM together with the Penalty Function Method, which is used to add constraints as well as to inter-connect the contiguous plate elements of the closed-box structures. The procedure used here is the same as the one used by (Yuan and Dickinson 1992a), although the set of admissible functions presented in Chapter 2 are used instead of the set of functions defined in (Bhat 1985). No symmetry is used to solve any of the vibration problems and penalty parameters of stiffness type or inertial type with positive or negative values are used to model constraints.

The procedure, is divided into two sections. In Section 6.2.1, two contiguous plates are inter-connected using penalty parameters, while in Section 6.2.2 the

matrices representing the stiffness and mass matrices of the box-type structure are built to formulate the eigen-problem.

6.2.1 Inter-connecting contiguous plate elements

Consider two contiguous thin plate elements (as shown in Fig. 6.1), similar to the plate element presented in Chapter 4. If subscript p is used to identify a plate, then plate element p has dimensions a_p and b_p along its local coordinates x_p and y_p, thickness h_p and flexural rigidity D_p defined as

$$D_p = \frac{E_p h_p^{\,3}}{12\left(1-\nu_p^{\,2}\right)}, \tag{6.1}$$

where ν_p is Poisson's ratio and E_p is Young's modulus.

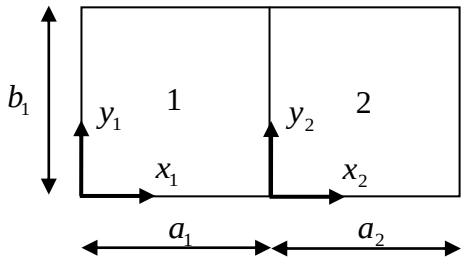

Figure 6.1. Coordinate axes and dimensions of two contiguous plate elements.

In this case, the amplitude of displacements of the plates 1 and 2 are denoted by W_1 and W_2 respectively and given by the following equations:

$$W_1(x_1,y_1) = \sum_{j}^{n}\sum_{i}^{n} c_{ij}\phi_i(x_1)\chi_j(y_1) \quad \text{and} \tag{6.2a}$$

$$W_2(x_2,y_2) = \sum_{j+n}^{2n}\sum_{i+n}^{2n} c_{ij}\phi_i(x_2)\chi_j(y_2), \tag{6.2b}$$

where the sets of admissible functions $\phi_i(x)$ and $\chi_j(x)$ are defined in Eqs. (4.2a)-(4.2d).

The process to build the stiffness and mass of each plate element in free condition is described in Chapter 4. Thus, the mass and stiffness matrices of the plates are

$$\mathbf{K}_p = a_p b_p D_p \left[\frac{1}{a_p^4} \mathbf{E}_{ki}^{(2,2)} \mathbf{F}_{lj}^{(0,0)} + \frac{1}{b_p^4} \mathbf{E}_{ki}^{(0,0)} \mathbf{F}_{lj}^{(2,2)} + \right.$$

$$\left. \frac{\nu_p}{a_p^2 b_p^2} \left[\mathbf{E}_{ki}^{(0,2)} \mathbf{F}_{lj}^{(2,0)} + \mathbf{E}_{ki}^{(2,0)} \mathbf{F}_{lj}^{(0,2)} \right] + \frac{2(1-\nu)}{a_p^2 b_p^2} \mathbf{E}_{ki}^{(1,1)} \mathbf{F}_{lj}^{(1,1)} \right], \tag{6.3}$$

$$\mathbf{M}_p = \rho_p a_p b_p h_p \mathbf{E}_{mi}^{(0,0)} \mathbf{F}_{nj}^{(0,0)}, \tag{6.4}$$

Boundary conditions along the edges of the plates are also modelled with penalty parameters in the same way as defined in Chapter 4, see Eq. (4.18).

Then, for the given example in Fig. 6.1, the strain energy of artificial stiffness to define inter-connection between the edge at $x_1 = a_1$ of plate 1 and the edge at $x_2 = 0$ of plate 2 are

$$V_{s,1-2} = \frac{1}{2} \int_0^L k \left(W_1 \big|_{x1=a1} - W_2 \big|_{x2=0} \right)^2 dy + \frac{1}{2} \int_0^L k_r \left(\left. \frac{\partial W_1}{\partial x_1} \right|_{x1=a1} - \left. \frac{\partial W_2}{\partial x_2} \right|_{x2=0} \right)^2 dy, \tag{6.5}$$

where the first term defines continuity in translation along the contiguous edges, while the second term defines continuity in rotation and k and k_r are the coefficients of the translational and rotational artificial springs per unit length.

Expanding Eq. (6.5) and developing the terms to inter-connect plates 1 and 2 gives:

$$V_{s,1-2} = \frac{1}{2}\int_0^L k\left(W_1^2\Big|_{x1=a1} - 2W_1\Big|_{x1=a1} W_2\Big|_{x2=0} + W_2^2\Big|_{x2=0}\right)dy$$

$$+\frac{1}{2}\int_0^L k_r\left(\left(\frac{\partial W_1}{\partial x_1}\right)^2\Bigg|_{x1=a1} - 2\frac{\partial W_1}{\partial x_1}\Bigg|_{x1=a1}\frac{\partial W_2}{\partial x_2}\Bigg|_{x2=0} + \left(\frac{\partial W_2}{\partial x_2}\right)^2\Bigg|_{x2=0}\right)dy \qquad (6.6)$$

In this case, to present results in non-dimensionalized form, the stiffness and mass matrices of both plates are divided by the properties of a plate p. Thus, the stiffness matrices are divided by $D_p / a_p b_p$, while the mass matrices are divided by $\rho_p a_p b_p h_p$.

Furthermore penalty matrices are non-dimensionalized using the non-dimensional parameters given in Eqs. (4.12a) and (4.12b), using the material and geometrical properties of plate p.

Then, the non-dimensional stiffness and mass matrices $\mathbf{K}$ and $\mathbf{M}$ of the system formed by stepped-plates using artificial stiffness are

$$\mathbf{K} = \begin{vmatrix} \mathbf{K}_1 + \mathbf{P}_{s,edge,1} + \mathbf{PI}_{s,1-2,1} & \mathbf{PC}_{s,1-2} \\ \mathbf{PC}_{s,1-2}^{\mathrm{T}} & \mathbf{K}_2 + \mathbf{P}_{s,edge,2} + \mathbf{PI}_{s,1-2,2} \end{vmatrix}, \quad \text{and} \qquad (6.7a)$$

$$\mathbf{M} = \begin{vmatrix} \mathbf{M}_1 & \mathbf{0} \\ \mathbf{0} & \mathbf{M}_2 \end{vmatrix}, \qquad (6.8)$$

where $\mathbf{K}_1$, $\mathbf{K}_2$, $\mathbf{M}_1$ and $\mathbf{M}_2$ are the mass and stiffness matrices of the plate elements in completely free condition given in Eqs. (6.3) and (6.4); $\mathbf{P}_{s,edge,1}$ and $\mathbf{P}_{s,edge,2}$ are the penalty matrices that define boundary conditions on plate 1 and 2, respectively; while $\mathbf{PI}_{s,1-2,1}$, $\mathbf{PI}_{s,1-2,2}$ and $\mathbf{PC}_{s,1-2}$ are the matrices that define inter-connection between plate elements.

Assuming that boundary conditions are defined only along the exterior edges of the stepped-plate, the penalty matrices that define boundary conditions are

$$\mathbf{P}_{s,edge,1} = \hat{k}\Big[\phi_k(0)\phi_i(0)\mathbf{F}_{lj}^{(0,0)} + \mathbf{E}_{ki}^{(0,0)}\chi_l(0)\chi_j(0) + \mathbf{E}_{ki}^{(0,0)}\chi_l(1)\chi_j(1) + \frac{\partial\phi_k(0)}{\partial\xi}\frac{\partial\phi_i(0)}{\partial\xi}\mathbf{F}_{lj}^{(0,0)} + \mathbf{E}_{ki}^{(0,0)}\frac{\partial\chi_l(0)}{\partial\eta}\frac{\partial\chi_j(0)}{\partial\eta} + \mathbf{E}_{ki}^{(0,0)}\frac{\partial\chi_l(1)}{\partial\eta}\frac{\partial\chi_j(1)}{\partial\eta}\Big] \quad (6.7b)$$

$$\mathbf{P}_{s,edge,2} = \hat{k}\Big[\phi_k(1)\phi_i(1)\mathbf{F}_{lj}^{(0,0)} + \mathbf{E}_{ki}^{(0,0)}\chi_l(0)\chi_j(0) + \mathbf{E}_{ki}^{(0,0)}\chi_l(1)\chi_j(1) + \frac{\partial\phi_k(1)}{\partial\xi}\frac{\partial\phi_i(1)}{\partial\xi}\mathbf{F}_{lj}^{(0,0)} + \mathbf{E}_{ki}^{(0,0)}\frac{\partial\chi_l(0)}{\partial\eta}\frac{\partial\chi_j(0)}{\partial\eta} + \mathbf{E}_{ki}^{(0,0)}\frac{\partial\chi_l(1)}{\partial\eta}\frac{\partial\chi_j(1)}{\partial\eta}\Big] \quad (6.7c)$$

The penalty matrices that define inter-connection between plates 1 and 2 are

$$\mathbf{PI}_{s,1-2,1} = \hat{k}\left(\phi_k(1)\phi_i(1)\mathbf{F}_{lj}^{(0,0)} + \frac{\partial\phi_k(1)}{\partial\xi}\frac{\partial\phi_i(1)}{\partial\xi}\mathbf{F}_{lj}^{(0,0)}\right), \quad (6.7d)$$

$$\mathbf{PI}_{s,1-2,2} = \hat{k}\left(\phi_k(0)\phi_i(0)\mathbf{F}_{lj}^{(0,0)} + \frac{\partial\phi_k(0)}{\partial\xi}\frac{\partial\phi_i(0)}{\partial\xi}\mathbf{F}_{lj}^{(0,0)}\right), \quad (6.7e)$$

$$\mathbf{PC}_{s,1-2} = -\hat{k}\left(\phi_k(0)\phi_i(1)\mathbf{F}_{lj}^{(0,0)} + \frac{\partial\phi_k(0)}{\partial\xi}\frac{\partial\phi_i(1)}{\partial\xi}\mathbf{F}_{lj}^{(0,0)}\right) \quad (6.7f)$$

As in all other cases in this thesis, penalty matrices defined by artificial inertia are identical to the penalty matrices defined by artificial springs when the non-dimensional penalty parameter $\hat{k}$ is substituted by $\hat{m}$.

6.2.2 Box-type structures

The box type structures modelled in this work are built by six plates as shown in Fig. 6.2. It is important to note that to model closed-boxes the coordinate systems of the plates have been defined in such a way that a point on any edge of the box

has the same value on both axes of the adjacent plates. For instance, plates four and five have a contiguous edge. Every point on this edge has the same location on axes y_4 and x_5. This allows carrying out the integrations in a straight forward way, without having to perform a coordinate transformation.

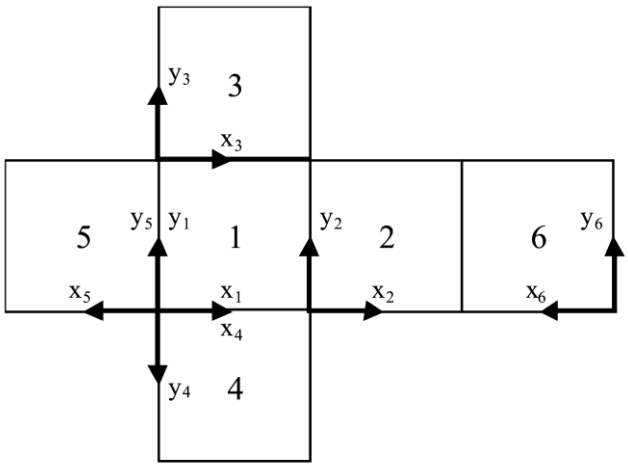

Figure 6.2. Unfolded box-type structure.

The procedure to build the stiffness and mass matrices of the whole box-type structure is the same as in 6.2.1, except for two points. First, it is assumed that stretching of the middle surface of each plate of a closed-box structure is neglected as in the work by Yuan and Dickinson (1992a). This causes a constraint in translation in all edges or in other words, creates a simply-supported condition on all edges of the box. Second, as translation is already constrained, coupling between plates is defined only by rotational springs.

It is also important to note here that as not all local coordinate systems of the plates are aligned in the same direction, the minus sign of the second term in

Eq. (6.6) that defines coupling in rotation changes to positive, when plates 2 and 3 and plates 4 and 5 are inter-connected.

With the present approach it is possible to add rotational constraints to any edge of the box to create a clamped condition, as well as translational and/or rotational point and/or line constraints in the interior of any plate of the box.

Results are again presented in non-dimensional form defined as

$$\lambda = \omega a_p^2 \sqrt{\frac{\rho_p h_p}{D_p}}, \tag{6.9}$$

where ω is the circular natural frequency of the plate.

The first box-type structure analyzed in this work is built by identical square plates, while the plates of the second structure are square plates of the same size and differ only in thickness. Then for both cases, results were non-dimensionalized using the properties of plate 2 to keep the thickness to side length ratio $a / h_2 = 100$, where a is the length of all sides of the box and h_2 is the thickness of plate 2.

6.3 Results and discussion

Results in this chapter are the average of the last pair of results with monotonic convergence of each type of penalty parameter with the same magnitude, but opposite sign. In both cases presented in this chapter, the average of the results using inertial penalty parameters matched the results using stiffness type penalty parameters up to the fifth significant figure. Results were obtained setting the

penalty parameters of stiffness and inertial type with values equal to $\pm 10^{p}$, where $p \in [1,2,3,...]$.

As mentioned earlier, results of two box-type structures built from six plate elements as shown in Fig.6.2 are presented in this work. The first box case corresponds to a simply-supported cubic box. The second case corresponds to a non-symmetrical cubic box. The non-symmetry of the box is due to the different thickness of each plate of the box and two non-symmetric boundary conditions. The normalized thickness of plates 1 to 6 can be described by the ratio $1:2:3:4:5:6 = 0.8:1:1.2:1.4:1.6:1.8$ when normalized with respect to the thickness of plate 2. The boundary conditions of the box are clamped conditions on edges at $\xi_1 = 0$ and $\eta_1 = 1$ of plate 1, while all other edges are simply supported. See Fig. 6.2 for the corresponding identification number of each plate. Results for this case are compared with the results obtained using the FEM program ABAQUS, as these results do not exist in the literature.

6.3.1 Frequency parameters of a box-type structure completely simply-supported

The purpose of producing results of a simply supported cubic box was to build a base line for comparisons between the results presented by Yuan and Dickinson (1992a) and the method proposed here. Yuan and Dickinson simplified the model to an eighth of the box and modelled the edges of the box as simply-supported, while the edges of the plates on the planes of symmetry were treated as sliding or simply supported to model symmetric or antisymmetric modes.

Table 6.1. Frequency parameters of a completely SS cubic closed box.

Approach	Sine series	Orthog. Polynom.	Present	Present	ABAQUS
No. terms	$n=4$	$n=8$	$n=15$	$n=20$	
Active DOFs	12	192	858	1728	37860
Penalty stiffness			$\widehat{k}=10^{13}$	$\widehat{k}=10^{13}$	
Penalty inertia			$\hat{m}=10^{11}$	$\hat{m}=10^{11}$	
Mode					
1	24.884	24.887	24.897	24.891	24.864
2	24.884	24.887	24.897	24.891	24.865
3	27.422	27.424	27.436	27.429	27.401
4	27.422	27.424	27.436	27.429	27.402
5	27.422	27.424	27.436	27.429	27.405
6	35.988	35.985	36.005	35.994	35.988
7	52.511	52.515	52.549	52.526	52.539
8	52.511	52.515	52.549	52.526	52.542
9	52.511	52.515	52.549	52.526	52.549
10	58.201	58.206	58.249	58.219	58.282
11	58.201	58.206	58.249	58.219	58.284
12	58.201	58.206	58.249	58.219	58.294
13	63.938	63.941	64.002	63.962	64.022
14	63.938	63.941	64.002	63.962	64.031
15	63.938	63.941	64.002	63.962	64.040
16	70.236	70.239	70.321	70.263	70.385
17	70.236	70.239	70.321	70.263	70.398
18	70.236	70.239	70.321	70.263	70.406
19	87.376	87.388	87.494	87.417	87.406
20	87.376	87.388	87.494	87.417	87.425
21	93.716	93.729	93.865	93.771	93.783
22	93.716	93.729	93.865	93.771	93.793
23	93.716	93.729	93.865	93.771	93.820
24	98.696	98.697	98.743	98.717	99.074
25	101.75	101.76	101.85	101.80	102.10
26	101.75	101.76	101.85	101.80	102.13
27	108.21	108.22	108.46	108.29	108.41

The results by Yuan and Dickinson (1992a) were obtained using two methods. The first set of results was obtained using orthogonal polynomials as published by Bhat (1985) in the RRM, setting the number of terms in both sets of admissible functions to $n=8$. This is equivalent to setting $n=15$ in the present work as each plate of the box is represented in full scale. The second set of results in Yuan and Dickinson (1992a) were obtained using the sine series solution using 4 terms for

each direction x, y and z. These results were reported to be accurate at least to four significant figures (Yuan and Dickinson 1992a). Unfortunately, while sine functions work well for SSSS plates, numerical experiments show that modelling CCCC plates with a sine series and rotational artificial stiffness, does not practically lead to fully converged results.

Table 6.1 presents the results obtained using the present approach, both sets of results in Yuan and Dickinson (1992a) and the results obtained in the finite element program ABAQUS. The FEM of the completely simply-supported cubic box was built using free meshing capabilities in ABAQUS using 90 S3 shell elements and 7639 S4R shell elements, giving 37860 unrestrained DOF. The finite element model included a relatively high number of DOF to give frequencies close to the published results in all of the 27 modes presented in Table 6.1.

6.3.2 Frequency parameters of a non-symmetrical box-type structure

The second set of results corresponds to a cubic box formed by plates of the same material, but different thickness. Boundary conditions also contribute to the non-symmetry by clamping edges at $\xi_1 = 0$ and $\eta_1 = 1$ of plate 1. Table 6.2 only shows results obtained by the present approach and ABAQUS as no results for non-symmetrical boxes were found in the literature.

Table 6.2. Frequency parameters of a cubic closed box with two adjacent clamped edges and different wall thickness on each side.

Approach	Present	Present	ABAQUS	ABAQUS	ABAQUS
No. terms	$n=15$	$n=20$			
Active DOFs	836	1696	28963	46047	53470
Penalty stiffness	$\widehat{k}=10^{14}$	$\widehat{k}=10^{14}$			
Penalty inertia	$\hat{m}=10^{11}$	$\hat{m}=10^{11}$			
Mode					
1	32.840	32.831	32.835	32.822	32.820
2	37.089	37.077	37.049	37.039	37.034
3	45.749	45.731	45.626	45.607	45.602
4	46.270	46.255	46.193	46.175	46.173
5	52.301	52.280	52.111	52.087	52.079
6	62.789	62.769	62.660	62.632	62.622
7	67.841	67.797	67.964	67.921	67.849
8	70.758	70.703	70.943	70.848	70.784
9	78.485	78.438	78.562	78.478	78.414
10	81.582	81.522	81.719	81.640	81.556
11	95.920	95.859	95.981	95.878	95.783
12	98.800	98.734	98.756	98.647	98.580
13	100.63	100.56	100.63	100.53	100.43
14	104.07	104.00	104.13	104.01	103.91
15	105.21	105.09	105.35	105.21	105.13
16	118.62	118.54	118.45	118.34	118.22
17	120.26	120.14	120.27	120.07	119.97
18	123.31	123.22	123.25	123.10	122.96
19	125.02	124.92	125.80	125.52	125.21
20	128.32	128.21	128.74	128.47	128.30
21	132.77	132.65	133.11	132.83	132.64
22	137.00	136.89	136.90	136.72	136.54
23	147.48	147.37	148.13	147.88	147.60
24	149.50	149.35	149.83	149.56	149.34
25	152.45	152.30	152.93	152.66	152.38
26	156.64	156.46	156.72	156.46	156.28
27	159.14	158.91	160.01	159.55	159.29

Once again the finite element model included a relatively high number of DOFs to give frequencies close to the results obtained by the procedure proposed in this work for all of the 27 modes presented in Table 6.2.

6.3.3 Concluding remarks

In both cases, the results of the present RRM approach where a set of admissible functions derived in Chapter 2, together with penalty terms as needed give close approximations to those used for comparisons. Although results given by Yuan and Dickinson (1992a) are closer to the exact solution, the set of admissible functions given here is simpler. Thus, with the present method, it is easier to define the terms to build the mass and stiffness matrices, as well as the matrices to define boundary conditions or inter-connect structural elements, which are formed by artificial stiffness or inertia. In fact, using this approach the vibration problems of a box-type structure can be solved with only one code regardless of the number of terms, boundary conditions, or geometry of the box.

Another advantage of the set of admissible functions used here in comparison with the set presented in (Bhat 1985) is that no orthonormalization or orthogonalization is required to build the set of admissible functions. This makes very easy to increase the maximum number of terms n included in the solution.

It is also worth noting that it is advantageous to use the same set of admissible functions to define the deflection of several types of structural elements in completely free conditions. This is because many matrices will be commonly used by the different types of elements and especially in the penalty matrices. For instance, the penalty matrices to define a constraint along an edge in a single DOF are identical for plates and shells, although for the latter, this would be just a submatrix.

In the next chapter, the procedure using the RRM together with the Penalty Function Method is described to solve structural stability problems of beams and frames.

Chapter 7

Buckling of Beams and Frames

7.1 Introduction

This chapter aims to extend the penalty parameter family showing that it is possible to use penalty parameters of geometric stiffness type to solve structural stability problems of Euler-Bernoulli beams. This is the same type of element presented in Chapter 3.

The use of penalty parameters of geometrical stiffness type is backed-up by a recent publication (Ilanko and Williams 2008), where a general mathematical proof has been presented to show that in linear eigenvalue problems, positive and negative penalty terms can be applied to the system matrix associated with the eigenvalue. In (Ilanko and Williams 2008) this type of penalty parameter has been referred to as the "eigenpenalty parameter", while the penalty parameter of stiffness type is called "ordinary penalty parameter". In (Ilanko and Williams 2008) the application was limited to a vibration problem where the eigenpenalty parameter is the inertial penalty parameter introduced in (Ilanko 2005b).

This chapter presents solutions for critical loads of tapered beams with different boundary conditions, a CC tapered beam with 49 intermediate constraints and a CC two-beam frame. In all cases the proposed set of admissible functions defined in Chapter 2 were used in the RRM and all constraints and inter-connections were modelled with ordinary and eigenpenalty parameters of positive and negative values.

Again, as in the previous chapters the monotonic convergence and bracketing of the constraint solution by a pair of results obtained by penalty parameters of the same type and magnitude, but opposite sign are used to avoid numerical instabilities.

7.2 Theoretical derivations

In order to simplify the theoretical derivations of the cases presented in this work and because the vibration problem for straight beams has already been presented in Chapter 3, only the theoretical derivations of the tapered beam and the procedure to inter-connect beams to form a two-beam frame are given below. The derivations for straight beams can be easily obtained from the equations modelling a tapered beam.

It is important to note that distortions of the cross-section of the beam are not taken into account in this work as in a recent paper by Andrade *et al.* (2007), where the RRM was used to determine the critical loads of a tapered *I*-beam, which gave close results to those obtained using the FEM software ABAQUS.

7.2.1 Tapered beam

The first example analyses the equilibrium of tapered beams of varying second moment of area $I(x)$ subject to an axial compressive force P as shown in Fig 7.1. The relevant second moment of area of the beam at the left end is denoted by I_0. The beam is made of a homogeneous material of elastic modulus E and is of length L. The cross-section of the beam is taken as solid circular, with the variation of the radius of the cross-section given by

$$r(x)=\left(r_0-\frac{x}{L}(r_0-r_L)\right), \tag{7.1}$$

where r_0 is the radius at the origin and r_L is the radius at the opposite end $x=L$.

The second moment of area $I(x)$ of the beam is

$$I(x)=\frac{\pi(r(x))^4}{4} \tag{7.2}$$

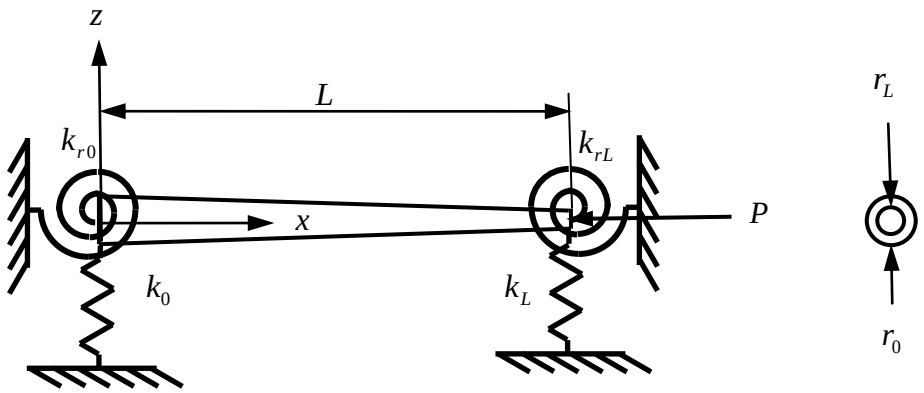

Figure 7.1. Tapered beam under compression axial force constrained by spring elements.

Again the method to solve the stability analysis of the beam proposed here is to use the RRM with the set of admissible functions that model the deflection of a

FF beam presented in Chapter 2 together with penalty parameters to model all constraints. For completeness the set of functions is given below

$$\phi_i = \left(\frac{x}{L}\right)^{i-1} \qquad \text{for } i = 1,2,3 \tag{7.3a}$$

$$\phi_i(x) = \cos\frac{(i-3)\pi x}{L} \qquad \text{for } i = 4,5,\ldots n \tag{7.3b}$$

where n is the number of terms used in the set of admissible functions.

For a single structural unit the amplitude of the displacement may be expressed by a single series $W(x)$, as follows:

$$W(x) = \sum_{i=1}^{n} c_i \phi_i(x) \tag{7.4}$$

where c_i are unknown coefficients.

The potential energy of an Euler-Bernoulli beam due to bending is given by

$$V_{max} = \frac{EI}{2}\int_0^L \left(\frac{\partial^2 W}{\partial x^2}\right)^2 dx \tag{7.5}$$

The potential energy due to an axial compressive force P is given by

$$V_a = -\int_0^L \frac{P}{2}\left(\frac{\partial W}{\partial x}\right)^2 dx \tag{7.6}$$

As mentioned earlier, each constraint condition not satisfied by the set of admissible functions needs to be incorporated through the use of penalty functions. This may be achieved by including an energy term associated with an

artificial spring of large stiffness or an eigenpenalty parameter into the total potential energy.

Then, the strain energy of artificial translational and rotational springs of very large stiffness k_x and k_{rx} at a point x is given by

$$V_s = \frac{k_x}{2} W^2\Big|_x + \frac{k_{rx}}{2}\left(\frac{\partial W}{\partial x}\right)^2\Bigg|_x \tag{7.7a}$$

For instance, for a clamped-clamped beam, four penalty functions are necessary to enforce the four needed constraints. These include translational constraints at $x = 0$ and $x = L$ as well as rotational constraints at $x = 0$ and $x = L$ as follows:

$$V_s = \frac{k_0}{2} W^2\Big|_{x=0} + \frac{k_L}{2} W^2\Big|_{x=L} + \frac{k_{r0}}{2}\left(\frac{\partial W}{\partial x}\right)^2\Bigg|_{x=0} + \frac{k_{rL}}{2}\left(\frac{\partial W}{\partial x}\right)^2\Bigg|_{x=L}, \tag{7.8a}$$

where the stiffness coefficients k_x and k_{rx} serve as penalty parameters.

From the principle of stationary potential energy, the total potential energy of the structural system must be a minimum for a stable equilibrium. The Rayleigh-Ritz minimisation with ordinary penalty term would be of the form:

$$\left(\frac{\partial V_{max}}{\partial c_i} + \frac{\partial V_s}{\partial c_i}\right) - P_c\left(\frac{\partial V_a^*}{\partial c_i}\right) = 0, \tag{7.9a}$$

where the eigenvalue P_c is the critical load and $V_a^* = V_a / P$ is the geometric stiffness function, independent from the load.

The purpose of using large values for the penalty parameter is to minimise the value of the terms that are being multiplied by this parameter, thus constraining a

degree of freedom. This can also be achieved by including the penalty energy function as part of the geometric potential energy. In this case, the energy terms of artificial translational geometric stiffness γ and rotational geometric stiffness γ_r at a point x are given by

$$V_g = P\left(\frac{\gamma_x}{2}W^2\Big|_x + \frac{\gamma_{rx}}{2}\left(\frac{\partial W}{\partial x}\right)^2\Bigg|_x\right) \tag{7.7b}$$

Therefore the potential energy due to artificial translational and rotational geometric stiffness to model a clamped-clamped beam is

$$V_g = P\left(\frac{\gamma_0}{2}W^2\Big|_{x=0} + \frac{\gamma_L}{2}W^2\Big|_{x=L} + \frac{\gamma_{r0}}{2}\left(\frac{\partial W}{\partial x}\right)^2\Bigg|_{x=0} + \frac{\gamma_{rL}}{2}\left(\frac{\partial W}{\partial x}\right)^2\Bigg|_{x=L}\right) \tag{7.8b}$$

In this case, the eigenpenalty terms are multiplied by the axial force P in the same way the inertial penalty terms are multiplied by the square of the natural frequencies in vibration analysis. The derivations in (Ilanko and Williams 2008), although explained in the context of a vibratory system, are also applicable for structural stability analysis. The Rayleigh-Ritz minimisation equation when artificial geometric stiffness is used to enforce constraints is

$$\left(\frac{\partial V_{max}}{\partial c_i}\right) - P_c\left(\frac{\partial V_a^*}{\partial c_i} + \frac{\partial V_g^*}{\partial c_i}\right) = 0, \tag{7.9b}$$

where $V_g^* = V_g / P$ is the artificial geometric stiffness function, independent from the load.

For convenience results are presented in non-dimensional form. This is achieved introducing a non-dimensional axial coordinate, dividing the stiffness and

geometrical stiffness matrices obtained from the minimization of the terms defined in Eqs. (7.5) and (7.6) by EI_0 / L^3 and by $1/L$ respectively and introducing non-dimensional penalty parameters in either Eq. (7.8a) or Eq. (7.8b) depending on the choice of penalty parameter used in the solution. These non-dimensional parameters are defined as follows:

- non-dimensional axial coordinate

$$\xi = x / L \tag{7.10}$$

- tapering ratio

$$\hat{\rho} = \frac{r_L}{r_0} \tag{7.11}$$

- elastic translational and rotational non-dimensional stiffness penalty parameter

$$\hat{k} = \frac{kL^3}{EI_0} = \frac{k_r L}{EI_0}, \tag{7.12a}$$

- translational and rotational non-dimensional geometric stiffness penalty parameter

$$\hat{g} = \gamma L = \frac{\gamma_r}{L} \tag{7.12b}$$

Then the Rayleigh-Ritz minimization using artificial elastic springs and non-dimensional parameters gives:

$$[\mathbf{K} + \mathbf{P}_s]\{\mathbf{c}\} - \lambda[\mathbf{G}]\{\mathbf{c}\} = \{\mathbf{0}\} \tag{7.13a}$$

where $\mathbf{K}$, $\mathbf{G}$ and $\mathbf{P}_s$ are the elastic stiffness, geometric stiffness and penalty matrices, while $\mathbf{c}$ is a vector of unknown coefficients and λ is the non-dimensional critical load defined as

$$\lambda = \frac{P_c L^2}{EI_0}, \tag{7.14}$$

Similarly, if eigenpenalty parameters are used, the Rayleigh-Ritz minimization gives:

$$[\mathbf{K}]\{\mathbf{c}\} - P_c[\mathbf{G} + \mathbf{P}_g]\{\mathbf{c}\} = \{\mathbf{0}\} \tag{7.13b}$$

Then the non-dimensional elastic stiffness, geometric stiffness and penalty matrices are

$$\mathbf{K} = \mathbf{E}_{ki}^{(2,2)}, \tag{7.15}$$

$$\mathbf{G} = \mathbf{E}_{ki}^{(1,1)}, \tag{7.16}$$

where

$\mathbf{E}_{ki}^{(r,s)} = \int_0^L \left(\frac{d^r \phi_k}{d\xi^r}\right)\left(\frac{d^s \phi_i}{d\xi^s}\right) d\xi$, and

$$\mathbf{P}_s = (\hat{k})\left(\phi_k(0)\phi_i(0) + \phi_k(1)\phi_i(1) + \frac{\phi_k(0)}{\partial\xi}\frac{\phi_i(0)}{\partial\xi} + \frac{\phi_k(1)}{\partial\xi}\frac{\phi_i(1)}{\partial\xi}\right), \tag{7.17a}$$

$$\mathbf{P}_g = (\hat{\gamma})\left(\phi_k(0)\phi_i(0) + \phi_k(1)\phi_i(1) + \frac{\phi_k(0)}{\partial\xi}\frac{\phi_i(0)}{\partial\xi} + \frac{\phi_k(1)}{\partial\xi}\frac{\phi_i(1)}{\partial\xi}\right) \tag{7.17b}$$

It is important to note that intermediate constraints on the beam can be modelled using either artificial stiffness (ordinary penalty term) or artificial geometric stiffness (eigenpenalty term) using either Eq. (7.7a) or Eq. (7.7b).

7.2.2 A two-beam frame

The second type of structure analyzed in this chapter is a simple two-beam frame consisting of two identical beams of length L and homogeneous material of flexural rigidity EI under a load P equally distributed on both beams. Each beam is fully constrained at the origin and joined to the other beam at an angle θ at $x = L$ as shown in Fig. 7.2. In section 7.3 results for frames at different angles θ are presented.

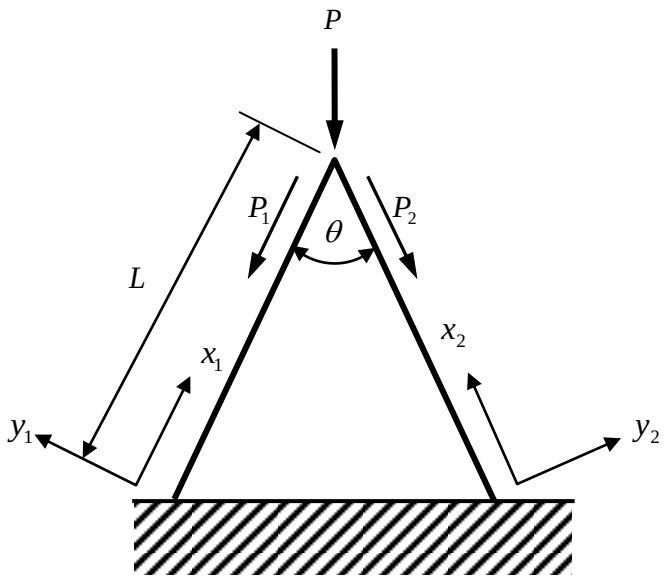

Figure 7.2. Two-beam frame under a compression force P.

The procedure in this section starts with the definition of the energy equations of the system. These energy equations are given in the following order: potential energy of the beams due to bending; potential energy due to axial compressive load; energy to define inter-connection of the beams using penalty parameters; energy to define boundary conditions. After all energy terms are defined the Rayleigh-Ritz minimization is carried out to define the matrices of the system and

then the eigen-problem is solved with a specific set of boundary conditions and angle between beams θ.

In this case, the amplitudes of the displacement of the left and right beams are denoted by W_1 and W_2 respectively and given by the following equations:

$$W_1(x_1) = \sum_{i=1}^{n} c_i \phi_i(x_1) \quad \text{and} \tag{7.18a}$$

$$W_2(x_2) = \sum_{i=1+n}^{2n} c_{i+n} \phi_i(x_2), \tag{7.18b}$$

where the sets of admissible functions $\phi_i(x)$ are defined in Eqs. (7.3a,7.3b).

The total potential energy of the two-beam frame due to bending is

$$V_{max} = \frac{EI}{2} \int_0^{L_1} \left(\frac{\partial^2 W_1}{\partial {x_1}^2} \right)^2 dx_1 + \int_0^{L_2} \frac{EI}{2} \left(\frac{\partial^2 W_2}{\partial {x_2}^2} \right)^2 dx_2 \tag{7.19}$$

The potential energy due to an axial compressive force P is

$$V_a = -\int_0^{L_1} \frac{P_1}{2} \left(\frac{\partial W_1}{\partial x_1} \right)^2 dx_1 - \int_0^{L_2} \frac{P_2}{2} \left(\frac{\partial W_2}{\partial x_2} \right)^2 dx_2 \tag{7.20}$$

where P_1 and P_2 are the axial loads acting on the beams as shown in Fig. 7.2.

Then, for symmetry

$$P_1 = P_2 = \frac{P}{2\cos(\theta/2)} \tag{7.21}$$

The necessary ordinary penalty functions to define the interconnection of two aligned beams as given in (Yuan and Dickinson 1992b) are

$$V_{s,1-2} = \frac{k}{2}\left(W_1\big|_{x=L} - W_2\big|_{x=L}\right)^2 + \frac{k_r}{2}\left(\frac{\partial W_1}{\partial x_1}\bigg|_{x=L} + \frac{\partial W_2}{\partial x_2}\bigg|_{x=L}\right)^2 \tag{7.22}$$

Thus, the degrees of freedom at the end of both beams are fully coupled when springs of very large stiffness (positive or negative) are used to model the inter-connections, making the difference of the relative translation and change in the slope between the end-points of both beams equal to zero. It is important to mention, that in this case the sign inside the second parenthesis of Eq. (7.22) is positive because of the coordinate used (see Fig. 7.2).

Another relevant point is that when beams are joined to form a two-beam frame ($\theta \neq 180°$) instead of a stepped-beam, it is necessary to include an extra translational penalty parameter modelling a pin at the joint. This is because the transverse displacement of beams at the joint is negligible when they form part of a frame, as their axial stiffness is substantially greater than their transverse stiffness. This effect holds for a large range of the angle θ between the beams shown in Fig. 7.2. The extra constraint can be added to either of the beams at the joint multiplying the translational penalty parameter at $x = L$ by two, but in this work the extra constraint is added to the first beam.

Then, expanding Eq. (7.22) and adding the extra constraint to model a frame ($\theta \neq 180°$) gives:

$$V_{s,1-2,\theta} = \frac{k}{2}\left(2\left(W_1\big|_{x=L}\right)^2 - 2W_1\big|_{x=L} W_2\big|_{x=L} + \left(W_2\big|_{x=L}\right)^2\right)$$

$$+\frac{k_r}{2}\left(\left(\left.\frac{\partial W_1}{\partial x_1}\right|_{x=L}\right)^2+\left.\frac{\partial W_1}{\partial x_1}\right|_{x=L}\left.\frac{\partial W_2}{\partial x_2}\right|_{x=L}+\left(\left.\frac{\partial W_2}{\partial x_2}\right|_{x=L}\right)^2\right) \tag{7.23}$$

It is possible to observe in Eq. (7.23) that, without the extra constraint, the first and last penalty terms in translation and rotation are the same energy terms that could define boundary conditions at $x=L$ on beam 1 and 2, respectively. The other two terms in translation and rotation define the coupling between the beams.

Boundary conditions at the origin of each beam are defined in the exact same way as in Section 7.2.1. Thus, the energy terms to define boundary conditions using artificial stiffness are

$$V_s=\hat{k}\left(W_1|_0 W_1|_0+W_2|_0 W_2|_0+\left.\frac{\partial W_1}{\partial x}\right|_0\left.\frac{\partial W_1}{\partial x}\right|_0+\left.\frac{\partial W_2}{\partial x}\right|_0\left.\frac{\partial W_2}{\partial x}\right|_0\right) \tag{7.24}$$

Once again, the Rayleigh-Ritz minimisation with ordinary penalty term would be of the form:

$$\left(\frac{\partial V_{max}}{\partial c_i}+\frac{\partial V_s}{\partial c_i}+\frac{\partial V_{s,1-2,\theta}}{\partial c_i}\right)-P_c\left(\frac{\partial V_a^*}{\partial c_i}\right)=0 \tag{7.25}$$

where $V_a^*=V_a/P$

To define the two-beam frame problem in non-dimensional terms, some of the non-dimensional parameters in 7.2.1 are introduced in the solution. These are the non-dimensional axial coordinate defined in Eq. (7.10) and the non-dimensional penalty parameters in Eqs. (7.12a) and (7.12b). To obtain results in non-

dimesional form it is also necessary to divide Eq. (7.19) by EI / L^3 and Eq. (7.20) by $1/L$.

Then, after the Rayleigh-Ritz minimization of the non-dimensional system, the eigen-problem is defined as

$$\begin{bmatrix} \mathbf{K}_1 + \mathbf{P}_{s,1} & \mathbf{PC}_{s,1-2} \\ \mathbf{PC}_{s,1-2}^{\mathrm{T}} & \mathbf{K}_2 + \mathbf{P}_{s,2} \end{bmatrix} \{\mathbf{c}\} - \lambda \begin{bmatrix} \mathbf{G}_1 & \mathbf{0} \\ \mathbf{0} & \mathbf{G}_2 \end{bmatrix} \{\mathbf{c}\} = \{\mathbf{0}\}, \tag{7.26a}$$

where $\mathbf{P}_{s,1}$, $\mathbf{P}_{s,2}$ and $\mathbf{PC}_{s,1-2}$ are the penalty matrices due to artificial elastic stiffness,

Alternatively, eigenpenalty parameters can be used to define constraints. In this case, it is enough to include the penalty matrices in the geometric stiffness matrix, substituting the ordinary penalty parameter $\hat{k}$ by the eigenparameter $\hat{\gamma}$. This gives the following eigen-problem:

$$\begin{bmatrix} \mathbf{K}_1 & 0 \\ 0 & \mathbf{K}_2 \end{bmatrix} \{\mathbf{c}\} - \lambda \begin{bmatrix} \mathbf{G}_1 + \mathbf{P}_{g,1} & \mathbf{PC}_{g,1-2} \\ \mathbf{PC}_{g,1-2}^{T} & \mathbf{G}_2 + \mathbf{P}_{g,2} \end{bmatrix} \{\mathbf{c}\} = \{\mathbf{0}\}, \tag{7.26b}$$

where $\mathbf{P}_{g,1}$, $\mathbf{P}_{g,2}$ and $\mathbf{PC}_{g,1-2}$ are the penalty matrices due to artificial geometric stiffness.

In this case the non-dimensional critical load is defined as

$$\lambda = \frac{P_c L^2}{EI}, \tag{7.27}$$

Then the non-dimensional stiffness, geometric stiffness and penalty matrices included in Eqs. (7.26a) and (7.26b) are

$$\mathbf{K}_1 = \mathbf{K}_2 = \mathbf{E}_{ki}^{(2,2)}, \tag{7.28}$$

$$\mathbf{G}_1 = \mathbf{G}_2 = \frac{1}{2\cos(\theta/2)}\mathbf{E}_{ki}^{(1,1)}, \tag{7.29}$$

where

$$\mathbf{E}_{ki}^{(r,s)} = \int_0^1 \left(\frac{d^r \phi_k}{d\xi^r}\right)\left(\frac{d^s \phi_i}{d\xi^s}\right) d\xi,$$

$$\mathbf{P}_{s,1} = \hat{k}\left(\phi_k(0)\phi_i(0) + 2\phi_k(1)\phi_i(1) + \frac{\phi_k(0)}{\partial\xi}\frac{\phi_i(0)}{\partial\xi} + \frac{\phi_k(1)}{\partial\xi}\frac{\phi_i(1)}{\partial\xi}\right), \tag{7.30a}$$

$$\mathbf{P}_{s,2} = \hat{k}\left(\phi_k(0)\phi_i(0) + \phi_k(1)\phi_i(1) + \frac{\phi_k(0)}{\partial\xi}\frac{\phi_i(0)}{\partial\xi} + \frac{\phi_k(1)}{\partial\xi}\frac{\phi_i(1)}{\partial\xi}\right), \tag{7.30b}$$

$$\mathbf{PC}_s = \hat{k}\left(-\phi_k(1)\phi_i(1) + \frac{\phi_k(1)}{\partial\xi}\frac{\phi_i(1)}{\partial\xi}\right), \tag{7.30c}$$

Similarly, penalty matrices due to artificial geometric stiffness ($\mathbf{P}_{g,1}$, $\mathbf{P}_{g,1}$ and $\mathbf{PC}_g$) can be obtained substituting $\hat{k}$ by $\hat{\gamma}$ in Eqs. (7.30a-7.30c).

7.3 Results and discussion

As in the previous chapters, the solution of the proposed method uses penalty functions to model constraints and inter-connections of the beam, which results in an asymptotic analysis to obtain the critical loads of the structures.

As mentioned earlier in this chapter the structural stability analysis is carried out using positive and negative non-dimensional penalty parameters of elastic stiffness and geometric stiffness type with values equal to $\pm 10^p$, where $p \in [1,2,3,...]$.

All sets of results correspond to the set of results in which convergence up to the fifth significant figure was reached or to the last set of results before monotonic convergence was interrupted.

This section shows the results of tapered beam cases. Results using the RRM and penalty parameters were compared with results obtained using the RRM together with the Lagrangian Multiplier Method and the FEM with standard beam elements. The matrices defining the elastic stiffness and geometrical stiffness of a beam element in the FEM are defined in Appendix A. In the Penalty Function Method as well as in the Lagrangian Multiplier Method, the same set of displacement functions were used in the Rayleigh-Ritz procedure so that the effect of constraint violation would be the only cause of any discrepancy. For the same reason, all results were obtained from codes written for MATLAB, including the FEM results. In the FEM solution each element used to build the tapered beam model has a constant radius, but the radius of each element decreases (for $\hat{\rho} < 1$) or increases (for $\hat{\rho} > 1$) as to have the same radius as the tapered beam at the centre of each element.

7.3.1 Critical loads of CC tapered beam varying the number of DOFs

First, tapered beams with CC boundary conditions and tapering ratio $\hat{\rho} = 2$ were analyzed to show the convergence with respect to the number of terms used in the set of admissible functions as shown in Table 7.1. Critical loads in Table 7.1 were obtained using 10, 20, 50 and 100 terms in the RRM (for both, the Penalty Method and the Lagrangian Multiplier Method) and 5, 10, 25 and 50 elements in

the FEM. In all approaches, four degrees of freedom (DOF) were eliminated by the applied constraints.

It is worth noting that when Lagrangian multipliers are used to define the constraints of a system, the elastic stiffness and geometric stiffness matrices of the system increases by one row and one column for each applied constraint.

Results in Table 7.1 show that the Penalty Function Method gives the same results as the Lagrangian Multiplier Method which models the constraints exactly. From the results it was also observed that the RRM requires fewer DOFs to converge than the FEM, even when boundary conditions are applied through penalty parameters in the RRM. For instance the accuracy obtained with the RRM containing 16 active DOFs is slightly better than the results obtained with the FEM containing 96 DOFs. This can be stated because results from the RRM are upperbounds and in all cases in Table 7.1 the results using the RRM are slightly lower than the results from the FEM. On the other hand, the band-width of the stiffness and geometrical stiffness of the beam in the FEM are smaller in comparison with the matrices of the same number of DOFs using the RRM. A test solving a CC beam with $\hat{\rho} = 2$ using the RRM with 16 DOFs show that it is 30% faster than the FEM with 196 DOFs. A second test with elastic stiffness and geometric stiffness matrices of size 96x96 in both methods, showed that the solution using FEM was six and a half times faster than a single run of the eigen-problem defined by the RRM with penalty parameters. It is also worth noting that the RRM used together with the Penalty Function Method is an asymptotic

method and requires several runs with different penalty values to find the converged results due to constraint violation.

Table 7.1. Critical loads of CC beams with tapering ratio $\hat{\rho} = 2$.

DOF	Method	Penalty Value	P_c		
		$+\hat{k},-\hat{k},+\hat{g},-\hat{g}$	1	2	3
6	RRM & Penalty	$10^8,10^8,10^6,10^5$	158.45	330.09	667.44
	RRM & Lagrangian		158.45	330.09	667.44
	FEM		169.33	320.99	761.74
16	RRM & Penalty	$10^7,10^9,10^6,10^5$	157.93	323.19	631.78
	RRM & Lagrangian		157.93	323.19	631.78
	FEM		159.58	327.52	647.56
46	RRM & Penalty	$10^8,10^7,10^5,10^5$	157.91	323.06	631.66
	RRM & Lagrangian		157.91	323.06	631.66
	FEM		158.11	323.47	632.68
96	RRM & Penalty	$10^7,10^9,10^6,10^5$	157.91	323.05	631.65
	RRM & Lagrangian		157.91	323.05	631.65
	FEM		157.96	323.15	631.85

7.3.2 Critical loads of CC tapered beam varying the penalty value

This section presents again results for a CC beam with tapering ratio $\hat{\rho} = 2$. But in this case, the convergence of the results due to the penalty value is investigated.

Table 7.2 shows the convergence of the critical loads with respect to the magnitude of the penalty parameters with solutions including 96 DOFs. As in all previous chapters, numerical instabilities occurred only when very large penalty parameters were used and were not found to be associated with the number of terms included in the series.

Table 7.2. Convergence of the critical loads of CC beams with tapering ratio $\hat{\rho} = 2$ with respect to the penalty parameters.

Penalty Type	Penalty Value	P_c 1	2	3
$+\hat{k}$	10^1	18.302	72.239	199.26
	10^2	76.570	136.50	306.24
	10^3	153.08	277.70	531.94
	10^4	157.47	319.96	629.82
	10^5	157.87	322.75	631.48
	10^6	157.91	323.02	631.64
	10^7	157.91	323.05	631.65
$-\hat{k}$	10^1	306.37	582.25	937.37
	10^2	193.48	423.83	746.42
	10^3	162.10	344.88	646.65
	10^4	158.35	325.91	633.37
	10^5	157.96	323.35	631.83
	10^6	157.92	323.08	631.67
	10^7	157.91	323.06	631.66
	10^8	157.91	323.05	631.66
	10^9	157.91	323.05	631.65
$+\hat{g}$	10^1	160.57	331.10	634.32
	10^2	158.19	323.96	631.93
	10^3	157.94	323.14	631.68
	10^4	157.92	323.06	631.66
	10^5	157.91	323.05	631.66
	10^6	157.91	323.05	631.65
$-\hat{g}$	10^1	154.91	312.21	628.65
	10^2	157.63	322.12	631.37
	10^3	157.89	322.96	631.63
	10^4	157.91	323.04	631.65
	10^5	157.91	323.05	631.65

Results presented in Table 7.2 confirm the predicted monotonic convergence depending on the type and sign of penalty parameter as explained in Chapter 1 and shows that lower eigenparameter values are needed to obtain converged results than when using ordinary type parameters. Some of the results in Table 7.2

were plotted in Fig. 7.3, from where it is possible to observe that the eigenvalues or critical loads converged linearly with respect to the inverse value of the eigenpenalty parameters in a larger range than with ordinary penalty parameters.

Here it is worth noting that regardless of the type of penalty parameter, it is expected that the average of a pair of results using the same penalty type and magnitude, but opposite sign should give a very good approximation to the constrained solution, which should coincide with the lambda value corresponding to abscise equal to zero in Fig. 7.3.

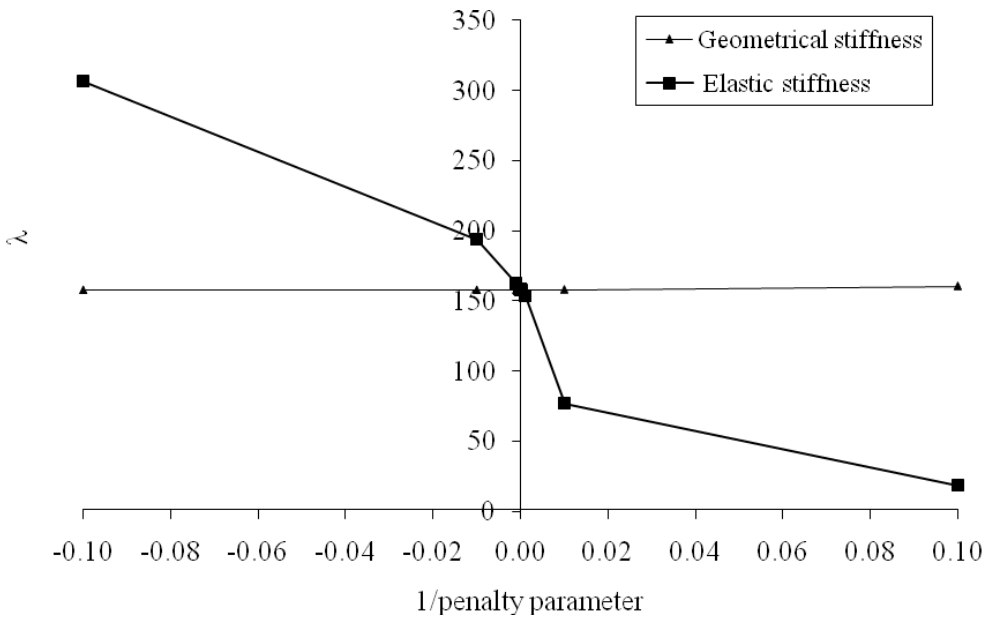

Figure 7.3. Non-dimensional critical load λ
versus inverse of stiffness and geometrical stiffness penalty parameters
of CC beams with $\hat{\rho}$ =2, using 96 DOFs in the RRM.

7.3.3 Critical loads of CS, CF and SS tapered beams

To further investigate the use of eigenparameters in structural stability analysis, beams with tapering ratio $\hat{\rho} = 2$ and CS, CF and SS boundary conditions are

given in Table 7.3. In all cases 96 DOFs were used as Table 7.1 shows that using more than 96 DOFs is not likely to significantly improve the results.

From the results in Table 7.3 it was observed that SS beams converged extremely rapidly for all types of penalty parameters. As in all other cases, when adding $\hat{h}$ constraints, $\hat{h}$ eigenvalues should be deleted from the set of results. As mentioned earlier it is very easy to identify the eigenvalues that do not correspond to the solution of the problem, checking if they converge to 0^+, 0^-, ∞ or $-\infty$. However, in the SS case it was detected that an eigenvalue converging towards ∞, that had to be deleted, had not fully converged and was still "mixed" with the valid eigenvalues when the penalty parameter was set to 10, which is the value given in Table 7.3.

Table 7.3. Critical loads of CS, CF and SS beams with tapering ratio $\hat{\rho} = 2$ using 96 DOFs.

BC	Method	Penalty Value	P_c		
		$+\hat{k},-\hat{k},+\hat{g},-\hat{g}$	1	2	3
CS	RRM & Penalty	$10^7,10^7,10^5,10^5$	80.763	238.72	475.60
	RRM & Lagrangian		80.763	238.72	475.60
	FEM		80.883	239.09	476.42
CF	RRM & Penalty	$10^6,10^7,10^6,10^5$	5.4341	84.795	242.73
	RRM & Lagrangian		5.4341	84.795	242.73
	FEM		5.4436	84.923	243.11
SS	RRM & Penalty	$10^1,10^1,10^1,10^1$	39.478	157.91	355.31
	RRM & Lagrangian		39.478	157.91	355.31
	FEM		39.446	157.78	355.03

7.3.4 Critical loads of CC tapered beams with 49 intermediate supports

The method presented in this work gives the RRM flexibility to apply boundary conditions at any point on the beam without having to change the set of

admissible functions, which has been identified in the past as one of the most significant drawbacks when using the RRM (Courant 1943). However, when intermediate supports are used, more terms are needed to obtain results with the desired accuracy. To illustrate this feature of the method, results for a CC beam with 49 equidistant pins varying the number of DOFs are presented on Table 7.4.

Table 7.4. Critical loads of CC beams with tapered ratio $\hat{\rho}$ = 2 and 49 intermediate and equidistant pins.

DOF	Method	Penalty Value	P_c		
		$+\hat{k},-\hat{k},+\hat{g},-\hat{g}$	1	2	3
149	RRM & Penalty	$10^{12},10^{12},10^{7},10^{8}$	34079	42294	49764
	RRM & Lagrangian		34079	42294	49764
	FEM		34395	42757	50395
349	RRM & Penalty	$10^{12},10^{12},10^{7},10^{8}$	34074	42286	49754
	RRM & Lagrangian		34074	42286	49754
	FEM		34097	42321	49803
749	RRM & Penalty	$10^{11},10^{12},10^{7},10^{7}$	34073	42285	49753
	RRM & Lagrangian		34073	42285	49753
	FEM		34075	42288	49757

7.3.5 Critical loads of CC beams with varying tapering ratio

Table 7.5 presents numerical experiments for CC beams with tapering ratios $\hat{\rho}$ equal to 0.01, 0.025 and 4 using 1000 terms in RRM and 1000 elements. This means that the RRM solutions contain 996 DOFs, while the FEM solution contains 1994 DOFs. By comparison of the results in Table 7.4, it was decided to include twice as many DOFs in the FEM than in the RRM to obtain results of about the same accuracy. Although, the tapering ratios may not be realistic, this is a way to test the robustness of the method.

Table 7.5. Critical loads of CC beams with various tapering ratios and 1000 terms in the RRM and 1000 elements in the FEM.

$\hat{\rho}$	Method	Penalty Value	P_c		
			1	2	3
			x10^{-7}	x10^{-7}	x10^{-6}
0.01	RRM & $+\hat{k}$	10^4	39488	80826	15799
	RRM & $-\hat{k}$	10^3	39491	80846	15802
	RRM & $+\hat{g}$	10^7	39488	80822	15799
	RRM & $-\hat{g}$	10^6	39494	80826	15798
	RRM & Lagrangian		39488	80822	15799
	FEM		39631	81094	15863
0.025			x10^{-6}	x10^{-6}	x10^{-6}
	RRM & $+\hat{k}$	10^4	24675	50477	98696
	RRM & $-\hat{k}$	10^5	24774	50479	98699
	RRM & $+\hat{g}$	10^9	24674	50478	98697
	RRM & $-\hat{g}$	10^6	24675	50478	98698
	RRM & Lagrangian		24674	50478	98697
	FEM		24689	50508	98757
4	RRM & $+\hat{k}$	10^8	631.65	1292.2	2526.6
	RRM & $-\hat{k}$	10^7	631.60	1292.2	2526.7
	RRM & $+\hat{g}$	10^7	631.65	1292.2	2526.6
	RRM & $-\hat{g}$	10^5	631.65	1292.2	2526.6
	RRM & Lagrangian		631.65	1292.2	2526.6
	FEM		631.66	1292.2	2526.6

From results in Table 7.5 it is observed that the only type of penalty parameter that gives results which agree with the results using the Lagrangian Multiplier Method is the positive geometrical stiffness type $+\hat{g}$. It is also observed that in a few cases the lower bounds are higher than the upper bounds. This is because small round-off errors were not identified with the series of values that defined the penalty parameters ($\pm 10^p$, where $p \in [1,2,3,...]$). This problem could be avoided using smaller increments in the series that defines the values of the penalty parameters, especially in the close range were the monotonic convergence is interrupted.

7.3.6 Critical loads for two-beam frames

Table 7.6 presents results for the two-beam frames attached at different angles obtained with the method proposed here and compared with results using the commercial FEM software ABAQUS building the two-beam frames with 20 beam elements B32 (3-node quadratic beams). Penalty values on Table 7.6 correspond to minimum value to reach convergence up to the fifth significant figure free of numerical instabilities. Results using the RRM were obtained fixing $n = 20$ in both beams.

From the cases analyzed in Table 7.6 it was observed that when negative stiffness was used many eigenvalues corresponding to constraint DOF gave small eigenvalues, even though these eigenvalues should converge towards infinity. This problem is easy to recognize, as it is clear that the eigenvalues have not converged. A similar problem occurred only for a frame with $\theta = 165$ when negative eigenparameters were used.

Table 7.6. Critical loads of two-beam frames joined at various angles θ.

θ	Method	Penalty Value	P_c		
		$+\hat{k},-\hat{k},+\hat{g},-\hat{g}$	1	2	3
30	RRM & Penalty	$10^8,10^7,10^5,10^6$	39.006	76.266	115.29
	FEM		38.920	76.081	114.81
90	RRM & Penalty	$10^7,10^6,10^4,10^5$	28.554	55.831	84.400
	FEM		28.522	55.719	84.136
165	RRM & Penalty	$10^6,10^7,10^6,10^5$	5.2708	10.306	15.579
	FEM		5.3539	10.458	15.793

Sets of results using the RRM and penalty parameters are given together as identical results up to the fifth significant number were obtained in all cases.

7.3.7 Concluding remarks

It has been shown that positive and negative eigenpenalty parameters can be used to determine the critical loads of a constrained structure. Unlike the ordinary penalty parameter which corresponds to the application of an artificial elastic stiffness, the eigenpenalty is applied using an artificial geometric stiffness term. The results obtained using a Rayleigh-Ritz procedure with penalty parameters were compared with results generated using the RRM and Lagrange multipliers as well as with results obtained by the FEM either using standard beam elements or using the commercial program ABAQUS. Results of both methods using the RRM converged to virtually identical results. Numerical results show that convergence towards a constrained solution is obtained at a lower magnitude of the penalty parameter when using the eigenpenalty method compared to the ordinary penalty method.

Chapter 8

Conclusions

8.1 The set of admissible functions

It has been shown that a set of admissible functions consisting of a combination of a second order polynomial and a Fourier cosine series may be used in the RRM for calculating the natural frequencies and modes of FF beams, completely free rectangular plates and completely free shallow shells. The same set of admissible functions can be used to obtain the natural frequencies of the same structures subject to various combinations of classical boundary conditions at their ends (in the case of beams) or along their edges (for plates and shells). In addition the same series has been used successfully to obtain the natural frequencies of plates subject to additional point constraints and closed-box type structures, as well as to obtain the critical loads of tapered beams and two-beam frames.

For all cases including constraints, some or all terms in this series may individually violate the constraints for some boundary conditions, but in each case, the constraint conditions can be satisfied to any reasonable degree of accuracy by using positive and negative ordinary penalty parameters or eigenpenalty parameters.

Another important property of the set of admissible functions developed in this work is that the number of terms that can be used in the solution was limited only by the memory of the PC with 1 Gb in RAM, as ill-conditioning was in no case found to be due to the number of terms included in the solution. Ill-conditioning found in this work, was always due to too high penalty values.

The convenience to use the same set of admissible functions to model the deflection of different structural elements was also noted, as they have common matrices and for instance the penalty matrices of plates are identical to the penalty submatrices of shallow shells.

In the study of the different types of penalty parameters, it was also noted, that it is important to identify a priori the number of rigid body modes modelled in the set of admissible functions, as well as the number of zero rows and columns in each of the system matrices to anticipate the number of zero or infinite eigenvalues of the solution with or without using penalty parameters.

8.2 Penalty parameters

As noted in recent publications, the use of inertial penalty parameters appears to be advantageous compared to the stiffness penalty parameters as results converge with lower magnitude of the penalty parameter. It was found that small absolute values of inertial penalty parameters are sufficient to obtain the frequency parameters of high modes. The results using artificial inertia also show that if constraint violation is checked for the first mode, then it is not necessary to check for higher modes, as higher modes converge first. Thus, the use of inertial penalty

parameters is recommended for vibration analysis of constrained systems, when the number of terms is small. It was also shown solving vibration problems of shallow shells that the eigenpenalty parameters are in disadvantage, when the number of terms included in the solution is large as the fundamental frequency is the last one to converge. Thus, it is possible that numerical instabilities will appear before the convergence of the fundamental frequency. Furthermore, when using a large number of terms it could be expected that the range of eigenpenalty parameters that would give converged results would be small, making very difficult to find a penalty parameter that gives a good approximation to the constraint solution for lower modes.

It was also found that critical values are also present when eigenpenalty parameters are used to model constraints, but that the number of these critical values is limited to the number of rigid-body modes included in the solution without penalty parameters.

The present work also demonstrated the efficacy of the use of the monotonic convergence property, as well as the bracketing property to check for round-off errors.

8.3 Future Work

Further development of this procedure is possible. The following points are recommended for future work:

a) Develop matrices of other structural elements using the same set of admissible functions. These could be in geometry such as circular plates

and spherical cups, as well as elements using different beam, plate and shell theories that take into account shear deformation and rotary inertia, three-dimensional effects, etc. It may be that new coordinate systems need to be developed to facilitate the use of the selected functions. In dealing with higher order theories, it would be interesting to see if any additional low order polynomial terms would be needed.

b) This project can also be extended to analyse problems of complex geometries mixing different structural element types. In assembling different types of elements, ensuring continuity conditions along boundaries, particularly any curved boundaries, using penalty approach may pose some interesting questions such as whether penalty terms should be computed using numerical integration and how to simplify any coordinate transformations in situations where the elements being connected use different coordinate systems.

c) Using penalty parameters to produce hybrid structural models combining the present approach with the FEM. It is well known that in the FEM techniques such as the Guyan reduction have been used to condense the matrices of the system in an attempt to reduce the computation time. One of drawbacks of this technique is the loss of accuracy in the inertia representation, especially if the DOFs containing high inertia are not included in the resulting substructure. On the other hand, solving problems of complex geometries is a drawback of the RRM. But the combination of these techniques could lead to a reduction of the size of the system matrices, whilst still allowing the analysis of structures of complex

geometries and incrementing the accuracy of the solution per DOF included in the solution.

d) Another possibility is to analyse other type of engineering problems, such as radiation of noise, interaction between structural elements and fluid, etc.

References

Amabili, M. (1997). "Shell-plate interaction in the free vibrations of circular cylindrical tanks partially filled with a liquid: the artificial spring method." Journal of Sound and Vibration, 199(3), 431-452.

Amabili, M. (2008). Nonlinear vibrations and stability of shells and plates, Cambridge University Press, Cambridge; New York.

Amabili, M., and Garziera, R. (1999). "A technique for the systematic choice of admissible functions in the Rayleigh-Ritz method." Journal of Sound and Vibration, 224(3), 519-539.

Amabili, M., Pierandrei, R., and Frosali, G. (1997). "Analysis of vibrating circular plates having non-uniform constraints using the modal properties of free-edge plates: application to bolted plates." Journal of Sound and Vibration, 206(1), 23-38.

Andrade, A., Camotim, D., and Dinis, P. B. (2007). "Lateral-torsional buckling of singly symmetric web-tapered thin-walled I-beams: 1D model vs. shell FEA." Computers & Structures, 85(17-18), 1343-1359.

Askes, H., and Ilanko, S. (2006). "The use of negative penalty functions in linear systems of equations." Proceedings of the Royal Society A, 462, 2965-2975.

Baruh, H., and Tadikonda, S. S. K. (1989). "Another look at admissible functions." Journal of Sound and Vibration, 132(1), 73-87.

Bassily, S. F., and Dickinson, S. M. (1975). "On the use of beam functions for problems of plates involving free edges." Journal of Applied Mechanics, Transactions ASME, Ser E, 42(4), 858-864.

Bhat, R. B. (1985). "Natural frequencies of rectangular plates using characteristic orthogonal polynomials in Rayleigh-Ritz method." Journal of Sound and Vibration, 102(4), 493-499.

Bhat, R. B. (1996). "Effect of normal mode contents in assumed deflection shapes in Rayleigh-Ritz method." Journal of Sound and Vibration, 189(3), 407-419.

Blevins, R. D. (2000). Formulas for natural frequency and mode shape, Krieger Pub. Co., Malabar, Fla.

Brown, R. E., and Stone, M. A. (1997). "On the use of polynomial series with the Rayleigh-Ritz method." Composite Structures, 39(3-4), 191-196.

Budiansky, B., and Hu, P. C. (1946). "The Lagrangian multiplier method of finding upper and lower limits to critical stresses of clamped plates." NACA report 848.

Burnett, D. S. (1987). Finite element analysis: from concepts to applications, Addison-Wesley Pub. Co., Reading, Mass.

Courant, R. (1943). "Variational methods for the solution of problems of equilibrium and vibration." Bulletin of the American Mathematical Society, 49, 1-23.

Crossland, J. A., and Dickinson, S. M. (1997). "The free vibration of thin rectangular planform shallow shells with slits." Journal of Sound and Vibration, 199(3), 513-521.

De Rosa, M. A., and Auciello, N. M. (1996). "Free vibrations of tapered beams with flexible ends." Computers & Structures, 60(2), 197-202.

de Silva, C. W. (1999). Vibration Fundamentals and Practice, CRC Press, Boca Raton, Florida.

Dickinson, S. M. (1968). "Vibration of box-type structures with flexible joints between constituent plates." Journal of Mechanical Engineering Science, 10, 294-296.

Dickinson, S. M., and Warburton, G. B. (1967). "Vibration of box-type structures." Journal of Mechanical Engineering Science, 9, 325-335.

Dill, E. H., and Pilster, K. S. (1958). "Vibration of rectangular plates and plate systems." Proceedings of the Third U.S. National Congress of Applied Mechanics, 123-132.

Dowell, E. H. (1972). "Free vibrations of an arbitrary structure in terms of component modes." Jounal of Applied Mechanics, 39(3), 727-732.

Dowell, E. H. (1984). "On asymptotic approximations to beam model shapes." Journal of Applied Mechanics, Transactions ASME, 51(2), 439.

Filipich, C. P., and Rosales, M. B. (2000). "Arbitrary precision frequencies of a free rectangular thin plate." Journal of Sound and Vibration, 230(3), 521-539.

Garcia, A. L. (1994). Numerical methods for physics, Prentice Hall, Englewood Cliffs, N.J.

Gorman, D. J. (1978). "Free vibration analysis of the completely free rectangular plate by the method of superposition." Journal of Sound and Vibration, 57(3), 437-447.

Gorman, D. J. (1999). Vibration analysis of plates by the superposition method, World Scientific, Singapore, River Edge, N.J.

Huang, C. S., and Leissa, A. W. (2009). "Vibration analysis of rectangular plates with side cracks via the Ritz method." Journal of Sound and Vibration, In Press, Corrected Proof.

Ilanko, S. (2002a). "Existence of natural frequencies of systems with artificial restraints and their convergence in asymptotic modelling." Journal of Sound and Vibration, 255(5), 883-898.

Ilanko, S. (2002b). "The use of negative penalty functions in constrained variational problems." Communications in Numerical Methods in Engineering 18, 659-668.

Ilanko, S. (2003). "The use of asymptotic modelling in vibration and stability analysis of structures." Journal of Sound and Vibration, 263(5), 1047-1054.

Ilanko, S. (2005a). "Asymptotic modelling theorems for the static analysis of linear elastic structures." Proceedings of the Royal Society A, 461, 3525-3542.

Ilanko, S. (2005b). "Introducing the use of positive and negative inertial functions in asymptotic modelling." Proceedings of the Royal Society A, 461, 2545-2562.

Ilanko, S. (2006). "On the bounds of Gorman's superposition method of free vibration analysis." Journal of Sound and Vibration, 294(1-2), 418-420.

Ilanko, S., and Dickinson, S. M. (1987). "The vibration and post-buckling of geometrically imperfect, simply supported, rectangular plates under uni-axial loading, part I: Theoretical approach." Journal of Sound and Vibration, 118(2), 313-336.

Ilanko, S., and Dickinson, S. M. (1999). "Asymptotic modelling of rigid boundaries and connections in the Rayleigh-Ritz method." Journal of Sound and Vibration, 219(2), 370-378.

Ilanko, S., and Williams, F. (2008). "Wittrick-Williams algorithm proof of bracketing and convergence theorems for eigenvalues of constrained structures with positive and negative penalty parameters." International Journal of Numerical Methods in Engineering, 75, 83-102.

Jaworski, J. W., and Dowell, E. H. (2008). "Free vibration of a cantilevered beam with multiple steps: Comparison of several theoretical methods with experiment." Journal of Sound and Vibration, 312(4-5), 713-725.

Kapania, R. K., and Kim, Y. Y. (2006). "Flexural-torsional coupled vibration of slewing beams using various types of orthogonal polynomials." Journal of Mechanical Science and Technology, 20, 1790-1800.

Kapania, R. K., and Liu, Y. (2000). "Static and vibration analyses of general wing structures using equivalent-plate models." AIAA Journal, 38, 1269-1277.

Karnovsky, I. A., and Lebed, O. I. (2000). Formulas for structural dynamics: tables, graphs and solutions, McGraw-Hill Professional Book Group, Blacklick, OH, USA.

Karnovsky, I. A., and Lebed, O. I. (2004). Free vibrations of beams and frames : eigenvalues and eigenfunctions, McGraw-Hill, New York.

Kim, C. S. (1995). "Free vibration of rectangular plates with an arbitrary straight line support." Journal of Sound and Vibration, 180(5), 769-784.

Klein, L. (1974). "Transverse vibrations of non-uniform beams." Journal of Sound and Vibration, 37(4), 491-505.

Kurpa, L. V., Lyubitska, K. I., and Shmatko, A. V. (2005). "Solution of vibration problems for shallow shells of arbitrary form by the R-function method." Journal of Sound and Vibration, 279(3-5), 1071-1084.

Leissa, A. W. (1969a). "Vibration of plates." NASA, U. S. Government Printing Office.

Leissa, A. W. (1969b). "Vibration of shells." NASA, SP-288.

Leissa, A. W. (1973). "The free vibration of rectangular plates." Journal of Sound and Vibration, 31(3), 257-293.

Leissa, A. W., and Narita, Y. (1984). "Vibrations of completely free shallow shells of rectangular planform." Journal of Sound and Vibration, 96(2), 207-218.

Lévy, M. (1899). "Memoire sur la theorie des plaques elastiques planes." Journal des Mathematiques Pures et Appliquees, 3, 219.

Li, W. L. (2000). "Free vibrations of beams with general boundary conditions." Journal of Sound and Vibration, 237(4), 709-725.

Li, W. L. (2002). "Comparison of Fourier sine and cosine series expansions for beams with arbitrary boundary conditions." Journal of Sound and Vibration, 255(1), 185-194.

Li, W. L. (2004). "Vibration analysis of rectangular plates with general elastic boundary supports." Journal of Sound and Vibration, 273(3), 619-635.

Li, W. L., and Daniels, M. (2002). "A Fourier series method for the vibrations of elastically restrained plates arbitrarily loaded with springs and masses." Journal of Sound and Vibration, 252(4), 768-781.

Li, W. L., Zhang, X., Du, J., and Liu, Z. (2009). "An exact series solution for the transverse vibration of rectangular plates with general elastic boundary supports." Journal of Sound and Vibration, 321(1-2), 254-269.

Liew, K. M., and Lim, C. W. (1994). "Vibration of perforated doubly-curved shallow shells with rounded corners." International Journal of Solids and Structures, 31(11), 1519-1536.

Liew, K. M., and Wang, C. M. (1993). "pb-2 Rayleigh-Ritz method for general plate analysis." Engineering Structures, 15(1), 55-60.

Lim, C. W., and Liew, K. M. (1994). "A pb-2 Ritz formulation for flexural vibration of shallow cylindrical shells of rectangular planform." Journal of Sound and Vibration, 173(3), 343-375.

Liu, G. R., and Chen, X. L. (2001). "A mesh-free method for static and free vibration analyses of thin plates of complicated shape." Journal of Sound and Vibration, 241(5), 839-855.

Logan, D. L. (2007). A first course in the finite element method, Thomson, Toronto, Ont.

Mikhlin, S. G. (1964). Variational methods in mathematical physics, Pergamon Press, Oxford

Mikhlin, S. G. (1971). The Numerical Performance of Variational Methods, Wolters-Noordhoff, Groningen, The Netherlands.

Mukhopadhyay, M. (2008). Structural dynamics: vibration and systems, Ane Books India for CRC Press, New Delhi, India.

Navier, C. L. M. N. (1823). Bulletin des Science de la Societe Philomarhique de Paris.

Oosterhout, G. M., van der Hoogt, P. J. M., and Spiering, R. M. E. J. (1995). "Accurate calculation methods for natural frequencies of plates with special attention to the higher modes." Journal of Sound and Vibration, 183(1), 33-47.

Rao, S. S. (2007). Vibration of continuous systems Wiley, Hoboken, N.J.

Reddy, J. N. (1990). "A general nonlinear third-order theory of plates with moderate thickness." International Journal of Non-Linear Mechanics, 25, 677-686.

Ritz, W. (1908). "Ueber eine neue Methode zur Loesung gewisser Variationsprobleme der mathmatischen Physik." Journal fuer reine and angewandte Mathematik, 135, 1-61.

Singhvi, S., and Kapania, R. K. (1994). "Comparison of simple and Chebychev polynomials in Rayleigh-Ritz analysis." Journal of Engineering Mechanics, 120, 2126-2135.

Smith, S. T., Bradford, M. A., and Oehlers, D. J. (1999). "Numerical convergence of simple and orthogonal polynomials for the unilateral plate buckling problem using the Rayleigh-Ritz method." International Journal for Numerical Methods in Engineering, 44(11), 1685-1707.

Szilard, R. (2004). Theories and applications of plate analysis: classical, numerical, and engineering methods, John Wiley, Hoboken, NJ, USA.

Thomson, W. T., and Dahleh, M. D. (1998). Theory of vibration with applications, Prentice Hall, Upper Saddle River, N.J.

Ventsel, E., and Krauthammer, T. (2001). Thin plates and shells: theory, analysis, and applications, T. Krauthammer, translator, Marcel Dekker, New York.

von Kármán, T. (1910). "Festigkeitprobleme in Maschinenbau." Encyklopadie der Mathematischen Wissenschaften, 4(4), 311-385.

Warburton, G. B. (1954). "The vibration of rectangular plates." Proceedings of the Institute of Mechanical engineers, ser. A, 168, 371-381.

Williams, F. W., and Ilanko, S. (2006). "The use of the reciprocals of positive and negative inertial functions in asymptotic modelling." Proceedings of the Royal Society A 462, 1909-1915.

Williams, T. W. C. (1987). "Rounding error effects on computed Rayleigh-Ritz estimates." Journal of Sound and Vibration, 117(3), 588-593.

Wu, J. S., and Chou, H. M. (1998). "Free vibration analysis of a cantilever beam carrying any number of elastically mounted point masses with the analytical-and-numerical-combined-method." Journal of Sound and Vibration, 213, 317-332.

Wu, J. S., and Luo, S. S. (1997). "Use of analytical-and-numerical-combined method in the free vibration analysis of a rectangular plate with any number of point masses and translational springs." Journal of Sound and Vibration, 200, 179-194.

Young, P. G. (2000). "Application of a three-dimensional shell theory to the free vibration of shells arbitrarily deep in one direction." Journal of Sound and Vibration, 238(2), 257-269.

Young, P. G., and Dickinson, S. M. (1993). "On the free flexural vibration of rectangular plates with straight or curved internal line supports." Journal of Sound and Vibration, 162(1), 123-135.

Young, P. G., and Dickinson, S. M. (1994). "Further studies on the vibration of plates with curved edges, including complicating effects." Journal of Sound and Vibration, 177(1), 93-109.

Young, P. G., and Dickinson, S. M. (1995a). "Vibration of a class of shallow shells bounded by edges described by polynomials Part II: natural frequency parameters for shallow shells of various different planforms." Journal of Sound and Vibration, 181(2), 215-230.

Young, P. G., and Dickinson, S. M. (1995b). "Vibration of a class of shallow shells bounded by edges described by polynomials, part I: theoretical approach and validation." Journal of Sound and Vibration, 181(2), 203-214.

Yuan, J., and Dickinson, S. M. (1992a). "The flexural vibration of rectangular plate systems approached by using artificial springs in the Rayleigh-Ritz method." Journal of Sound and Vibration, 159(1), 39-55.

Yuan, J., and Dickinson, S. M. (1992b). "On the use of artificial springs in the study of the free vibrations of systems comprised of straight and curved beams." Journal of Sound and Vibration, 153(2), 203-216.

Zhou, D. (1996). "Natural frequencies of rectangular plates using a set of static beam functions in Rayleigh-Ritz method." Journal of Sound and Vibration, 189(1), 81-87.

Zienkiewicz, O. C., Taylor, R. L. R. L., 1934- , and Zhu, J. Z. (2005). The finite element method : its basis and fundamentals, R. L. Taylor, J. Z. Zhu, and O. C. Zienkiewicz, translator, Elsevier Butterworth-Heinemann, Amsterdam, London

Appendix A

Matrices of a Standard Beam Element in the FEM

The properties of a standard beam element used in this work are defined by the stiffness matrix **K** and the mass matrix **M** as given by Logan (2007), as well as by the geometrical stiffness matrix **G** as given by Burnett (1987) presented below.

$$\mathbf{K} = \frac{EI}{L^3}\begin{bmatrix} 12 & 6L & -12 & 6L \\ 6L & 4L^2 & -6L & 2L^2 \\ -12 & -6L & 12 & -6L \\ 6L & 2L^2 & -6L & 4L^2 \end{bmatrix}, \tag{A.1}$$

$$\mathbf{M} = \frac{\rho AL}{420}\begin{bmatrix} 156 & 22L & 54 & -13L \\ 22L & 4L^2 & 13L & -3L^2 \\ 54 & 13L & 156 & -22L \\ -13L & -3L^2 & -22L & 4L^2 \end{bmatrix} \quad \text{and} \tag{A.2}$$

$$\mathbf{G} = \frac{1}{30L}\begin{bmatrix} 36 & 3L & -36 & 3L \\ 3L & 4L^2 & -3L & -L^2 \\ -36 & -3L & 36 & -3L \\ 3L & -L^2 & -3L & 4L^2 \end{bmatrix} \tag{A.3}$$

Appendix B

The Lagrangian Multiplier Method

B.1 Introduction

The Lagrangian Multiplier Method is one of the techniques commonly used in the RRM to define constraints and to inter-connect structural elements. Lagrange multipliers can be interpreted as generalized forces that maintain the modelled boundary conditions (Klein 1974).

A formal definition of the system of equations that define Lagrangian multipliers is given in (Budiansky and Hu 1946) as the minimization of

$$f - \Lambda\varphi, \tag{B.1}$$

where f is a function of $\hat{n}$ variables, Λ is the undetermined Lagrangian multiplier and φ is a relationship that bounds the $\hat{n}$ variables of the function $f(x_1, x_2, ...x_n)$

$$\varphi(x_1, x_2, ...x_n) = 0 \tag{B.2}$$

Then the minimization can be expressed as

$$\frac{\partial f}{\partial x_k} - \Lambda\frac{\partial \varphi}{\partial x_k} = 0, \tag{B.3}$$

$$\varphi = 0 \tag{B.4}$$

Thus, this technique adds a row and a column for each point constraint added to the system. For instance, to model a cantilever beam constraining the translational and rotational degrees of freedom at $x = 0$, two rows and columns should be added to the stiffness and mass matrices. These two rows and columns can be defined as

$$k_{n+1,j} = k_{j,n+1} = \frac{\partial\left(a_{n+1}\left(w(0)\right)\right)}{\partial a_j} = \phi_j(0), \qquad \text{for} \quad j = 1 \text{ to } n, \quad \text{and} \tag{B.5a}$$

$$k_{n+1,j} = k_{j,n+1} = 0, \qquad \text{for} \quad j = n+1 \text{ and } n+2 \tag{B.5b}$$

$$k_{n+2,j} = k_{j,n+2} = \frac{\partial\left(a_{n+2}\left(w'(0)\right)\right)}{\partial a_i} = \phi'_j(0), \qquad \text{for} \quad j = 1 \text{ to } n, \quad \text{and} \tag{B.6a}$$

$$k_{n+2,j} = k_{j,n+2} = 0, \qquad \text{for} \quad j = n+1 \text{ and } n+2 \tag{B.6b}$$

where a_{n+1} and a_{n+2} define the Lagrangian multipliers. Eq. (B.5) adds a constraint in translation, while Eq. (B.6) adds a constraint in rotation.

It should be noted that this technique adds zeros to the main diagonal and for this reason, it was not possible to solve the set of equations in the same way described in Section 3.3. Instead a change of variables had to be carried out before solving for the eigenvalues. This change of variables consists in multiplying the elastic and geometric stiffness matrices by the inverse of the stiffness matrix.